Supplementary Material:
Novel Method to Estimate the Octane Ratings of Ethanol-Gasoline Mixtures using Base Fuel Properties

James E. Anderson[1]*

Timothy J. Wallington[1]

1. Research & Advanced Engineering, Ford Motor Company, Dearborn, Michigan, USA

Contents

SI-1. Ethanol blends with CRC FACE fuels

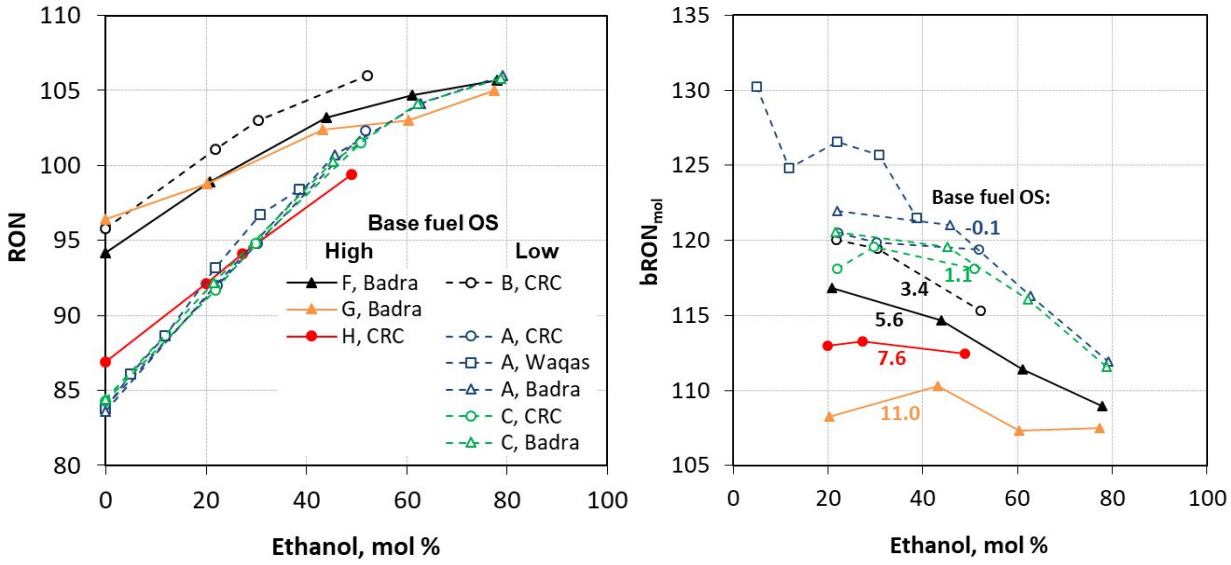

Figure S1. RON (left) and bRON$_{mol}$ (right) versus ethanol content in six CRC FACE gasoline test fuels (FACE A, B, C, F, G and H) from studies by CRC (Cannella et al., 2014), Waqas et al. (2016) and Badra et al. (2017).

SI-2. P_g ethanol octane blending model approach

Anderson et al.[16] added a new term to the linear molar octane blending model[27] which allows it to represent various degrees of synergistic or antagonistic blending. The equation includes a single empirical parameter, P_g, to provide gasoline-specific scaling for the non-linear molar octane blending. As defined, that parameter is multiplied by the octane number difference between ethanol and the gasoline, and further multiplied by the ethanol and gasoline fractions, as both are needed for the interaction). Positive or negative values of P_g indicate synergistic or antagonistic octane blending, respectively.

$$ON_b = (1 - x_a)ON_g + x_a ON_a + P_g x_a (1 - x_a)(ON_a - ON_g)$$

One limitation of the P_g approach occurs for cases in which ON_g is greater than ON_a. In this case the value of P_g would need to use the opposite sign to represent a synergistic or antagonistic interaction. This inconsistency is addressed by using the absolute value of the ON difference, $|ON_a\text{-}ON_g|$, as shown below.

$$ON_b = (1 - x_a)ON_g + x_a ON_a + P_g x_a (1 - x_a)(|ON_a - ON_g|)$$

A second limitation of the P_g approach is that as ON_g approaches the value of ON_a, the value of $|ON_a - ON_g|$ gets very small and P_g needs to become very large in order to compensate. For the special case in which ON_g equals ON_a, the interaction term is zero and cannot capture any interactions.

The equation for the implied bON_{mol} using the P_g approach is obtained by comparing the relevant equations for the P_g and bON_{mol} approaches.

$$ON_{blend} = (1 - x_a)ON_g + bON_{mol} x_a$$

$$ON_{blend} = (1 - x_a)ON_g + x_a ON_a + P_g x_a (1 - x_a)(|ON_a - ON_g|)$$

$$bON_{mol} = ON_a + P_g (1 - x_a)(|ON_a - ON_g|)$$

The implied bON_{mol} from the P_g approach is a linear function of alcohol content, x_a, with slope = $-P_g(|ON_a - ON_g|)$ and intercept = $ON_a + P_g(|ON_a - ON_g|)$. The $(1 - x_a)$ term ensures that $bON_{mol} = ON_a$ at 100% ethanol.

SI-3. Wang et al. (2017) model

The empirical model used by Wang et al.[28] is a function of volumetric ethanol content (C_e = 0-75 vol %), the RON of the base fuel (RON_{base}) and the RON of ethanol (RON_e).

$$RON_{blend} = \frac{NOI}{100}(RON_e - RON_{base}) + RON_{base}$$

$$NOI = -0.01983C_e^2 + 2.8512C_e$$

The blending octane number, therefore, is given as follows.

$$bRON_{vol} = \frac{-0.01983{C_e}^2 + 2.8512C_e}{100}(RON_e - RON_{base})$$

The 2nd order (parabolic) form of this empirical equation in terms of C_e leads to a maximum $bRON_{vol}$ value at 72 vol % ethanol rather than 100 vol % ethanol and would (incorrectly) lead to declining $bRON_{vol}$ values if used at higher ethanol content.

SI-4. Z ethanol octane blending model approach

The Z ethanol octane blending approach is a simplified variant of the P_g approach. The parameter Z is simply derived from the P_g approach by consolidating the $|ON_a - ON_g|$ term, which is fixed for a given base fuel and alcohol combination, and the coefficient P_g.

$$Z = P_g(|ON_a - ON_g|)$$

$$bON_{mol} = ON_a + Z(1 - x_a)$$

$$ON_{blend} = (1 - x_a)ON_g + x_a ON_a + Z x_a (1 - x_a)$$

Z describes the degree of deviation from linear blending for a given blend: $Z > 0$ for synergistic blending and $Z < 0$ for antagonistic blending.

One advantage of this approach is that it eliminates the $|ON_a - ON_g|$ term. This avoids the issue, seen primarily for MON, in which the $|ON_a - ON_g|$ term is very small, i.e., when ON_a is very close to ON_g, which in turn forces P_g to be a very large number to describe the interaction.

When Z does not include an ethanol content term, the maximum ON uplift due to synergistic blending behavior occurs at 50 mol % (~30 vol %) ethanol for most gasolines for which the uplift is Z/4 ON. If ethanol content is included as a term in Z, then the maximum ON uplift may occur at somewhat higher or lower ethanol content than 50 mol %.

SI-5. Calculation of ethanol octane blending values from literature data

Volumetric blending octane numbers (bON_{vol})

Volumetric ethanol blending octane numbers (bON_{vol}) are calculated from the reported octane ratings and ethanol content as follows:

$$ON_{blend} = C_g ON_g + C_e bON_{vol}$$

$$bON_{vol} = (ON_{blend} - C_g ON_g)/C_e$$

where C_e = volumetric ethanol fraction, $C_g = (1 - C_e)$ = volumetric gasoline fraction, ON_g = octane number of the base gasoline or base fuel (with ON = RON or MON) and ON_{blend} = octane number of the ethanol-gasoline blend

Molar blending octane numbers (bON_{mol})

Molar ethanol blending octane numbers (bON_{mol}) are calculated from the reported octane numbers and molar ethanol fraction (x_a) as follows:

$$ON_{blend} = (1 - x_a) ON_g + bON_{mol} x_a$$

$$bON_{mol} = ON_g + (ON_{blend} - ON_g)/x_a$$

P_g values

P_g values are calculated from the reported octane numbers and molar ethanol fraction (x_a) as follows:

$$ON_{blend} = (1 - x_a) ON_g + x_a ON_a + P_g x_a (1 - x_a)(|ON_a - ON_g|)$$

$$P_g = \frac{ON_{blend} - (1 - x_a)ON_g - x_a ON_a}{x_a(1 - x_a)(|ON_a - ON_g|)}$$

Z values

Z values are calculated from the reported octane numbers and molar ethanol fraction (x_a) as follows:

$$Z = \frac{\frac{(ON_{blend} - (1 - x_a)ON_g)}{x_a} - ON_a}{(1 - x_a)}$$

Note that Z can only be calculated for an ethanol blend—it is mathematically undefined for the base fuel ($x_a = 0$) and for neat ethanol ($x_a = 1$).

SI-6. Previously unpublished data

The data set indicated as reference [26] consists of ethanol blends from two base fuels that were prepared and characterized concurrent with our published 2012 study.[16] The base fuels and blends were prepared by Gage Products (Ferndale, MI) as described previously.[16] Nominal ethanol content for the prepared blends were 15, 30, 50 vol %. Octane ratings were measured by GE Energy Waukesha (Waukesha, WI) as described previously.[16] All other properties were measured by Paragon Laboratories (Livonia, MI) as described previously.[16] The base fuel and blend octane ratings and properties are provided in section SI-7 and are identified as "Anderson 2019" (reference 26).

Fuel property information for premium-grade CARBOB in reference 21 was obtained by personal communication with the authors.

MON for the RON91 base fuel in reference 23 was obtained by personal communication with the authors, who reported that the base fuel octane sensitivity was in the 8-10 range, thus 9 was used for this analysis.

SI-7. Fuel property and composition data

The complex base fuel data set was obtained from a total of 26 references[1-26] and included 299 ethanol-gasoline blends generated from 90 different base fuels, including full boiling range gasolines, blendstocks for oxygenate blending (BOBs), research gasolines, natural gasolines and refinery streams.

Table S1-A contains the composition and property data for the base fuels while Table S1-B contains the ethanol content and octane ratings of the base fuels, ethanol blends and (where measured) neat ethanol.

Table S1. Base fuel composition and property data set

				BOB or Base Fuel														
First Author, Year	Ref.	Base fuel ID	Type	Sat. (%)	Par., Total (%)	n-Par. (%)	iso-Par. (%)	Naph. (%)	Olef. (%)	Arom. (%)	ASTM HC method, units	Density (kg/L)	(R)eported or (E)stimated	MW (g/mol)	(R)eported or (E)st.	RON	MON	Notes
Brinkman 1975	1	P	M-Gas	62					3	35	vol	0.757	R	100	E	96.0	85.0	
Keller 1979	2	Fuel 10	M-Gas									0.73	E	100	E	90.9	82.5	
Keller 1979	2	Fuel 11	M-Gas									0.73	E	100	E	90.6	83.5	
Keller 1979	2	Fuel 12	M-Gas									0.73	E	100	E	92.0	84.0	
Keller 1979	2	Fuel 13	M-Gas									0.73	E	100	E	92.7	83.4	
Keller 1979	2	Fuel 14	M-Gas									0.73	E	100	E	92.0	82.4	
Marceglia 1982	3	Gasoline	M-Gas									0.73	E	100	E	94.3	84.3	
Kisenyi 1994	4	Gasoline	M-Gas	46.4					6	47.6	vol	0.7753	R	100	E	98.8	87.3	
Reynolds 2002	5	Alkylate	Refinery									0.69	E (typ. value)	114	E (typ. value)	96.5	93.5	
Reynolds 2002	5	LSR-A	Refinery									0.66	E (typ. value)	81	E (typ. value)	72.3	70.0	
Reynolds 2002	5	LSR-B	Refinery									0.66	E (typ. value)	81	E (typ. value)	69.8	67.8	
Reynolds 2002	5	CC-A	Refinery									0.77	E (typ. value)	107	E (typ. value)	60.7	59.5	
Reynolds 2002	5	CC-B	Refinery									0.77	E (typ. value)	107	E (typ. value)	87.6	78.9	
Reynolds 2002	5	Reformate A	Refinery									0.80	E (typ. value)	112	E (typ. value)	94.0	83.2	
Reynolds 2002	5	Reformate B	Refinery									0.80	E (typ. value)	112	E (typ. value)	84.1	76.8	
daSilva 2005	6	A	M-gas	64	60	12	48	4	3	33	mol DHA	0.734	R	111	R	98.0	89.5	
daSilva 2005	6	B	Refinery	88	71	14	57	17	3	9	mol DHA	0.706	R	98	R	81.7	79.5	
Yucesu 2006	7	Gasoline	M-Gas									0.7649	R	100	E	98.8	86.4	
Nakata 2007	8	A	M-Gas	63.4					9.9	26.7	vol	0.736	R	100	E	91.5	83.0	
Nakata 2007	8	B	M-Gas	37.1					19.7	43.2	vol	0.76	R	100	E	99.6	87.1	
Nakata 2007	8	D	Res.	38.2					0.4	61.4	vol	0.797	R	100	E	96.4	85.3	
Nakata 2007	8	E	Res.	45.8					36.8	17.4	vol	0.73	E	100	E	91.3	80.3	
Martini 2007	9	A, EU	M-Gas	55					8.7	36.3	vol	0.7555	R	100	E	98.4	86.1	
Martini 2007	9	B, Artic	M-gas	55.7					9.1	35.2	vol	0.7533	R	100	E	97.8	86.1	
Karonis 2008	10	I	M-gas	56.6	50.9			5.7	12	31.4	vol	0.7372	R	100	E	92.5	84.2	
Karonis 2008	10	II	Res.	65.4	58.6			6.8	13.5	21.1	vol	0.7155	R	100	E	94.0	84.1	
Milpied 2009	11	I	Res.									0.73	E (0.547 R)	100	E	95.5	85.0	
Milpied 2009	11	J	Res.									0.73	E (0.527 R)	100	E	98.1	87.8	
Milpied 2009	11	G	Res.									0.73	E (0.586 R)	100	E	91.6	81.6	
Wheeler 2009	12	A79D21	Refinery	57.4	49.5	17.6	31.9	7.9	1.5	41.1	vol DHA	0.7807	R	105	E (blend comp., typ. val.)	83.4	76.5	
Wheeler 2009	12	C50D50	Refinery	63.1	47.9	16.7	31.2	15.2	17.4	19.5	vol DHA	0.7412	R	94	E (blend comp., typ. val.)	77.2	72.6	
Wheeler 2009	12	B (Alkylate)	Refinery	94.8	93.7	5	88.7	1.1	0.3	4.9	vol DHA	0.698	R	114	E (typ. value)	90.0	89.9	
Wheeler 2009	12	B77D23	Refinery	91.4	85.9	12.4	73.5	5.5	0.6	8	vol DHA	0.7128	R	106	E (blend comp., typ. val.)	82.0	81.7	
API 2010	13	839056	M-Gas									0.7477	R	100	E	92.2	81.9	
API 2010	13	839061	M-Gas									0.7196	R	100	E	93.2	88.5	
API 2010	13	839062	M-Gas									0.7516	R	100	E	92.5	87.5	
API 2010	13	839064	M-Gas									0.7599	R	100	E	98.8	82.9	
API 2010	13	839058	M-Gas									0.7509	R	100	E	92.0	82.8	
API 2010	13	839066	M-Gas									0.7441	R	100	E	94.4	86.7	
API 2010	13	839067	M-Gas									0.7439	R	100	E	89.0	81.5	
API 2010	13	839070	M-Gas									0.7579	R	100	E	94.5	83.9	
API 2010	13	839071	M-Gas									0.7386	R	100	E	91.4	82.1	

API 2010	13	839074	M-Gas									0.7367	R	100	E	97.0	91.3	
API 2010	13	865535	M-Gas									0.7368	R	100	E	91.5	82.3	
API 2010	13	856595	M-Gas									0.7228	R	100	E	89.3	83.3	
API 2010	13	856613	BOB									0.6903	R	100	E	92.9	88.9	
API 2010	13	859062	BOB									0.7195	R	100	E	86.9	81.3	
API 2010	13	839043	BOB									0.7052	R	100	E	93.9	88.1	
API 2010	13	831491	BOB									0.7289	R	100	E	84.0	80.3	
API 2010	13	836035	BOB									0.7453	R	100	E	89.0	83.0	
API 2010	13	838796	BOB									0.7366	R	100	E	87.2	80.6	
API 2010	13	844187	BOB									0.7694	R	100	E	98.1	86.4	
API 2010	13	844188	BOB									0.7612	R	100	E	97.9	86.0	
API 2010	13	844189	BOB									0.7314	R	100	E	88.2	80.4	
Moore 2011	14	E0*	M-Gas									0.686	R	111.1	R	90.8	83.2	
Christensen 2011	15	BOB1	BOB	72.2					8	19.8	wt D1319	0.7242	R	100	E	86.8	80.7	
Christensen 2011	15	BOB2	BOB	76.2					4.6	19.2	wt D1319	0.7374	R	100	E	85.4	80.7	
Christensen 2011	15	BOB3	BOB	67.7					2.5	29.8	wt D1319	0.7335	R	100	E	96.5	87.3	
Anderson 2012	16	B82E0	Res.	69.77	65.61	28.4	37.21	4.16	5.56	24.67	vol DHA	0.724	R	96.6	R	81.7	76.5	
Anderson 2012	16	B88E0	Res.	68.46	63.59	21.21	42.38	4.87	5.84	25.7	vol DHA	0.727	R	97	R	88.2	81.7	
Anderson 2012	16	B92E0	Res.	68.18	64.26	15.92	48.34	3.92	5.81	26.01	vol DHA	0.728	R	98.1	R	92.2	84.7	
Anderson 2012	16	B95E0	Res.	60.43	57.18	13.71	43.47	3.25	6.19	33.39	vol DHA	0.743	R	100.6	R	95.4	86.4	
Anderson 2012	16	B97E0	Res.	58.85	56.4	11.08	45.32	2.45	5.3	35.85	vol DHA	0.747	R	101.6	R	97.4	87.9	
Storey 2012	17	US cert	M-gas							45	mass D5580	0.746	R	100	E	97.1	88.3	
Szybist 2013	18	UTG-96	M-gas	68					2.4	29.6	vol D1319	0.739	R	100	E	96.1	88.2	
Szybist 2013	18	LSRG	Refinery	95.2					3.3	1.4	vol D1319	0.658	R	81	E (blend comp. and prop.)	64.7	62.4	
Foong 2014	19	Gasoline	M-gas	60.4	48.9	13.7	35.3	11.4	8	31.7	vol D6730	0.73	E	100	E	91.5	82.1	
CRC 2014	20	FACE A	Res.	99.25	97.64	11.65	85.99	1.61	0.21	0.38	vol DHA	0.6805	R	100.8	E (Fig. 3.10)	83.9	83.5	
CRC 2014	20	FACE B	Res.	95.01	94.87	7.99	86.88	0.14	0.02	5.84	vol DHA	0.697	R	103.5	E (Fig. 3.10)	95.8	92.4	
CRC 2014	20	FACE C	Res.	94.52	94.16	24.43	69.73	0.36	1.27	3.92	vol DHA	0.691	R	100.3	E (Fig. 3.10)	84.3	83.0	
CRC 2014	20	FACE H	Res.	55.8	45.3	22.49	22.81	10.5	6.82	35.76	vol DHA	0.759	R	98.0	E (Fig. 3.10)	86.9	79.6	
Alleman 2015	21	CARBOB-prem	BOB	69.6	55.7	7	48.7	13.9	9.86	18.7	wt D6729	0.7434	R (pers. comm.)	99.8	R (pers. comm.)	86.8	80.7	(pers. comm.)
Alleman 2015	21	Nat Gas A	NG	95.4	80.6	37.7	42.9	14.8	0.712	3.72	wt D6729	0.6738	R	80.2	R (pers. comm.)	70.8	68.9	
Alleman 2015	21	Nat Gas D	NG	97.2	84.8	39.1	45.7	12.4	0.584	2.19	wt D6729	0.665	R	78.9	R (pers. comm.)	71.4	69.3	
Chupka 2015	22	WCBOB	BOB	70.4	65.69	9.59	56.1	4.71	3.6	25.8	vol D6729	0.7242	R	96.3	R	93.7	87.3	
Chupka 2015	22	CARBOB-reg	BOB	74.25	61.25	7.65	53.6	13	8.09	15.6	vol D6729	0.7318	R	100.5	R	84.8	80.8	
Chupka 2015	22	sCBOB	BOB	67.2	59.4	11.5	47.9	7.8	8.4	23.7	vol D6729	0.7374	R	95.9	R	87.9	81.9	
Rankovic 2015	23	RON91	M-gas	61.1	46.1	7.7	38.4	15	4.7	34.1	mass D6733	0.745	R	94.1	R	91.0	82.0	(OS=8-10, pers. comm.)
Rankovic 2015	23	RON71	Res.	76.6	54.6	15.4	39.2	22	2.1	21.3	mass D6733	0.738	R	99.3	R	71.0	69.0	
Waqas 2016	24	FACE I	Res.	92.23	88.93	14.39	74.54	3.3	6.35	1.15	vol DHA	0.697	R	98.3	E (CRC 2014, Fig. 3.10)	70.9	69.6	(CRC 2014, Table A.1)
Waqas 2016	24	FACE J	Res.	67.57	65.28	31.64	33.64	2.29	0.6	31.69	vol DHA	0.742	R	102.3	E (CRC 2014, Fig. 3.10)	72.7	69.5	(CRC 2014, Table A.1)
Waqas 2016	24	FACE A	Res.	99.25	97.64	11.65	85.99	1.61	0.21	0.38	vol DHA	0.681	R	100.8	E (CRC 2014, Fig. 3.10)	83.8	83.5	(CRC 2014, Table A.1)
Badra 2017	25	FACE A	Res.	99.25	97.64	11.65	85.99	1.61	0.21	0.38	vol DHA	0.681	R	100.8	E (CRC 2014, Fig. 3.10)	83.6	82.9	
Badra 2017	25	FACE C	Res.	94.52	94.16	24.43	69.73	0.36	1.27	3.92	vol DHA	0.691	R	100.3	E (CRC 2014, Fig. 3.10)	84.4	83.0	
Badra 2017	25	FACE F	Res.	82.94	71.96	4.4	67.56	10.98	9.42	7.72	vol DHA	0.707	R	97.8	E (CRC 2014, Fig. 3.10)	94.2	87.4	
Badra 2017	25	FACE G	Res.	56.68	45.16	6.73	38.43	11.52	8.11	33.63	vol DHA	0.76	R	101.9	E (CRC 2014, Fig. 3.10)	96.4	84.9	
Badra 2017	25	FACE I	Res.	92.23	88.93	14.39	74.54	3.3	6.35	1.15	vol DHA	0.697	R	98.3	E (CRC 2014, Fig. 3.10)	69.5	69.0	
Badra 2017	25	FACE J	Res.	67.57	65.28	31.64	33.64	2.29	0.6	31.69	vol DHA	0.742	R	102.3	E (CRC 2014, Fig. 3.10)	71.8	66.9	
Anderson 2019	26	B87bE0	Res.	73.4					4.47	22.14	vol D1319	0.734	R	100	E	86.8	79.0	
Anderson 2019	26	B95bE0	Res.	59.2					3.25	37.51	vol D1319	0.753	R	100	E	95.4	85.1	

Table S2. Base fuel and blend octane rating data set. Excluded RON values are indicated (based on evaluation discussed in section SI-9).

First Author, Year	Base fuel ID	Ethanol (vol %)	Octane Ratings RON exclude?	MON
Brinkman 1975	P	0	96.0	85
Brinkman 1975	P	10	99.0	86.6
Keller 1979	Fuel 10	0	90.9	82.5
Keller 1979	Fuel 10	10	95.1	84.5
Keller 1979	Fuel 11	0	90.6	83.5
Keller 1979	Fuel 11	10	94.5	84.7
Keller 1979	Fuel 12	0	92.0	84
Keller 1979	Fuel 12	10	96.4	86.8
Keller 1979	Fuel 13	0	92.7	83.4
Keller 1979	Fuel 13	10	96.3	86.1
Keller 1979	Fuel 14	0	92.0	82.4
Keller 1979	Fuel 14	10	96.3	85.0
Marceglia 1982	Gasoline	0	94.3	84.3
Marceglia 1982	Gasoline	10	97.2	85.5
Kisenyi 1994	Gasoline	0	98.8	87.3
Kisenyi 1994	Gasoline	5.2	99.5	87.0
Reynolds 2002	Alkylate	0	96.5	93.5
Reynolds 2002	Alkylate	10	101.9	94.3
Reynolds 2002	LSR-A	0	72.3	70
Reynolds 2002	LSR-A	10	80.4	77.1
Reynolds 2002	LSR-B	0	69.8	67.8
Reynolds 2002	LSR-B	10	77.6	74.8
Reynolds 2002	CC-A	0	60.7	59.5
Reynolds 2002	CC-A	10	70.6	68.4
Reynolds 2002	CC-B	0	87.6	78.9
Reynolds 2002	CC-B	10	91.7	80.9
Reynolds 2002	Reformate A	0	94.0	83.2
Reynolds 2002	Reformate A	10	96.9	85.4
Reynolds 2002	Reformate B	0	84.1	76.8
Reynolds 2002	Reformate B	10	89.5	80.6
daSilva 2005	A	0	98.0	89.5
daSilva 2005	A	5	99.8	91.1

daSilva 2005	A	10	101.3	91.8
daSilva 2005	A	15	102.4	92.3
daSilva 2005	A	20	103.4	93.1
daSilva 2005	A	25	103.8	93.4
daSilva 2005	B	0	81.7	79.5
daSilva 2005	B	5	86	84
daSilva 2005	B	10	89.4	86.2
daSilva 2005	B	15	93.3	87.8
daSilva 2005	B	20	96.4	89.2
daSilva 2005	B	25	99.1	89.7
Yucesu 2006	Gasoline	0	98.8	86.4
Yucesu 2006	Gasoline	10	99.9	87.4
Yucesu 2006	Gasoline	20	101.6	89.8
Yucesu 2006	Gasoline	40	~~101.7~~ Y	90.9
Yucesu 2006	Gasoline	60	~~102.8~~ Y	92.7
Nakata 2007	A	0	91.5	83
Nakata 2007	A	10	94.4	84.9
Nakata 2007	B	0	99.6	87.1
Nakata 2007	B	10	100.9	87.6
Nakata 2007	D	0	96.4	85.3
Nakata 2007	D	10	99.7	87.2
Nakata 2007	E	0	91.3	80.3
Nakata 2007	E	10	94.3	82.3
Martini 2007	A, EU	0	98.4	86.1
Martini 2007	A, EU	4.7	99	86.5
Martini 2007	A, EU	9.7	100	86.7
Martini 2007	B, Artic	0	97.8	86.1
Martini 2007	B, Artic	5.1	99	86.3
Martini 2007	B, Artic	10.2	99.9	86.7
Karonis 2008	I	0	92.5	84.2
Karonis 2008	I	1	92.7	84.4
Karonis 2008	I	2	92.9	84.6
Karonis 2008	I	3	93.3	84.6
Karonis 2008	I	4	93.6	84.9
Karonis 2008	I	5	93.8	85.0
Karonis 2008	I	6	94.1	85.0
Karonis 2008	II	0	94.0	84.1
Karonis 2008	II	1	94.2	84.3
Karonis 2008	II	2	94.4	84.5
Karonis 2008	II	3	94.7	84.7
Karonis 2008	II	4	95.1	84.8
Karonis 2008	II	5	95.3	84.9
Karonis 2008	II	6	95.6	84.9
Milpied 2009	I	0	95.5	85
Milpied 2009	I	21.2	100.5	87.6

Milpied 2009	J	0	98.1	87.8
Milpied 2009	J	10.7	100.0	88
Milpied 2009	G	0	91.6	81.6
Milpied 2009	G	30.5	100.5	87.1
Wheeler 2009	A79D21	0	83.4	76.5
Wheeler 2009	A79D21	10.8	88.5	80.4
Wheeler 2009	A79D21	21.6	94.7	83.4
Wheeler 2009	A79D21	34.8	99.1	86.9
Wheeler 2009	C50D50	0	77.2	72.6
Wheeler 2009	C50D50	15.6	87.3	78.8
Wheeler 2009	C50D50	30.2	94.6	82.5
Wheeler 2009	B (Alkylate)	0	90.0	89.9
Wheeler 2009	B (Alkylate)	15.7	100.4	92.7
Wheeler 2009	B (Alkylate)	29.7	105.9	94
Wheeler 2009	B77D23	0	82.0	81.7
Wheeler 2009	B77D23	15.7	94.2	88.5
Wheeler 2009	B77D23	29.4	101.2	90.8
API 2010	839056	0	92.2	81.9
API 2010	839056	10.1	95.2	83.9
API 2010	839056	12.7	96.4	84.3
API 2010	839056	15.3	96.9	84.7
API 2010	839056	20.3	98.2	85.3
API 2010	839056	31.5	~~100.0~~ Y	87.3
API 2010	839061	0	93.2	88.5
API 2010	839061	9.7	98.4	90.7
API 2010	839061	12.3	99.7	90.8
API 2010	839061	15.0	100.4	91.2
API 2010	839061	20.6	101.4	91.6
API 2010	839061	31.0	~~101.8~~ Y	91.1
API 2010	839062	0	92.5	87.5
API 2010	839062	9.9	95.9	88.8
API 2010	839062	12.9	96.7	88.6
API 2010	839062	15.4	96.6	89
API 2010	839062	20.7	98.6	88.8
API 2010	839062	31.8	~~100.5~~ Y	89.4
API 2010	839064	0	98.8	82.9
API 2010	839064	9.9	100.7	84.6
API 2010	839064	12.6	101.1	85.1
API 2010	839064	15.5	101.4	85.1
API 2010	839064	20.2	101.5	85.7
API 2010	839064	30.0	~~101.8~~ Y	88.1
API 2010	839058	0	92.0	82.8
API 2010	839058	10.3	95.6	84.2
API 2010	839058	12.8	96.4	84.7
API 2010	839058	15.5	97.2	85.4

API 2010	839058	20.5	98.4	87.1
API 2010	839058	31.3	~~100~~ Y	87.7
API 2010	839066	0	94.4	86.7
API 2010	839066	10.2	98.4	89.1
API 2010	839066	12.7	99	89.5
API 2010	839066	15.2	99.6	89.4
API 2010	839066	20.8	101	90.2
API 2010	839066	31.5	~~101.8~~ Y	90.4
API 2010	839067	0	89.0	81.5
API 2010	839067	10.2	93.4	83.8
API 2010	839067	12.7	94.7	84.2
API 2010	839067	15.2	95.7	84.6
API 2010	839067	20.8	97.3	85.6
API 2010	839067	31.5	~~99.9~~ Y	88.1
API 2010	839070	0	94.5	83.9
API 2010	839070	10.2	97.7	86.6
API 2010	839070	12.7	98.3	86.6
API 2010	839070	15.2	98.9	86.8
API 2010	839070	20.8	99.6	87.1
API 2010	839070	31.5	~~101.4~~ Y	88.7
API 2010	839071	0	91.4	82.1
API 2010	839071	9.8	95.6	84.4
API 2010	839071	12.7	96.2	84.8
API 2010	839071	15.4	96.8	85.2
API 2010	839071	20.1	98.3	85.7
API 2010	839071	30.2	~~100.2~~ Y	87.2
API 2010	839074	0	97	91.3
API 2010	839074	10.4	100.7	91
API 2010	839074	13.1	101.4	91.8
API 2010	839074	16.1	102	92.1
API 2010	839074	20.8	101.9	92.3
API 2010	839074	32.1	~~102.1~~ Y	91.8
API 2010	865535	0	91.5	82.3
API 2010	865535	9.9	95.3	85.3
API 2010	865535	12.3	96.3	85.3
API 2010	865535	14.7	97	85.5
API 2010	865535	19.6	98	86.3
API 2010	865535	30.7	~~99.8~~Y	87.8
API 2010	856595	0	89.3	83.3
API 2010	856595	10.5	95.3	87.2
API 2010	856595	12.6	96.4	87.5
API 2010	856595	15.0	97.4	88.1
API 2010	856595	20.0	99.1	88.5
API 2010	856595	29.6	101.6	89.5
API 2010	856613	0	92.9	88.9
API 2010	856613	12.5	99.5	90.9
API 2010	856613	13.3	99.6	91.1
API 2010	856613	15.5	100.5	91.1

API 2010	856613	20.2	101.7	91.2
API 2010	856613	30.7	~~101.8~~Y	91.2
API 2010	859062	0	86.9	81.3
API 2010	859062	10.3	91.9	82.5
API 2010	859062	12.6	93	83.2
API 2010	859062	15.3	94.2	84.4
API 2010	859062	20.8	96.1	85.9
API 2010	859062	30.8	~~98.9~~Y	87
API 2010	839043	0	93.9	88.1
API 2010	839043	10.6	98.6	90.2
API 2010	839043	12.7	99.4	90.3
API 2010	839043	15.4	100.4	90.8
API 2010	839043	20.2	101.7	91
API 2010	839043	25.8	102.2	91.3
API 2010	831491	0	84	80.3
API 2010	831491	9.9	90.9	83.8
API 2010	831491	12.7	91.9	84.4
API 2010	831491	15.1	93	86.9
API 2010	831491	19.5	95.9	87.7
API 2010	831491	29.3	99.9	89
API 2010	836035	0	89	83
API 2010	836035	9.9	94.4	85.5
API 2010	836035	12.9	95.2	87.2
API 2010	836035	15.1	96.6	87.4
API 2010	836035	20.3	98.5	88.5
API 2010	836035	31.1	~~100.9~~ Y	89.5
API 2010	838796	0	87.2	80.6
API 2010	838796	10.4	92.5	83.5
API 2010	838796	12.9	93.6	83.9
API 2010	838796	15.5	94.9	84.4
API 2010	838796	21.0	97.4	85.3
API 2010	838796	25.3	99.6	88.2
API 2010	844187	0	98.1	86.4
API 2010	844187	9.6	99.9	87.6
API 2010	844187	12.1	100.6	88.3
API 2010	844187	14.5	101	88.4
API 2010	844187	19.9	101.7	88.9
API 2010	844187	32.6	~~101.6~~ Y	89.5
API 2010	844188	0	97.9	86
API 2010	844188	10.2	99.1	86.9
API 2010	844188	13.1	99.6	88
API 2010	844188	16.3	100	88.3
API 2010	844188	19.6	100.8	88.3
API 2010	844188	32.9	~~101.6~~ Y	88.1
API 2010	844189	0	88.2	80.4
API 2010	844189	9.6	92.9	83
API 2010	844189	11.8	93.7	83.3
API 2010	844189	14.1	94.7	83.8

API 2010	844189	19.0	96.6	84.6
API 2010	844189	31.3	~~99.3~~ Y	87.9
Moore 2011	E0*	0	90.8	83.2
Moore 2011	E0*	10.46	95.6	n/a
Moore 2011	E0*	21	99.7	n/a
Moore 2011	E0*	49.7	104	n/a
Moore 2011	E0*	82.2	106	n/a
Christensen 2011	BOB1	0	86.8	80.7
Christensen 2011	BOB1	9.9	91.6	83.4
Christensen 2011	BOB2	0	85.4	80.7
Christensen 2011	BOB2	9.7	90.9	83.6
Christensen 2011	BOB3	0	96.5	87.3
Christensen 2011	BOB3	9.9	99.5	88.8
Anderson 2012	B82E0	0	81.7	76.5
Anderson 2012	B82E0	9.9	88.25	80.95
Anderson 2012	B82E0	20.0	93.75	85
Anderson 2012	B82E0	29.9	98.05	87.2
Anderson 2012	B82E0	50.2	103.5	88.95
Anderson 2012	B82E0	76.8	106.8	90.05
Anderson 2012	B82E0	100	108.7	90.6
Anderson 2012	B88E0	0	88.15	81.7
Anderson 2012	B88E0	10.5	93.1	85.25
Anderson 2012	B88E0	19.2	97.25	87.25
Anderson 2012	B88E0	29.9	100.75	88.35
Anderson 2012	B88E0	50.7	104.65	89.85
Anderson 2012	B88E0	74.7	107.7	90.45
Anderson 2012	B88E0	100	108.7	90.6
Anderson 2012	B92E0	0	92.15	84.7
Anderson 2012	B92E0	10.0	96.1	86.7
Anderson 2012	B92E0	19.8	99.7	88.25
Anderson 2012	B92E0	29.1	102.2	88.95
Anderson 2012	B92E0	51.4	105.55	90.7
Anderson 2012	B92E0	75.0	108.05	91.05
Anderson 2012	B92E0	100	108.7	90.6
Anderson 2012	B95E0	0	95.35	86.35
Anderson 2012	B95E0	9.7	98.9	87.7
Anderson 2012	B95E0	20.0	101.25	89.15
Anderson 2012	B95E0	30.0	103.5	89.8
Anderson 2012	B95E0	51.5	105.95	90.8
Anderson 2012	B95E0	74.9	108	91.2
Anderson 2012	B95E0	100	108.7	90.6
Anderson 2012	B97E0	0	97.4	87.9
Anderson 2012	B97E0	19.8	102.65	89.85
Anderson 2012	B97E0	100	108.7	90.6
Storey 2012	US cert	0	97.1	88.3
Storey 2012	US cert	9.1	100	89.7

Storey 2012	US cert	19.8	101.2	90.2
Szybist 2013	UTG-96	0	96.1	88.2
Szybist 2013	UTG-96	52.3	104.4	90.5
Szybist 2013	LSRG	0	64.7	62.4
Szybist 2013	LSRG	52.2	102	88
Szybist 2013	LSRG	68.9	104.1	88.9
Foong 2014	Gasoline	0	91.5	82.1
Foong 2014	Gasoline	10.0	95.2	84.2
Foong 2014	Gasoline	20.0	98.3	85.5
Foong 2014	Gasoline	40.0	102.1	87.7
Foong 2014	Gasoline	60.0	104.6	89
Foong 2014	Gasoline	80.0	106.4	90.2
Foong 2014	Gasoline	100	108	90.7
CRC 2014	FACE A	0	83.9	83.5
CRC 2014	FACE A	10.1	92	87.9
CRC 2014	FACE A	14.7	94.8	89.4
CRC 2014	FACE A	29.9	102.3	91.4
CRC 2014	FACE B	0	95.8	92.4
CRC 2014	FACE B	10.0	101.1	93.5
CRC 2014	FACE B	14.7	103	93.5
CRC 2014	FACE B	30.2	106	93.3
CRC 2014	FACE C	0	84.3	83
CRC 2014	FACE C	10.2	91.7	87.5
CRC 2014	FACE C	14.6	94.8	88.8
CRC 2014	FACE C	29.5	101.5	91.6
CRC 2014	FACE H	0	86.9	79.6
CRC 2014	FACE H	10.2	92.1	82.2
CRC 2014	FACE H	14.6	94.1	83.3
CRC 2014	FACE H	30.3	99.4	87
Alleman 2015	CARBOB-prem	0	86.8	80.7
Alleman 2015	CARBOB-prem	9.7	91.1	84.3
Alleman 2015	CARBOB-prem	19.8	96.4	85.9
Alleman 2015	CARBOB-prem	24.7	98.1	86.3
Alleman 2015	CARBOB-prem	29.4	99.7	88.7
Alleman 2015	CARBOB-prem	38.9	102.4	89.7
Alleman 2015	CARBOB-prem	48.2	103.6	90.1
Alleman 2015	Nat Gas A	0	70.8	68.9
Alleman 2015	Nat Gas A	30	94.3	86.5
Alleman 2015	Nat Gas A	40	98.8	87.7
Alleman 2015	Nat Gas A	54	102.9	n/a
Alleman 2015	Nat Gas A	65	104.4	n/a
Alleman 2015	Nat Gas D	0	71.4	69.3
Alleman 2015	Nat Gas D	40	99.4	88.3
Alleman 2015	Nat Gas D	57	103	n/a
Chupka 2015	WCBOB	0	93.7	87.3

Chupka 2015	WCBOB	11.1	98.1	87.8
Chupka 2015	WCBOB	20.9	101.6	88.6
Chupka 2015	WCBOB	26.3	102.5	89.4
Chupka 2015	WCBOB	30.6	103.2	89.5
Chupka 2015	WCBOB	45.2	104.8	89.7
Chupka 2015	WCBOB	50.3	105.5	89.7
Chupka 2015	CARBOB-reg	0	84.8	80.8
Chupka 2015	CARBOB-reg	10.2	91.1	84.3
Chupka 2015	CARBOB-reg	18.6	96.4	85.9
Chupka 2015	CARBOB-reg	25.3	98.1	86.3
Chupka 2015	CARBOB-reg	31.9	99.7	88.7
Chupka 2015	CARBOB-reg	40.7	102.4	89.7
Chupka 2015	CARBOB-reg	51.1	103.6	90.1
Chupka 2015	sCBOB	0	87.9	81.9
Chupka 2015	sCBOB	9.3	93	84.1
Chupka 2015	sCBOB	26	99.1	87.4
Chupka 2015	sCBOB	47.1	102.6	88.7
Rankovic 2015	RON91	0	91	82
Rankovic 2015	RON91	10	95	n/a
Rankovic 2015	RON91	20	99	n/a
Rankovic 2015	RON91	40	103	n/a
Rankovic 2015	RON91	60	105	n/a
Rankovic 2015	RON91	80	108	n/a
Rankovic 2015	RON91	100	108	n/a
Rankovic 2015	RON71	0	71	69.0
Rankovic 2015	RON71	10	81	76.0
Rankovic 2015	RON71	20	88	80.7
Rankovic 2015	RON71	30	94	84.2
Rankovic 2015	RON71	40	99	86.2
Rankovic 2015	RON71	60	104	88.6
Rankovic 2015	RON71	80	107	89.7
Rankovic 2015	RON71	100	108	90.1
Waqas 2016	FACE I	0	70.9	69.6
Waqas 2016	FACE I	2	72.8	n/a
Waqas 2016	FACE I	5	76.3	n/a
Waqas 2016	FACE I	10	81.1	n/a
Waqas 2016	FACE I	15	85.8	n/a
Waqas 2016	FACE I	20	90.7	n/a
Waqas 2016	FACE J	0	72.7	69.5
Waqas 2016	FACE J	2	74.2	n/a
Waqas 2016	FACE J	5	76.2	n/a
Waqas 2016	FACE J	10	80.1	n/a
Waqas 2016	FACE J	15	84.7	n/a
Waqas 2016	FACE J	20	89.4	n/a
Waqas 2016	FACE A	0	83.8	83.5
Waqas 2016	FACE A	2	86.1	n/a
Waqas 2016	FACE A	5	88.6	n/a
Waqas 2016	FACE A	10	93.2	n/a
Waqas 2016	FACE A	15	96.7	n/a

Waqas 2016	FACE A	20	98.4	n/a
Badra 2017	FACE A	0	83.6	82.9
Badra 2017	FACE A	10	92	88
Badra 2017	FACE A	25	100.7	90.6
Badra 2017	FACE A	40	104.1	91.7
Badra 2017	FACE A	60	106	91.3
Badra 2017	FACE C	0	84.4	83
Badra 2017	FACE C	10	92.2	87.1
Badra 2017	FACE C	25	100.3	90.5
Badra 2017	FACE C	40	104.1	91
Badra 2017	FACE C	60	105.8	91.3
Badra 2017	FACE F	0	94.2	87.4
Badra 2017	FACE F	10	98.9	88.5
Badra 2017	FACE F	25	103.2	89.5
Badra 2017	FACE F	40	104.7	90.3
Badra 2017	FACE F	60	105.7	90.5
Badra 2017	FACE G	0	96.4	84.9
Badra 2017	FACE G	10	98.8	86.1
Badra 2017	FACE G	25	102.4	87.9
Badra 2017	FACE G	40	103	88.5
Badra 2017	FACE G	60	105	88.9
Badra 2017	FACE I	0	69.5	69
Badra 2017	FACE I	10	79.9	78
Badra 2017	FACE I	25	92.6	85.3
Badra 2017	FACE I	40	100.4	88.3
Badra 2017	FACE I	60	104.1	89.7
Badra 2017	FACE J	0	71.8	66.9
Badra 2017	FACE J	10	79	73.6
Badra 2017	FACE J	25	89.8	81.7
Badra 2017	FACE J	40	98	85.9
Badra 2017	FACE J	60	103.6	88.2
Anderson 2019	B87bE0	0	86.8	79
Anderson 2019	B87bE0	14.6	95.2	85
Anderson 2019	B87bE0	29.1	99.7	88.1
Anderson 2019	B87bE0	47.4	103.7	90.4
Anderson 2019	B87bE0	100	108.6	91.4
Anderson 2019	B95bE0	0	95.4	85.1
Anderson 2019	B95bE0	15	99.7	88.4
Anderson 2019	B95bE0	29	102.7	89.7
Anderson 2019	B95bE0	48	105.9	91.5
Anderson 2019	B95bE0	100	108.6	91.4

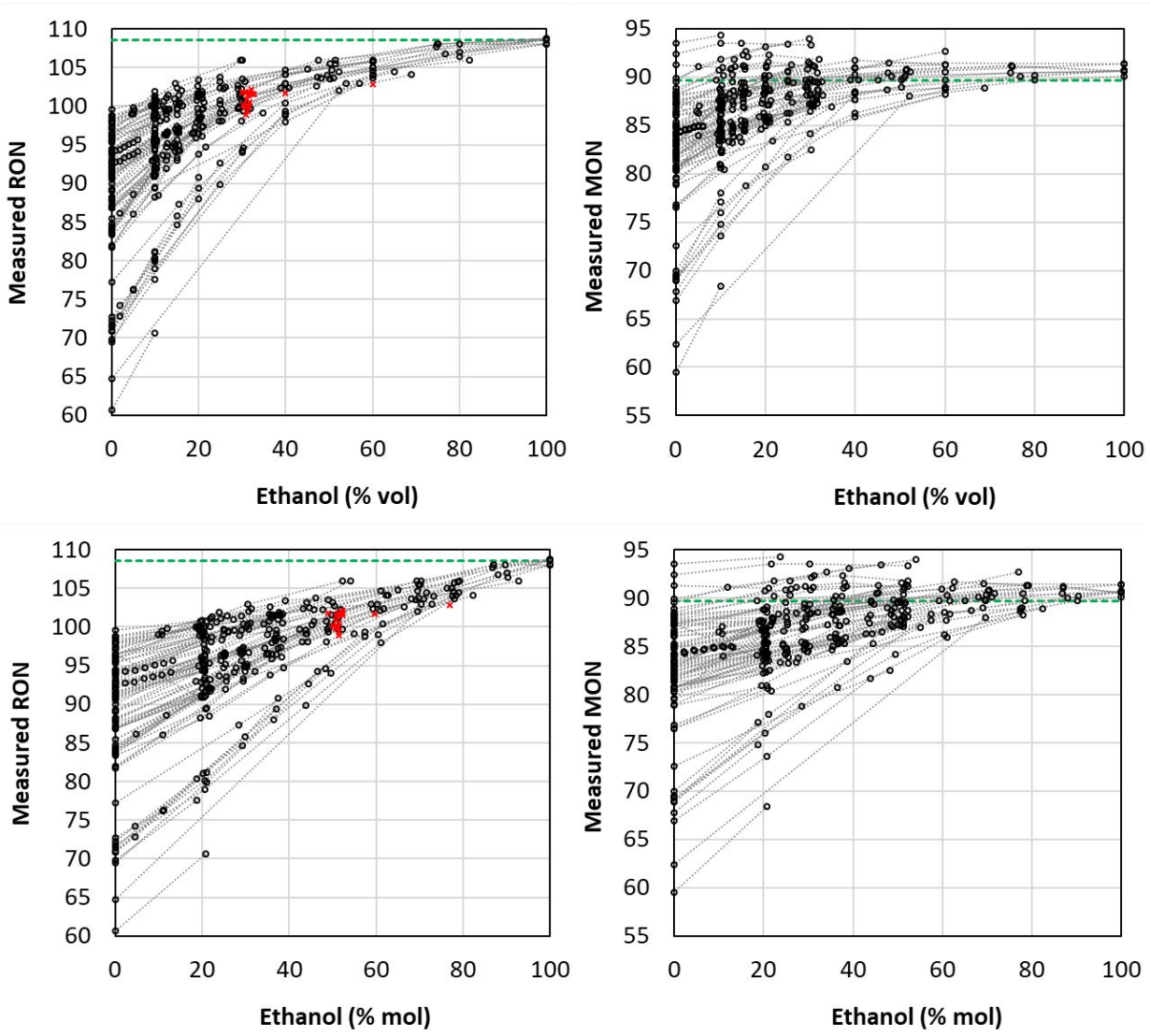

Figure S2. RON and MON of ethanol blends (280 RON values, 272 MON values) made from 88 different complex base fuels, as a function of ethanol content. Data plotted versus ethanol volumetric content (upper plots) and molar content (lower plots). Dashed green lines indicate octane ratings of neat ethanol. Dashed grey lines connect blends from a single base fuel. Red symbols indicate 19 RON values excluded from the analysis based on the discussion in section SI-8.

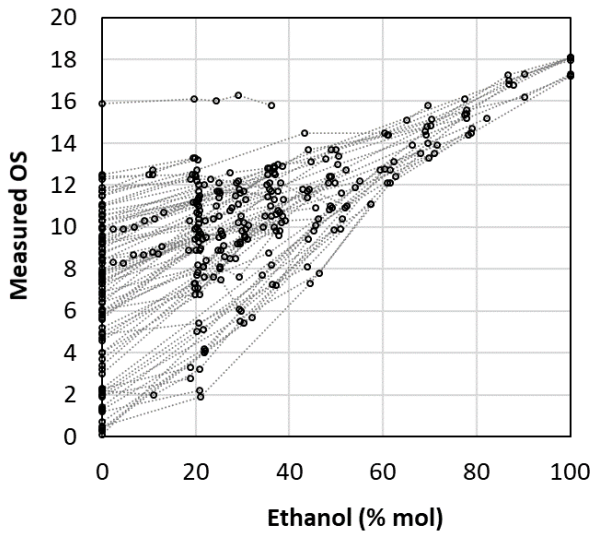

Figure S3. OS of base fuels and ethanol blends made from 88 different complex base fuels, as a function of ethanol content. Dashed grey lines connect blends from a single base fuel.

SI-8. Base fuel density and molecular weight and molar ethanol concentrations

To convert ethanol concentrations from volumetric terms to molar terms, the liquid molar volume of each base gasoline is required. Molar volume is calculated as the ratio of molecular weight and density (M_g/ρ_g). While the density of the base gasoline is commonly reported in most (but not all) studies, the molecular weight has typically not been reported as this requires a detailed hydrocarbon analysis (DHA) obtained by gas chromatography.

Figure S4 shows the densities of the various base gasolines used in this study for which density values were reported, generally at 15-25 °C but often unreported. Densities reported by Milpied et al.[11] were unrealistically low (specific gravities all between 0.53 and 0.61 kg/L at 15 °C) and were not used. The averages for the reported densities were 0.74, 0.73 and 0.72 kg/L for the market gasolines (n = 26), market BOBs (n = 16) and research gasolines (n = 24), respectively, but these values were not significantly different at a 95% confidence level. The average density for two natural gasolines was 0.67 kg/L (n = 2). Different refinery streams have widely varying composition and cuts, and therefore density. Reformate is high in aromatic hydrocarbon content and has a correspondingly high density, e.g. 0.70-0.88 kg/L.[29, 30] Alkylate is comprised of mostly iso-paraffins with lower density, e.g., 0.69-0.76 kg/L. [12, 29, 30] Catalytically-cracked gasoline contains aromatics, olefins and saturates and has intermediate density, e.g., 0.73-0.77 kg/L.[29, 30] Light straight run gasoline contains mostly saturates and its density can vary widely, e.g., 0.66-0.78 kg/L. .[18, 29, 30]

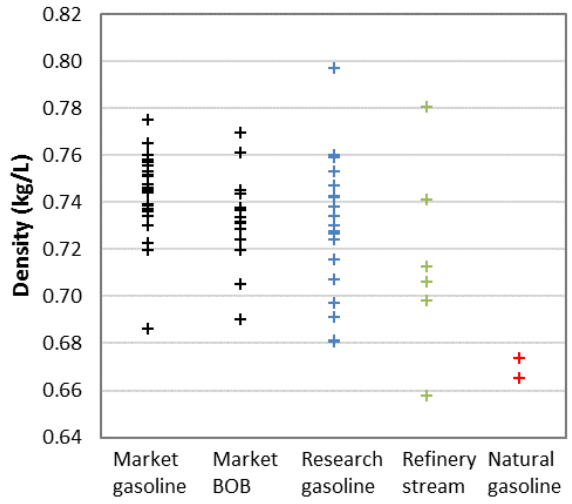

Figure S4. Densities of base fuels included in the study

Figure S5 shows a plot of reported molecular weights of base gasolines plotted versus density for which molecular weights were reported or could be calculated based on the reported DHAs. The averages for the reported molecular weights were 104, 98 and 100 g/mol for the market gasolines (n = 4), market BOBs (n = 4) and research gasolines (n = 19), respectively, but the differences were not statistically significant. The average molecular weight for natural gasolines was 80 g/mol (n = 2). In general, this analysis showed no discernable correlation between molecular weight and density, so molecular weight could not be estimated from density for those cases where only density was reported.

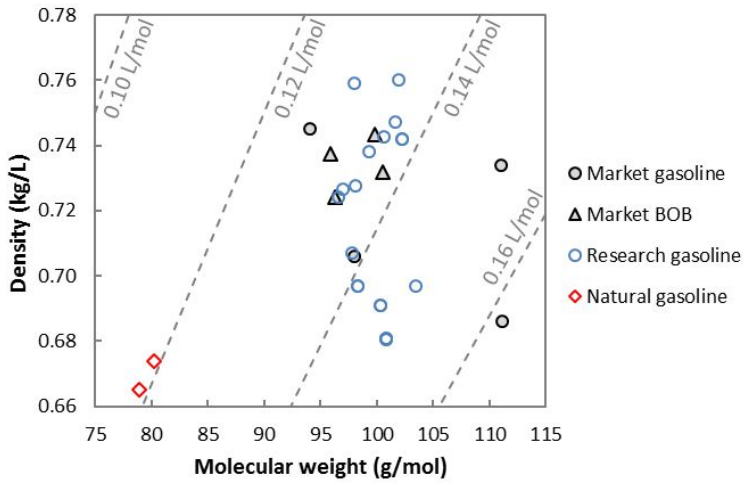

Figure S5. Molecular weight versus density for base gasolines included in the study. Fuels shown are only those for which both density and molecular weight were reported. Lines of constant molar volume are shown as dashed lines.

To obtain a better estimate of average density of U.S. market gasolines and BOBs, data from the Alliance of Automotive Manufacturers North American Fuel Survey was analyzed for two calendar years, 2008-2009 and 2016-2017.[31, 32] The year 2008 was selected as it occurred while ethanol blending was still increasing in the U.S. and significant volumes of E0 clear gasoline were still available. This year was also after MTBE use had been phased out.[33] Figure S6 shows the average density delineated by year, season (summer, winter), premium or regular grade (as labelled at pump), and by ethanol blending (E7-E10 BOBs or E0 gasoline). The densities of the BOBs were calculated from the reported density of the ethanol-containing fuel (primarily E10) after accounting for the density contribution of the reported ethanol content. Most of the data were for BOBs, while fewer data were available for clear gasoline, with the majority in winter 2008. As a result, confidence intervals (95%) are narrower for the BOBs as compared to E0 gasoline.

Densities of both BOBs and clear (E0) gasolines were greater in summer than in winter, presumably related to the use of light hydrocarbons in winter that cannot be used in summer due to RVP limits. Except for US summer grade BOBs (for which premium grade density was slightly less than regular grade), no statistically significant difference was found between regular and premium grade BOBs.

Pooling the data for regular and premium grades, the average U.S. BOB densities were 0.737 kg/L for summer (n = 412) and 0.720 kg/L for winter (n = 388). The annual average is therefore 0.729 kg/L for U.S. BOBs.

Fewer data were available for clear (E0) gasoline. Again pooling grades, the average U.S. clear gasoline densities were 0.738 kg/L for summer (n = 16) and 0.725 kg/L for winter (n = 19). The annual average is therefore 0.733 kg/L for U.S. clear gasoline. These were not significantly different from the U.S. BOB densities or from the clear gasoline samples from Canada (n = 42) and Mexico (n = 27).

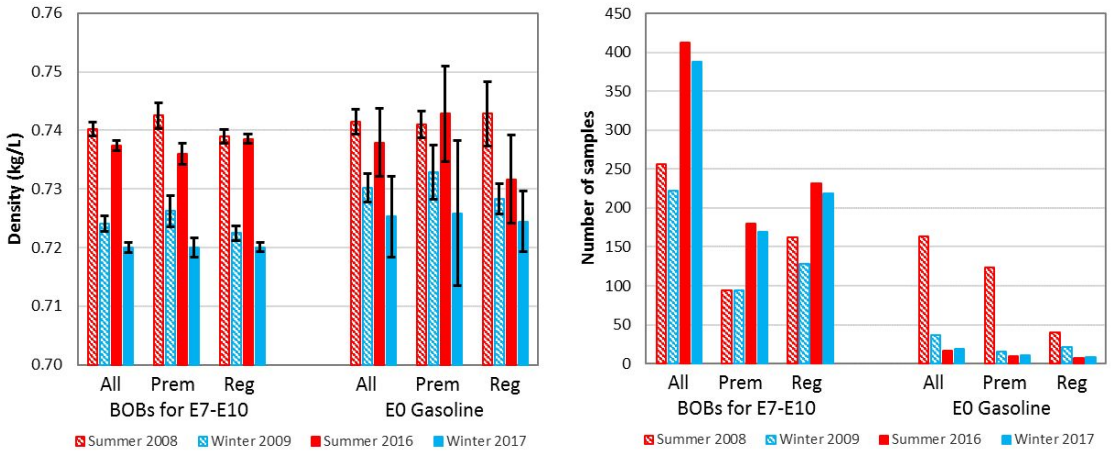

Figure S6. Average density of U.S. BOBs for E7-E10 and E0 gasolines (left), differentiated by premium and regular grades as labelled at pump. Error bars show 95% confidence interval (Alliance of Automotive Manufacturers North American Fuel Survey, Summer 2008, Winter 2009, Summer 2016, Winter 2017). Number of samples numbers shown in right plot.

Based on the trends above, the following values were assumed for market gasolines, BOBs and research gasolines that had no density and/or molecular weight reported:

- Market gasoline 0.73 kg/L 100 g/mol
- Market BOBs 0.73 kg/L 100 g/mol
- Research gasoline 0.73 kg/L 100 g/mol

No molecular weight information was reported for the refinery stream base fuels, however, their molecular weights will vary with their compositions, cuts and densities. Little to no information on average molecular weights of refinery streams is available in the public literature and only limited density information is available.[30] Molecular weights were therefore estimated based on reported compositions of the refinery streams, reported distillation curves, boiling points for various representative neat hydrocarbons and engineering judgment. The following densities and molecular weights were assumed when this information was not specifically reported:

- Full range alkylate 0.69 kg/L 114 g/mol
- Light straight run naphtha 0.66 kg/L 81 g/mol
- Cat cracked naphtha 0.77 kg/L 107 g/mol
- Full range reformate 0.80 kg/L 112 g/mol

In the data set, there were only 7 refinery streams and 7 associated ethanol blends without both density and molecular weight reported; there were 5 refinery streams (or blends of streams) and 11 associated ethanol blends with density data but without molecular weight. The use of the assumptions above therefore likely introduces very little uncertainty to the overall analyses.

The volume-to-mole conversion only requires molar volumes, i.e., the ratio of molecular weight and density (L/mol); these values are shown by iso-contour lines in Fig. S5. Ultimately, the molar volumes do not vary greatly between base gasolines and differences therefore have only a modest effect on the conversion from volume to molar ethanol concentrations.

Finally, for purposes of correlation development involving density as a predictor of octane blending values, only fuels with reported densities were used—no density estimates were included.

SI-9. Octane rating data evaluation

Challenges with accurate RON measurement for high ethanol content fuels have been reported, though such issues can be avoided through appropriate RON measurement methods. [34, 35] Specifically, RON measurements are sometimes biased low for high ethanol blends. As ethanol is added to a given gasoline base fuel or BOB, the RON steadily increases up to approximately 20-40 vol % ethanol, but then stabilizes in the 102-104 RON range as ethanol content is increased further. In contrast, most studies report that RON continues to increase as ethanol is added, albeit at a slowing rate, until reaching 108-109 RON at 100% ethanol.

In a given data set, the existence of this issue is difficult to ascertain and prove in the absence of RON measurements on a high ethanol content fuel with well-established octane ratings, such as neat ethanol. Of the 26 studies evaluated that report data on full boiling range base fuels, only 4 reported RON and MON measurements for neat ethanol.[16, 19, 23, 26] For these, no such RON measurement issue was identified as RON increased continuously as ethanol content increased.

For the 22 data sets without octane rating measurements for neat ethanol, it is helpful to plot the data versus molar ethanol content as this removes much of the nonlinearity that would exist if plotted versus volumetric ethanol content.[27] Even with this molar basis, nonlinearity remains for many blend series (i.e., the subject of this study). Four examples are shown in Fig. S7 along with linear molar model lines for BOBs with 92 and 100 RON. Both Foong et al.[19] and Anderson et al.[16] (red curves) report relatively smooth curves, without plateaus, that reach 108-109 RON at 100% ethanol content. In contrast, two blend series from Yucesu et al.[7] and API[13] show octane ratings that do not approach 108-109 RON and instead trend towards a plateau at approximately 35 mol % ethanol (approximately 15-20 vol %) and above.

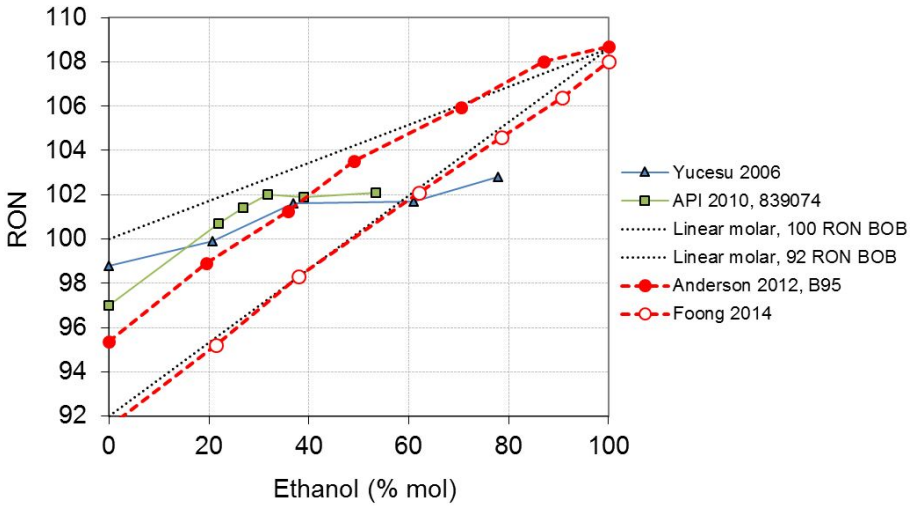

Figure S7. Comparison of selected ethanol-gasoline blend series with 92-100 RON base fuels.

While Yucesu et al. presented a blend series for a single base fuel, the API report included octane ratings for 21 different base fuels. Several blend series from this report with base fuels having RON greater than 92 are shown in Fig. S8. Each series appears to reach or approach a plateau at 102 RON. In contrast, data from this report for base fuels having RON less than 92 (Fig. S9) exhibit the expected linear behavior without reaching a plateau. Based on this examination, it appears that RON measurements above 102 RON and perhaps above 101 RON were somehow inadvertently curtailed for these samples. While this issue presumably relates to high ethanol content, it cannot be proven because no data for gasolines without ethanol at these RON levels were presented in in this report. Based on this assessment, data for all ethanol blends with ethanol content >30 vol % (>50 mol %) from these two publications[7,13] were excluded from the analysis

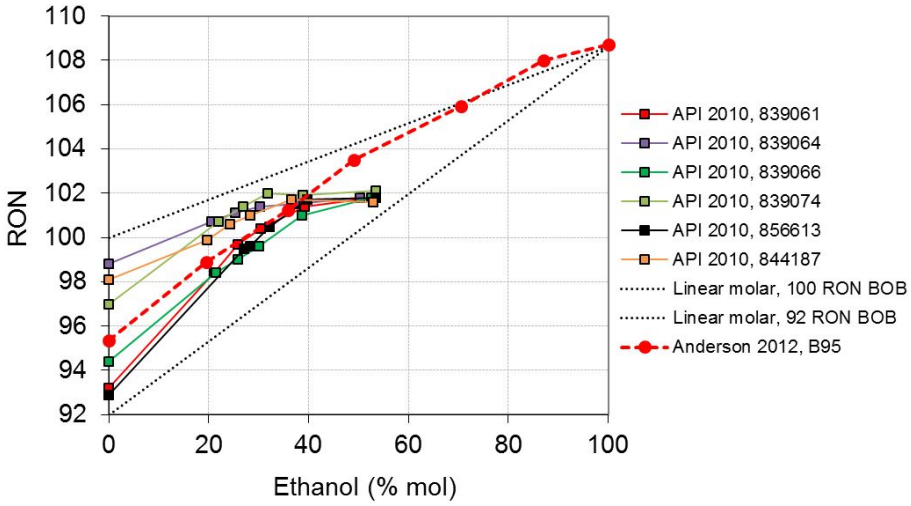

Figure S8. Comparison of selected ethanol-gasoline blend series with 92-100 RON base fuels.

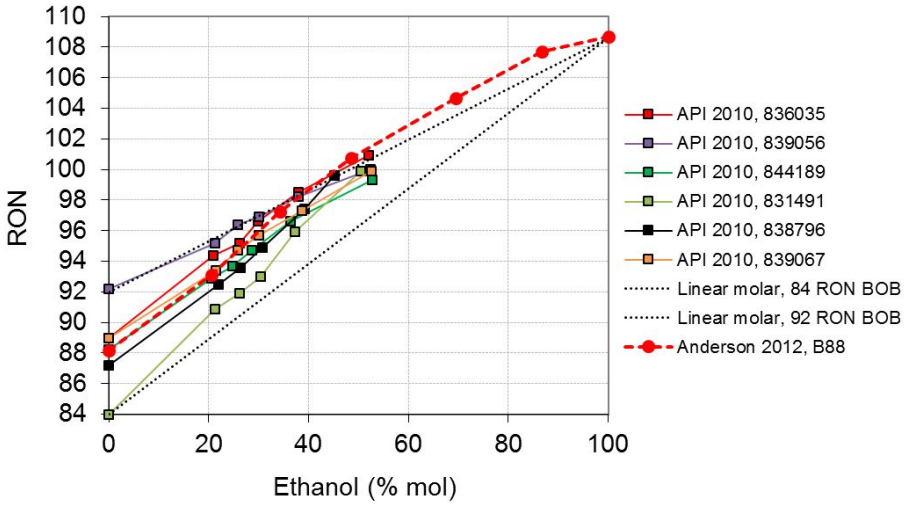

Figure S9. Comparison of selected ethanol-gasoline blend series with 84-92 RON base fuels.

SI-10. Analytical approach

Table S2. Parameters included in forward-step multivariate regressions

model name [a]	parameters allowed in regression	data set [b]
ON_g	OS_g, RON_g	1
ON_g+E	x_a, OS_g, RON_g	1
ON_g (vol) [a]	OS_g, RON_g	1
ON_g+E (vol) [a]	x_a, OS_g, RON_g	1
ON_{blend}	OS_b, RON_b	2
ON_{blend}+E	x_a, OS_b, RON_b	2
ON_{blend} (vol) [a]	OS_b, RON_b	2
ON_{blend}+E (vol) [a]	x_a, OS_b, RON_b	2
SOA	Sat_g, $Arom_g$	1A
SOA+E	x_a, Sat_g, $Arom_g$	1A
SOA+E+ON_g	x_a, OS_g, RON_g, Sat_g, $Arom_g$	1A
SOA+E+ON_g+D	x_a, OS_g, RON_g, Sat_g, $Arom_g$, ρ_g	1A
ON_g (SOA set)	OS_g, RON_g	1A
ON_g+E (SOA set)	x_a, OS_g, RON_g	1A
PIONA	$Arom_g$, $nPar_g$, $iPar_g$, $Naph_g$	1B
PIONA+E	x_a, $Arom_g$, $nPar_g$, $iPar_g$, $Naph_g$	1B
PIONA+E+ON_g	x_a, OS_g, RON_g $Arom_g$, $nPar_g$, $iPar_g$, $Naph_g$	1B
PIONA+E+ON_g +D	x_a, OS_g, RON_g $Arom_g$, $nPar_g$, $iPar_g$, $Naph_g$, ρ_g	1B
ON_g (PIONA set)	OS_g, RON_g	1B
ON_g+E (PIONA set)	x_a, OS_g, RON_g	1B
SOA (PIONA set)	Sat_g, $Arom_g$,	1B
SOA+E (PIONA set)	x_a, Sat_g, $Arom_g$,	1B

[a] Molar basis used for ethanol content and bON_{mol} for all cases except those for which "(vol)" indicates the use of a volume basis.

[b] Group 1 includes all blends with base fuel RON and MON values. Group 2 includes all blends with blend RON and MON values (some studies did not report blend MON). Group 1A and 1B are subsets of Group 1 for which SOA and PIONA data was reported, respectively. See Table S3 for number of data points in each group.

Table S3. Number of data points included in regressions

	n, data points included in regressions			
	RON models		MON models[a]	
	all data	E,R-limited[b]	all data	E,R-limited[b]
base fuel ONs	280	152	272 (253)[a]	151 (145)
blend ONs	253	145	253 (236)	145 (139)
base fuel SOA	168	73	145 (138)	68 (67)
base fuel PIONA	134	47	111 (104)	42 (41)

[a] For MON data sets, first value shows data points used in standard bMON, $P_{g,MON}$ and Z_{MON} approaches. Value in brackets shows smaller data set used in refined $P_{g,MON}$ models in which base fuels with MON between 88.3 and 91.1 were excluded.
[b] "E,R-limited" range subsets include only blends with less than 35 vol % ethanol and with blend RON between 91 and 100.

SI-11. Ethanol octane blending value data: bON_{mol}, P_g, Z and bON_{vol}

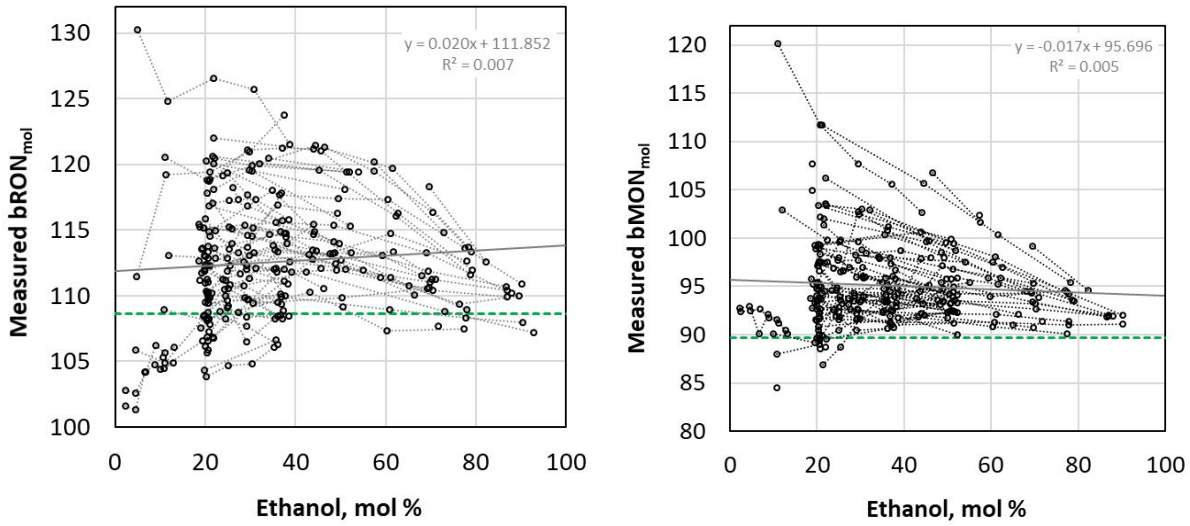

Figure S10. Measured $bRON_{mol}$ (left) and $bMON_{mol}$ (right) values versus molar ethanol content. Thin lines connect blends from single base fuel. Dashed green lines indicate the ON of neat ethanol. Grey solid line shows linear regression.

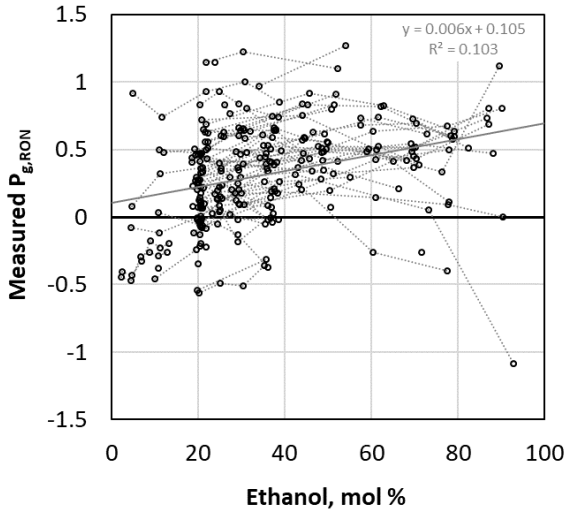

Figure S11. Measured $P_{g,RON}$ interaction values versus molar ethanol content. Thin lines connect blends from single base fuel. Grey solid line shows linear regression.

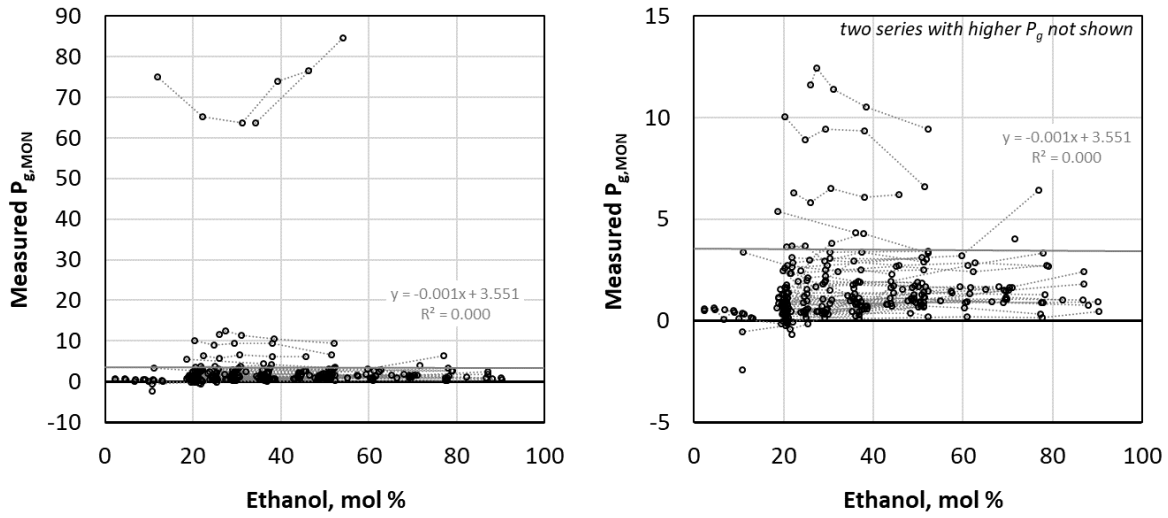

Figure S12. Measured $P_{g,MON}$ interaction values versus molar ethanol content. Thin lines connect blends from single base fuel. Grey solid line shows linear regression.

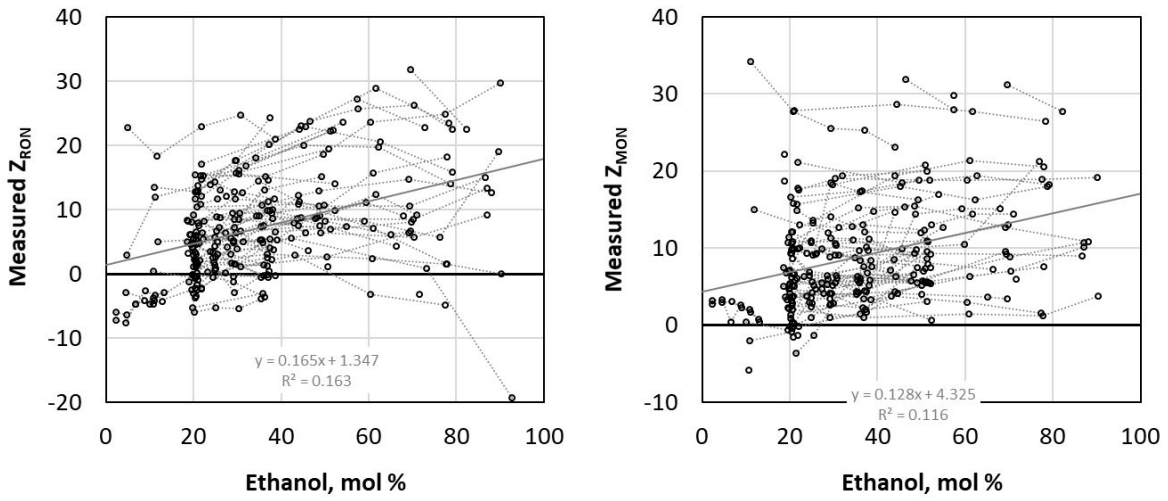

Figure S13. Measured Z interaction values for RON (left) and MON (right) versus molar ethanol content. Thin lines connect blends from single base fuel. Grey solid line shows linear regression.

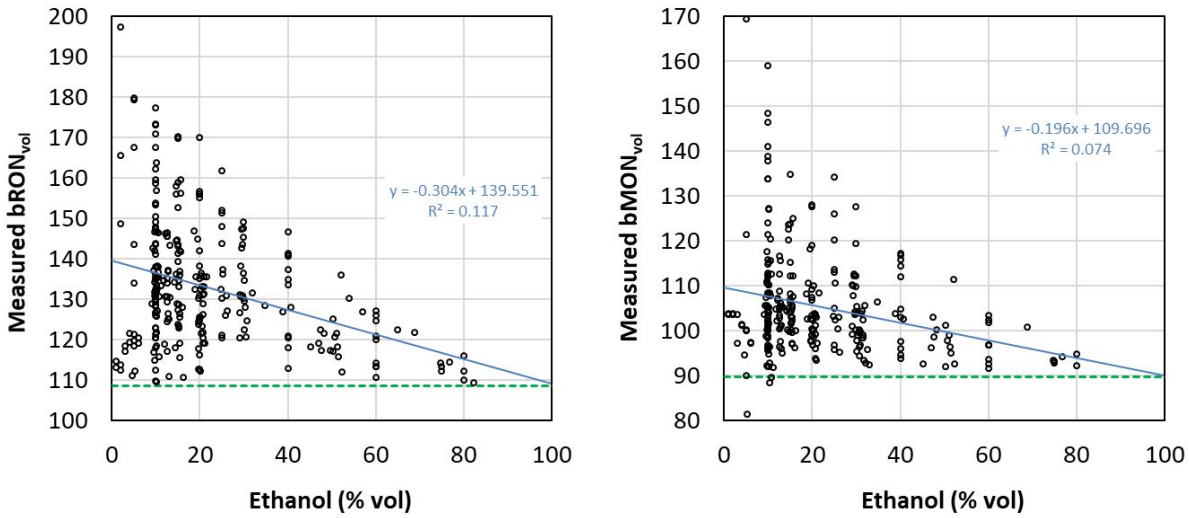

Figure S14. Measured volume-based bRON$_{vol}$ (left) and bMON$_{vol}$ (right) versus volumetric ethanol content. Dashed green lines indicate the RON and MON of neat ethanol. Blue solid line shows linear regression.

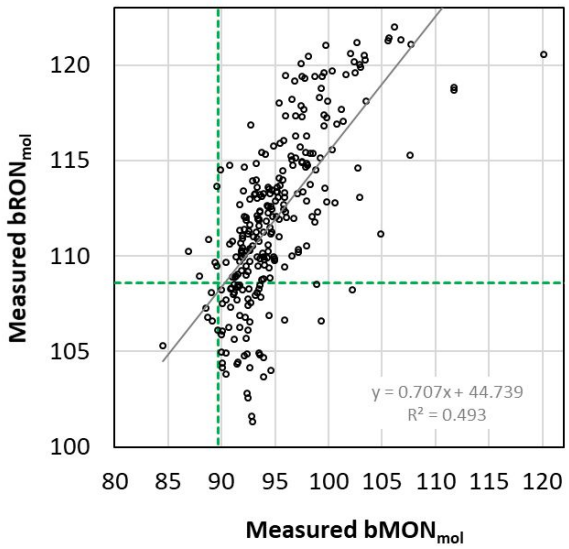

Figure S15. Measured bRON$_{mol}$ values plotted versus measured bMON$_{mol}$ values. Dashed green lines indicate the octane ratings of neat ethanol. Grey solid line shows linear regression.

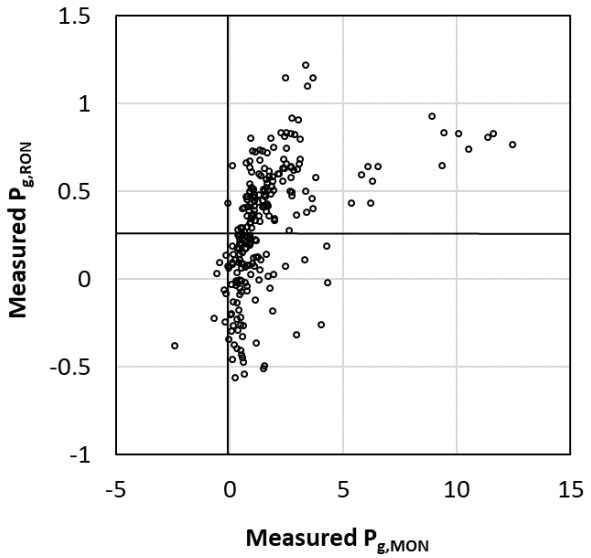

Figure S16. Measured $P_{g,RON}$ values plotted versus $P_{g,MON}$ values. Full data set shown except for several blends with very high $P_{g,MON}$ values (which are outside plot range). For this reason, no linear correlations are shown.

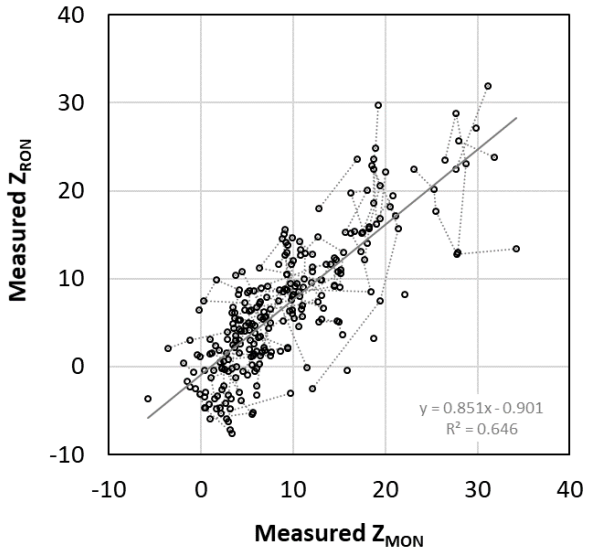

Figure S17. Measured $Z_{,RON}$ values plotted versus $Z_{,MON}$ values. Full data set shown. Thin lines connect blends from single base fuel. Grey solid line shows linear regression.

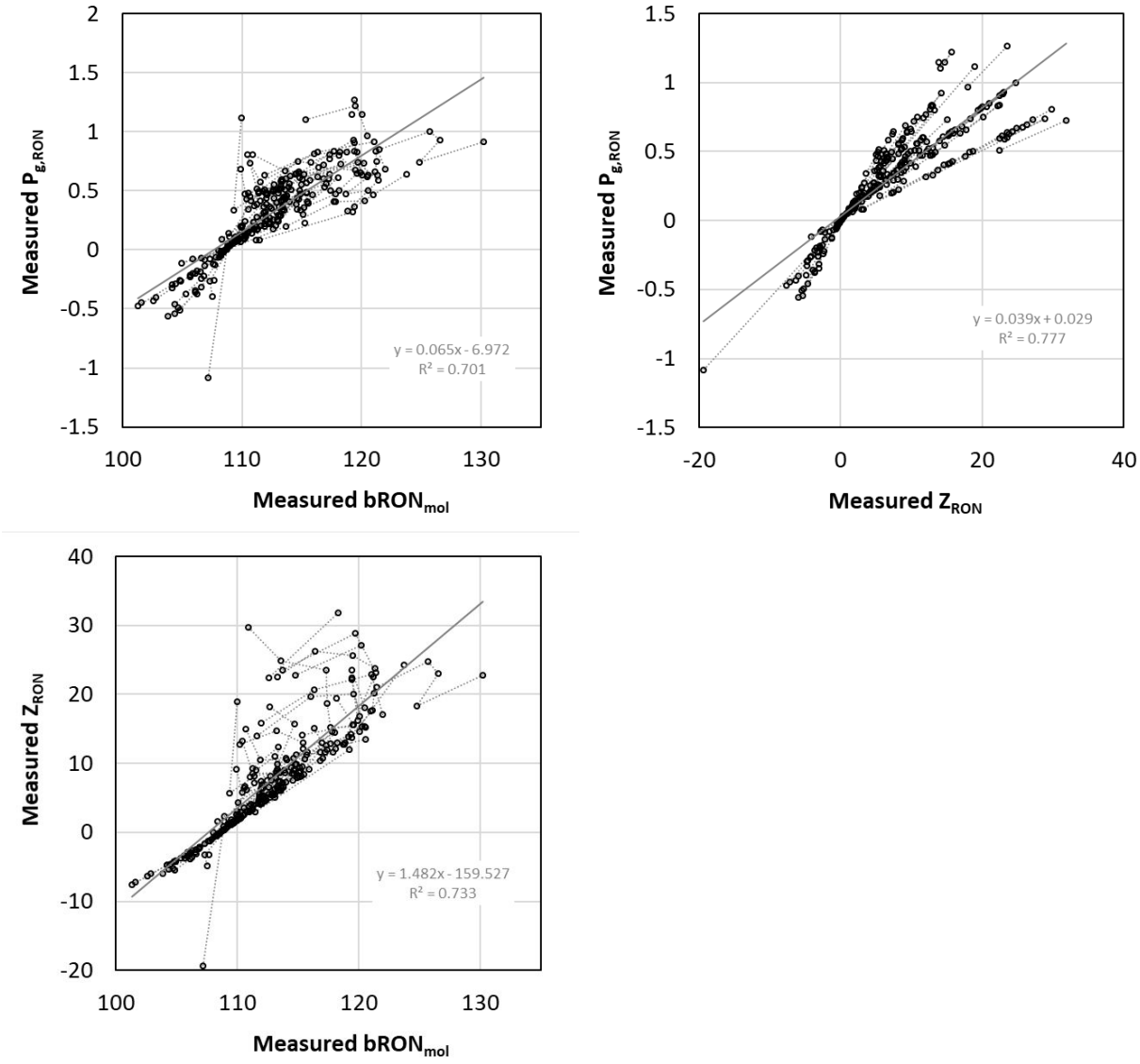

Figure S18. Correlation between $bRON_{mol}$, $P_{g,RON}$ and Z_{RON} values. Distinct groupings in $P_{g,RON}$ vs. Z_{RON} are due to their close mathematical relationship and groups of blends from base fuels having similar base fuel RON (e.g., natural gasolines and FACE fuels I and J having ~71 RON).

SI-12. Models without base fuel dependence

As a baseline, various ethanol octane blending models are assessed without incorporating information about variations in base fuel properties and composition. The linear molar blending model ("neat bON_{mol}") uses $bRON_{mol}$ and $bMON_{mol}$ values equal to neat ethanol's RON and MON, respectively. Models using least-squares best-fit bON and Z values were obtained, the former using both molar ("best bON_{mol}") and volume-based ("best bON_{vol}") blending, with values given in Table S4. Model errors are shown in two ways: bar charts with percentage of errors within 1, 2 and >2 ON (Fig. S19) and traditional box plots (Fig. S20).

For the bar chart approach (Fig. S19), the central dark bar segments represent positive and negative errors within 1 ON of measured values (roughly the accuracy of the ON methods), the lighter bar segments for errors 1-2 ON, and the open bar segments for errors > 2 ON. Better fits are indicated by wider dark segments centered over the origin and by smaller white segments. The linear molar model underestimates RON for most blends because most show synergistic blending. Wang et al.'s model,[28] in which $bRON_{vol}$ varies with ethanol content, overestimates RON for most of the data set. The best-fit $bRON_{vol}$ value provides a poor overall fit with large errors. The best-fit bON_{mol}, P_g and Z models provide a considerably improved overall fit for both RON and MON, with 50-60% of blends within 1 ON and 80-90% within 2 ON of the measured RON or MON.

In the box plots (Fig. S20), the median error is shown as a central diamond, the middle two quartiles (25-75%) are indicated by a thick horizontal line, and the 5-95% error range is given by a thin horizontal line.

Table S4. Ethanol octane blending parameters for generic ethanol octane blending models without base fuel dependence.

model	basis	RON	MON
neat bON_{mol}	molar	$bRON_{mol} = 108.6$	$bMON_{mol} = 89.7$
best-fit bON_{mol}	molar	$bRON_{mol} = 112.6$	$bMON_{mol} = 94.6$
best-fit P_g	molar	$P_{g,RON} = 0.446$	$P_{g,MON} = 1.082$
best-fit Z	molar	$Z_{,RON} = 8.53$	$Z_{,MON} = 9.69$
best-fit bON_{vol}	volume	$bRON_{vol} = 124.0$	$bMON_{vol} = 100.6$
Wang et al. (2017)	volume	$bRON_{mol} = 110.0\text{-}125.8$ (varies with ethanol content)	no MON model

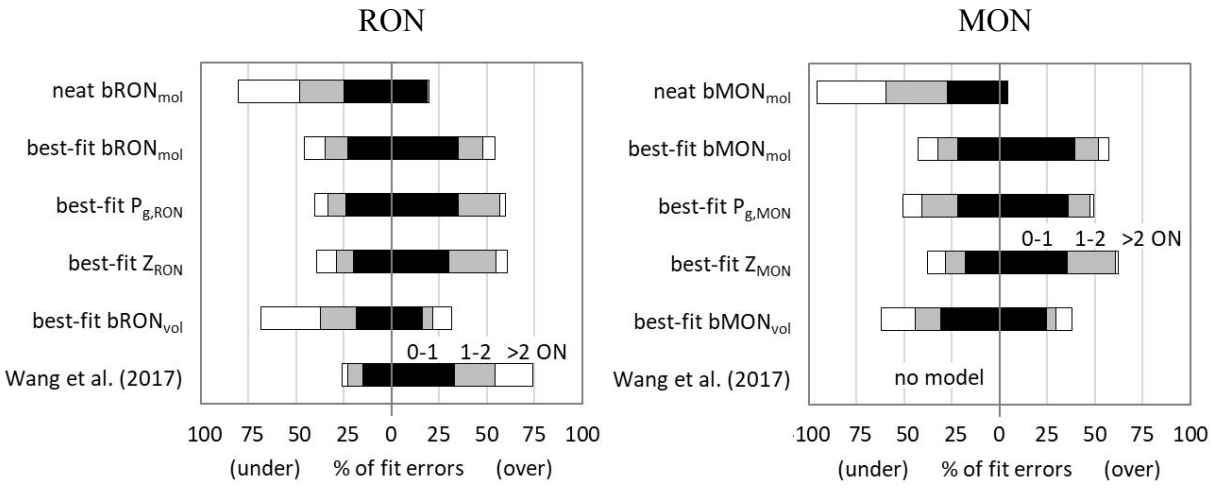

Figure S19. Goodness of fit for generic ethanol octane blending models without base fuel dependence (left RON, right MON). Bars show percentage of data with fit error of percentage of data with fit error 0-1 ON, 1-2 ON and >2 ON.

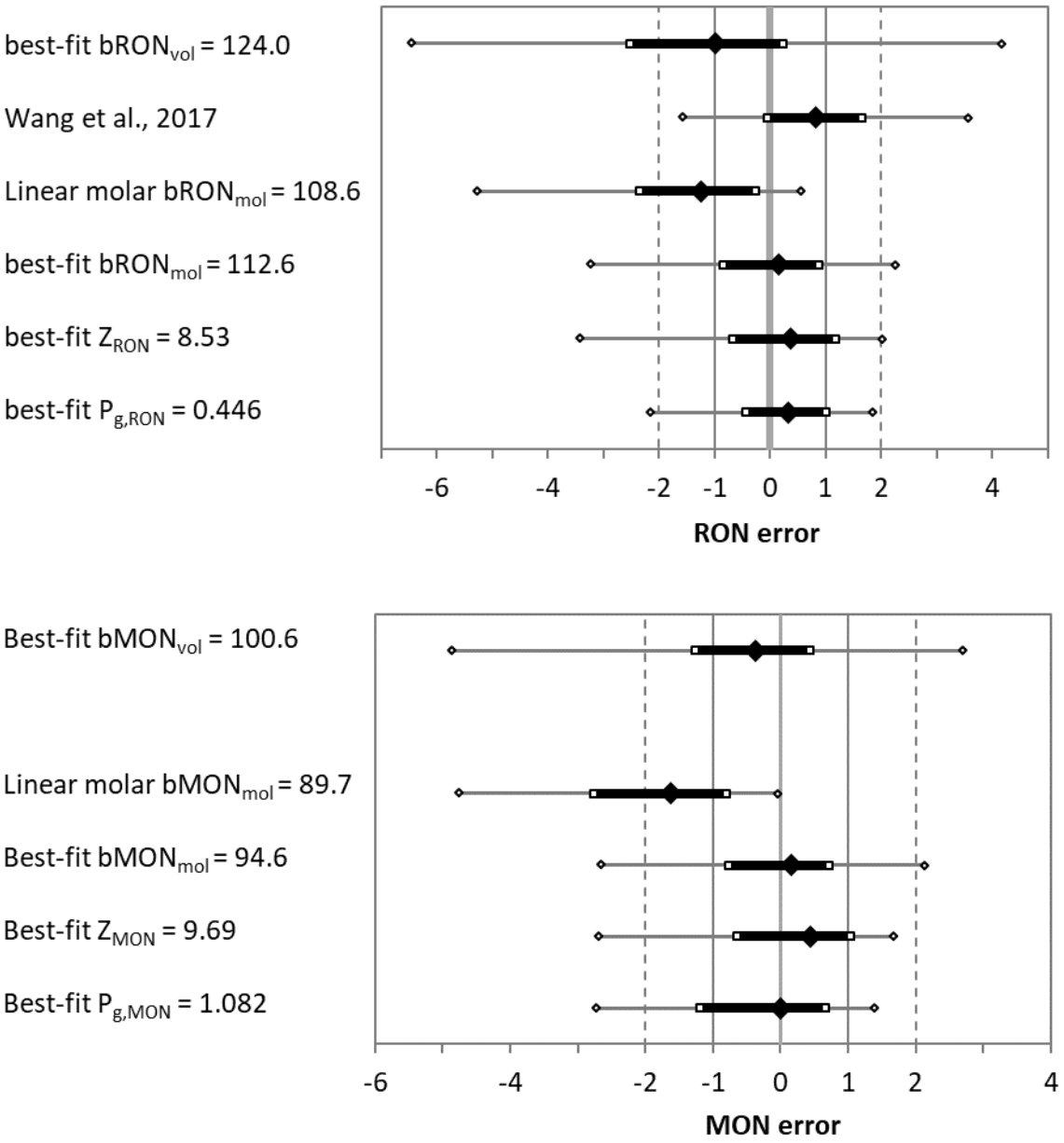

Figure S20. Box plots of RON_{blend} (top) and MON_{blend} (bottom) fitting errors for generic ethanol RON and MON blending models. Central diamonds = 50th percentile (median), inner dark bars = 25-75th percentile, and outer whiskers = 5-95th percentile of errors.

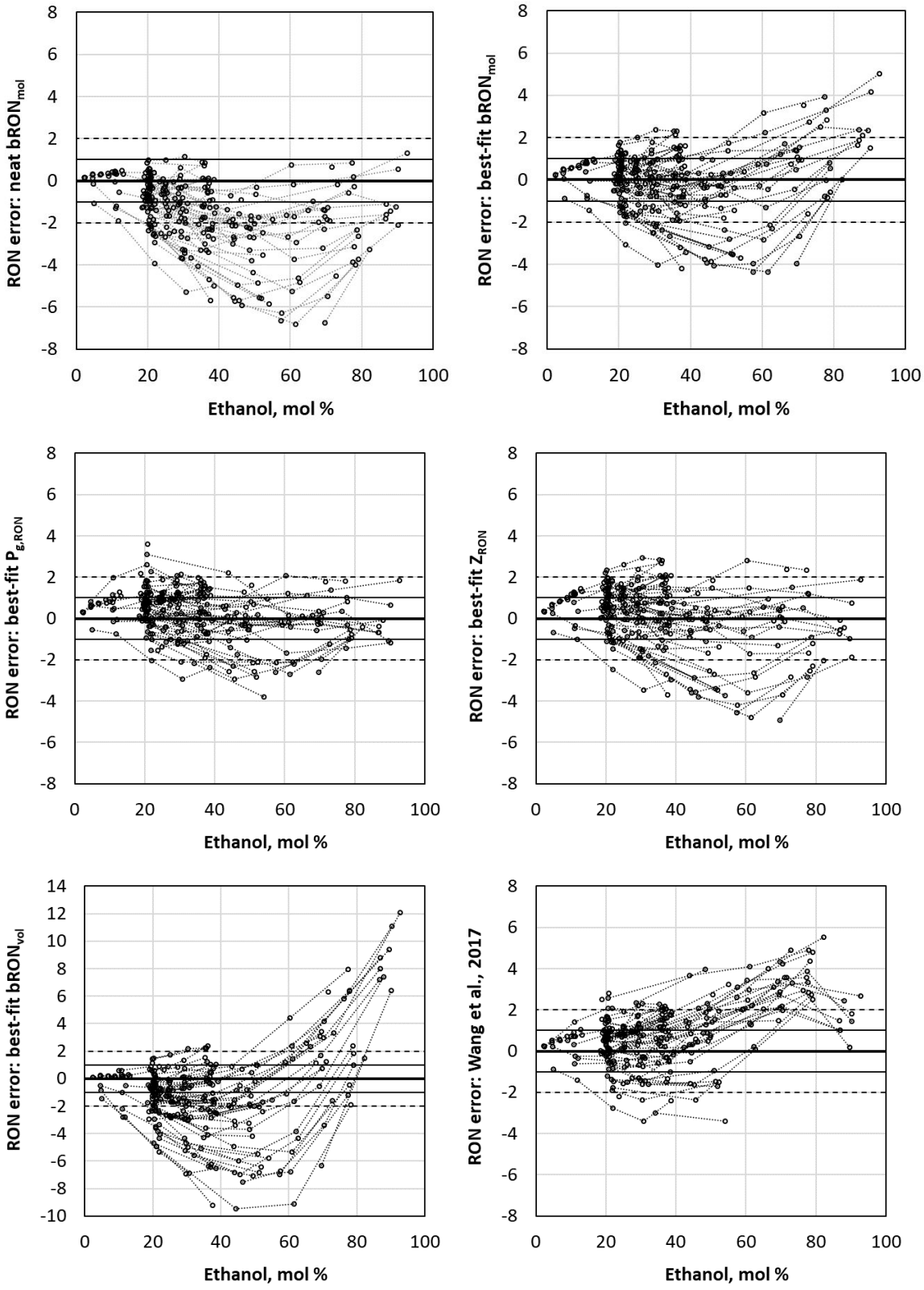

Figure S21. Error of RON prediction for ethanol blends using generic $bRON_{mol}$ models without base fuel dependence versus ethanol content. Thin lines connect blends from single base fuel. Model parameter values shown in Table S4.

SI-13.Models with dependence on individual fuel parameters

Least-squares regressions were conducted for the calculated bON, P_g and Z values against individual base fuel properties and composition (Table S5). Coefficients of determination between individual base fuel (and blend) properties and composition are shown in Table S6. Scatter plots of bON, Pg and Z values are shown against selected properties and composition in Figures S22 to S30.

Ethanol octane blending models were developed by inserting the least-squares best-fit correlations for OS_g versus bON_{mol}, P_g and Z (Table S5) into their respective octane blending terms. Utilizing OS_g as an explanatory variable, all three model approaches gave greatly improved RON predictions (Fig. S32), with ~80% of the predictions within 1 RON of the measured values versus 50-60% for the equivalent models without base fuel dependence. Large errors were similarly improved, with only 4-6% greater than 2 RON versus 10-17% for the generic models. Likewise, 70-74% of the model errors were within 1 RON for the Sat_g-based approaches and only 2-8% had errors greater than 2 RON. The $bRON_{mol}$ models, however, continue to show greater prediction error at high ethanol content (Fig. S33-S34). For MON, the P_g and Z models also improved when utilizing OS_g or Sat_g, but there was no benefit for the P_g approach (Fig S32).

Table S5. Least squares linear regressions of ethanol octane blending model coefficients with individual base fuel and blend parameters.

Parameter		Ethanol mol % x_a	Ethanol vol % C_a	RON base fuel RON_g	MON base fuel MON_g	AKI base fuel AKI_g	OS base fuel OS_g	RON blend RON_{blend}	MON blend MON_{blend}	OS blend OS_{blend}	Saturates base fuel Sat_g	Paraffins base fuel Par_g	n-Paraffins base fuel $nPar_g$	iso-Paraffins base fuel $iPar_g$	Napthenes base fuel $Naph_g$	Olefins base fuel $Olef_g$	Aromatics base fuel $Arom_g$	Density base fuel ρ_g
$bRON_{mol}$	r^2	0.007	0.000	0.204	0.031	0.116	0.575	0.011	0.058	0.153	0.595	0.489	0.000	0.433	0.007	0.296	0.463	0.358
	slope	0.0202	0.0043	-0.2611	-0.1364	-0.2299	-1.0372	-0.0802	0.3029	-0.5996	0.2718	0.2248	0.0026	0.1705	-0.0796	-0.6089	-0.2693	-107.6
	intercept	111.85	112.48	135.62	123.74	132.12	119.29	120.39	85.88	118.75	93.28	98.57	114.65	105.63	114.41	116.57	118.91	191.00
	n	280	280	280	280	280	280	280	253	253	168	146	134	134	146	168	170	280
$bMON_{mol}$	r^2	0.005	0.012	0.291	0.125	0.222	0.378	0.165	0.005	0.450	0.380	0.240	0.068	0.095	0.006	0.212	0.275	0.221
	slope	-0.0168	-0.0299	-0.3138	-0.2756	-0.3211	-0.7943	-0.3447	-0.0859	-1.0556	0.2170	0.1607	0.1728	0.0939	0.0707	-0.4820	-0.2086	-83.19
	intercept	95.70	95.74	123.14	117.82	122.68	100.55	128.92	102.58	106.61	80.04	85.56	94.10	91.80	95.70	98.54	100.30	155.96
	n	272	272	272	272	272	272	272	272	253	145	123	111	111	123	145	147	272
$P_{g,RON}$	r^2	0.103	0.065	0.084	0.000	0.030	0.440	0.047	0.232	0.010	0.462	0.374	0.012	0.395	0.013	0.349	0.310	0.278
	slope	0.00588	0.00546	-0.0129	-0.0007	-0.0091	-0.0701	0.0128	0.0493	-0.0127	0.0166	0.0130	-0.0036	0.0101	-0.0069	-0.0458	-0.0153	-7.333
	intercept	0.1050	0.1968	1.4575	0.3740	1.0897	0.7698	-0.9335	-3.9912	0.4439	-0.8394	-0.4599	0.5486	-0.0447	0.4761	0.6297	0.7017	5.6590
	n	280	280	280	280	280	280	280	253	253	168	146	134	134	146	168	170	280
$P_{g,MON}$	r^2	0.000	0.001	0.023	0.069	0.042	0.009	0.030	0.112	0.007	0.003	0.010	0.032	0.024	0.042	0.039	0.000	0.015
	slope	-0.0014	-0.0274	0.2285	0.5278	0.3587	-0.3188	0.3786	1.1054	-0.3542	0.0604	0.1018	-0.3963	0.1557	-0.5848	-0.6198	0.0186	-55.09
	intercept	3.551	4.107	-16.939	-40.063	-27.346	5.693	-33.668	-93.022	7.400	0.299	-1.384	11.935	-2.253	9.810	8.273	4.265	43.813
	n	272	272	272	272	272	272	272	272	253	145	123	111	111	123	145	147	272
$P_{g,MON}$	r^2	0.042	0.026	0.003	0.084	0.025	0.118	0.056	0.297	0.040	0.527	0.639	0.019	0.670	0.075	0.258	0.407	0.120
(excluding blends	slope	0.0130	0.0122	0.0090	0.0646	0.0300	-0.1241	0.0555	0.2021	-0.0828	0.0499	0.0468	-0.0157	0.0440	-0.0438	-0.1032	-0.0510	-17.36
w/ base fuel MON	intercept	0.857	1.065	0.539	-3.959	-1.229	2.209	-4.094	-16.238	2.213	-2.343	-1.731	1.721	-0.811	1.709	1.882	2.356	14.064
of 88.3-91.1)	n	253	253	253	253	253	253	253	253	236	138	116	104	104	116	138	138	253
Z_{RON}	r^2	0.163	0.126	0.350	0.126	0.250	0.601	0.014	0.106	0.008	0.607	0.415	0.036	0.250	0.003	0.306	0.476	0.374
	slope	0.165	0.170	-0.593	-0.477	-0.585	-1.834	0.158	0.723	-0.237	0.466	0.339	0.170	0.217	0.077	-1.050	-0.464	-190.5
	intercept	1.347	3.584	59.593	46.343	57.050	19.161	-8.059	-56.147	9.437	-24.804	-12.608	9.030	0.221	9.797	15.156	19.154	146.083
	n	280	280	280	280	280	280	280	253	253	168	146	134	134	146	168	170	280
Z_{MON}	r^2	0.116	0.099	0.495	0.269	0.409	0.496	0.009	0.017	0.108	0.555	0.344	0.147	0.118	0.009	0.282	0.424	0.303
	slope	0.128	0.141	-0.666	-0.659	-0.710	-1.483	-0.130	0.271	-0.842	0.430	0.301	0.385	0.158	0.134	-0.912	-0.426	-158.9
	intercept	4.32	5.91	68.62	63.45	70.08	19.25	21.77	-14.59	18.22	-20.24	-8.35	6.83	4.37	10.64	16.19	20.16	125.31
	n	272	272	272	272	272	272	272	272	253	145	123	111	111	123	145	147	272
$bRON_{vol}$	r^2	0.092	0.117	0.344	0.130	0.249	0.563	0.386	0.048	0.575	0.432	0.392	0.009	0.267	0.028	0.168	0.362	0.241
	slope	-0.231	-0.304	-1.091	-0.903	-1.086	-3.303	-1.526	-0.827	-3.476	0.767	0.675	0.194	0.512	-0.527	-1.521	-0.790	-284.5
	intercept	141.19	139.55	229.18	206.73	225.26	154.27	281.58	203.52	168.86	78.06	90.41	134.82	110.70	140.12	142.76	151.02	340.18
	n	280	280	280	280	280	280	280	253	253	168	146	134	134	146	168	170	280
$bMON_{vol}$	r^2	0.065	0.074	0.398	0.274	0.359	0.287	0.479	0.182	0.586	0.225	0.111	0.079	0.026	0.021	0.098	0.181	0.116
	slope	-0.153	-0.196	-0.959	-1.068	-1.068	-1.810	-1.536	-1.426	-3.131	0.437	0.291	0.514	0.135	0.348	-0.860	-0.444	-157.5
	intercept	110.99	109.70	191.13	193.48	197.14	117.80	256.17	229.85	139.63	75.14	88.48	100.74	101.48	105.18	111.74	116.40	220.61
	n	272	272	272	272	272	272	272	272	253	145	123	111	111	123	145	147	272

Table S6. Least squares linear correlation coefficients (r^2) between individual base fuel and blend parameters

	Ethanol mol %	Ethanol vol %	RON base fuel	MON base fuel	AKI base fuel	OS base fuel	RON blend	MON blend	OS blend	Saturates base fuel	Paraffins base fuel	n-Paraffins base fuel	iso-Paraffins base fuel	Napthenes base fuel	Olefins base fuel	Aromatics base fuel	Density base fuel
Ethanol mol %	-	0.930	0.010	0.008	0.009	0.006	0.467	0.286	0.490	0.004	0.009	0.000	0.029	0.022	0.020	0.001	0.007
Ethanol vol %	0.930	-	0.011	0.012	0.012	0.003	0.401	0.215	0.471	0.000	0.020	0.002	0.045	0.025	0.012	0.000	0.006
RON base fuel	0.010	0.011	-	0.852	0.972	0.549	0.303	0.299	0.138	0.310	0.106	0.342	0.000	0.036	0.090	0.288	0.192
MON base fuel	0.008	0.012	0.852	-	0.949	0.181	0.287	0.442	0.038	0.074	0.000	0.389	0.098	0.096	0.017	0.079	0.036
AKI base fuel	0.009	0.012	0.972	0.949	-	0.383	0.308	0.372	0.091	0.195	0.038	0.373	0.021	0.061	0.054	0.189	0.115
OS base fuel	0.006	0.003	0.549	0.181	0.383	-	0.128	0.014	0.275	0.795	0.656	0.060	0.413	0.017	0.258	0.684	0.487
RON blend	0.467	0.401	0.303	0.287	0.308	0.128	-	0.841	0.701	0.044	0.030	0.075	0.002	0.001	0.001	0.053	0.022
MON blend	0.286	0.215	0.299	0.442	0.372	0.014	0.841	-	0.301	0.000	0.020	0.133	0.083	0.055	0.016	0.002	0.000
OS blend	0.490	0.471	0.138	0.038	0.091	0.275	0.701	0.301	-	0.172	0.151	0.013	0.112	0.004	0.034	0.156	0.129
Saturates base fuel	0.004	0.000	0.310	0.074	0.195	0.795	0.044	0.000	0.172	-	0.885	0.009	0.700	0.044	0.268	0.891	0.818
Paraffins base fuel	0.009	0.020	0.106	0.000	0.038	0.656	0.030	0.020	0.151	0.885	-	0.015	0.774	0.279	0.328	0.780	0.784
n-Paraffins base fuel	0.000	0.002	0.342	0.389	0.373	0.060	0.075	0.133	0.013	0.009	0.015	-	0.132	0.015	0.126	0.000	0.031
iso-Paraffins base fuel	0.029	0.045	0.000	0.098	0.021	0.413	0.002	0.083	0.112	0.700	0.774	0.132	-	0.216	0.126	0.688	0.571
Napthenes base fuel	0.022	0.025	0.036	0.096	0.061	0.017	0.001	0.055	0.004	0.044	0.279	0.015	0.216	-	0.067	0.020	0.075
Olefins base fuel	0.020	0.012	0.090	0.017	0.054	0.258	0.001	0.016	0.034	0.268	0.328	0.126	0.126	0.067	-	0.043	0.081
Aromatics base fuel	0.001	0.000	0.288	0.079	0.189	0.684	0.053	0.002	0.156	0.891	0.780	0.000	0.688	0.020	0.043	-	0.836
Density base fuel	0.007	0.006	0.192	0.036	0.115	0.487	0.022	0.000	0.129	0.818	0.784	0.031	0.571	0.075	0.081	0.836	-

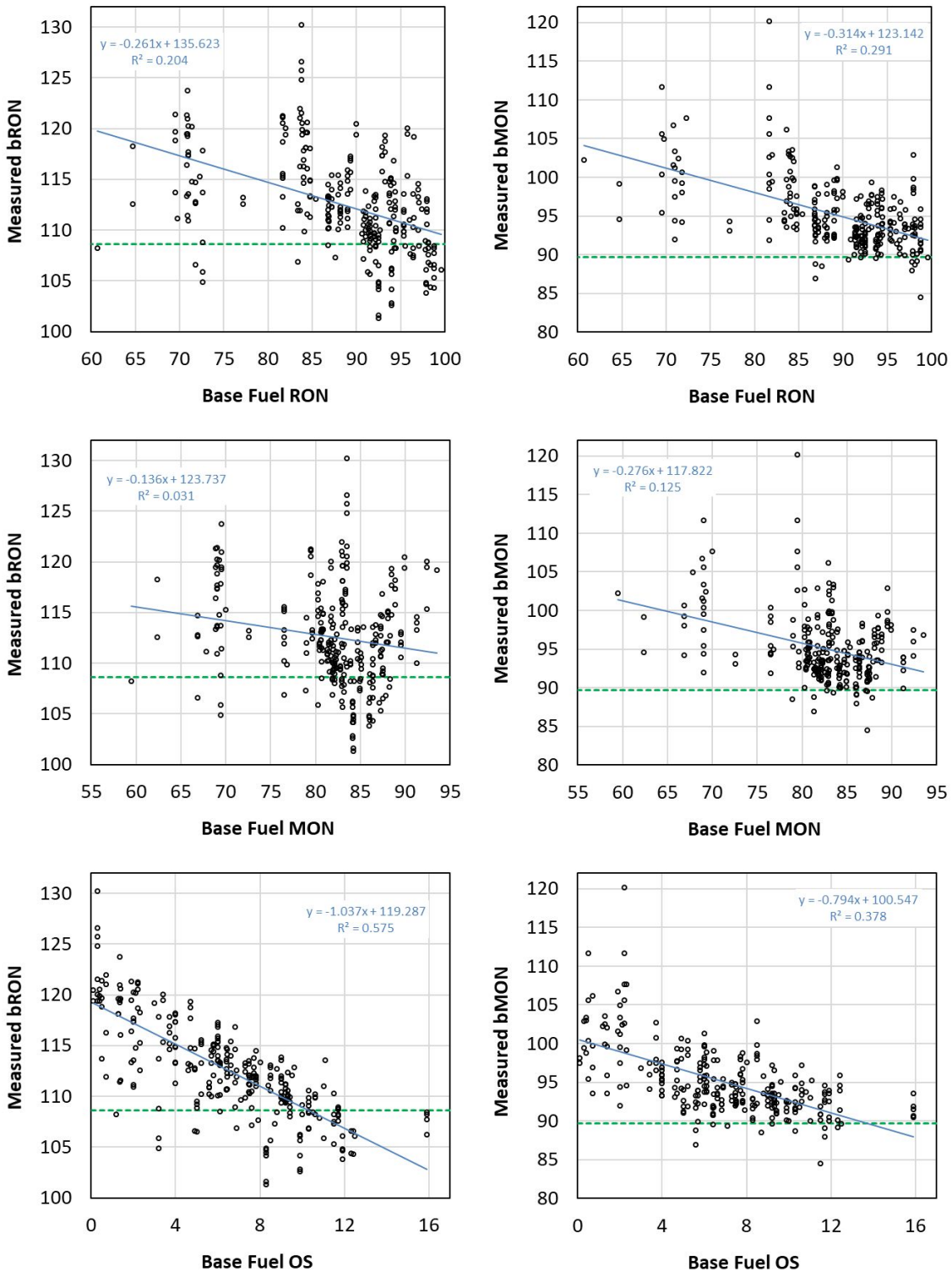

Figure S22. Measured $bRON_{mol}$ and $bMON_{mol}$ values plotted versus base fuel RON, base fuel MON and base fuel OS. Dashed green line indicates the RON or MON of neat ethanol.

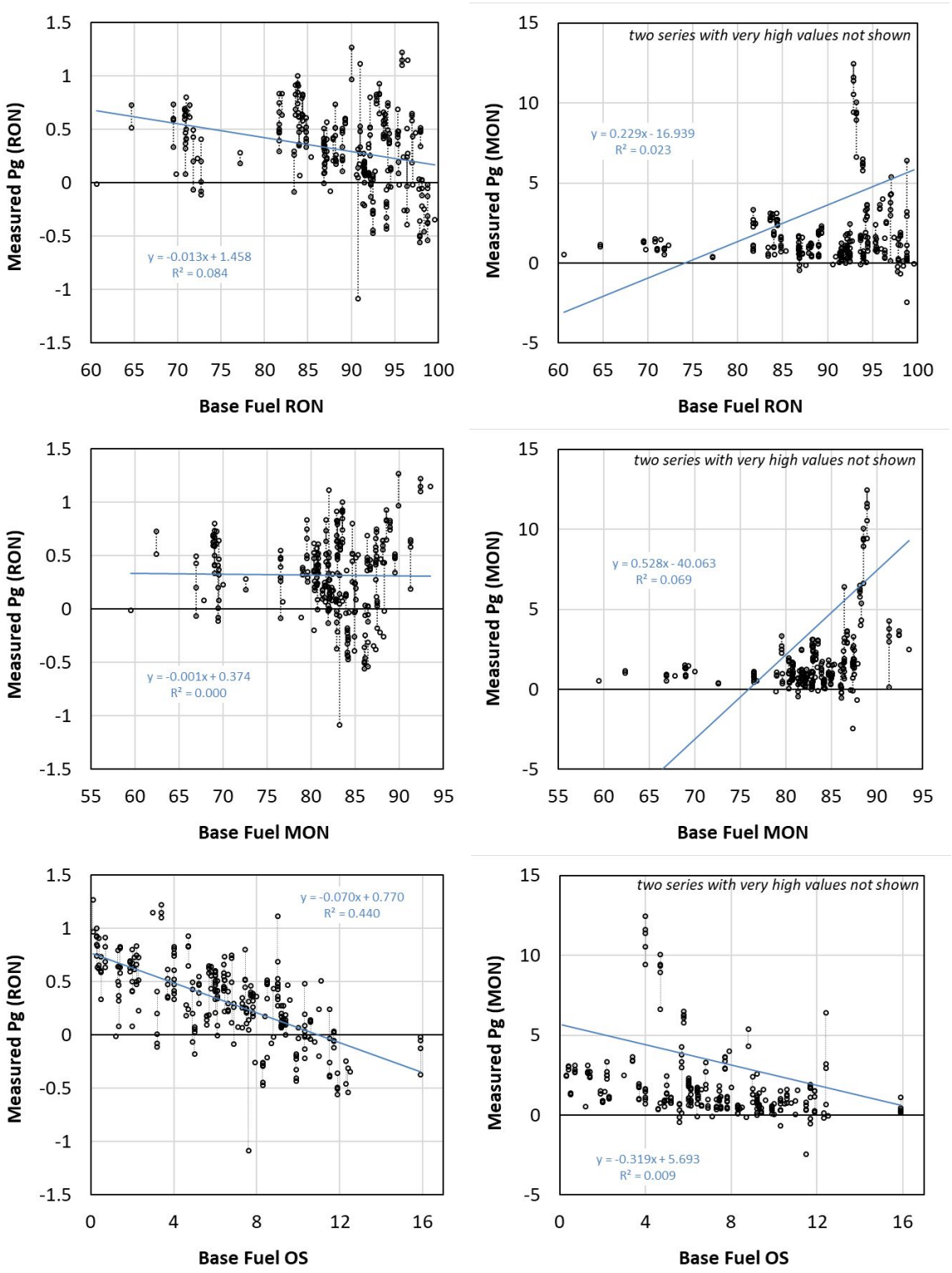

Figure S23. Measured $P_{g,RON}$ and $P_{g,MON}$ values plotted versus base fuel RON, base fuel MON and base fuel OS.

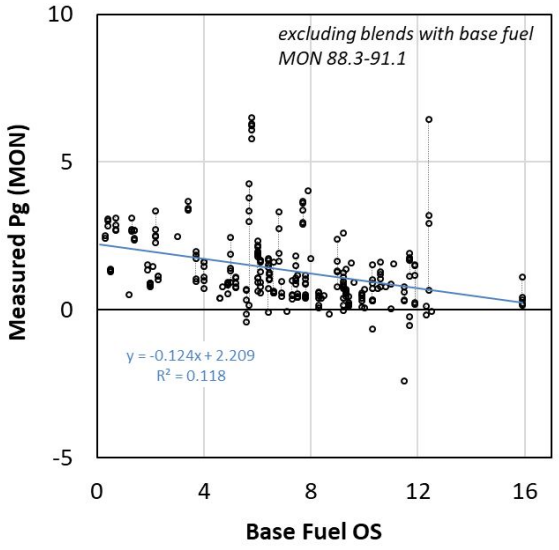

Figure S24. Measured $P_{g,MON}$ values plotted versus base fuel OS for a limited MON data set (excluding MON_g = 88.3-91.1).

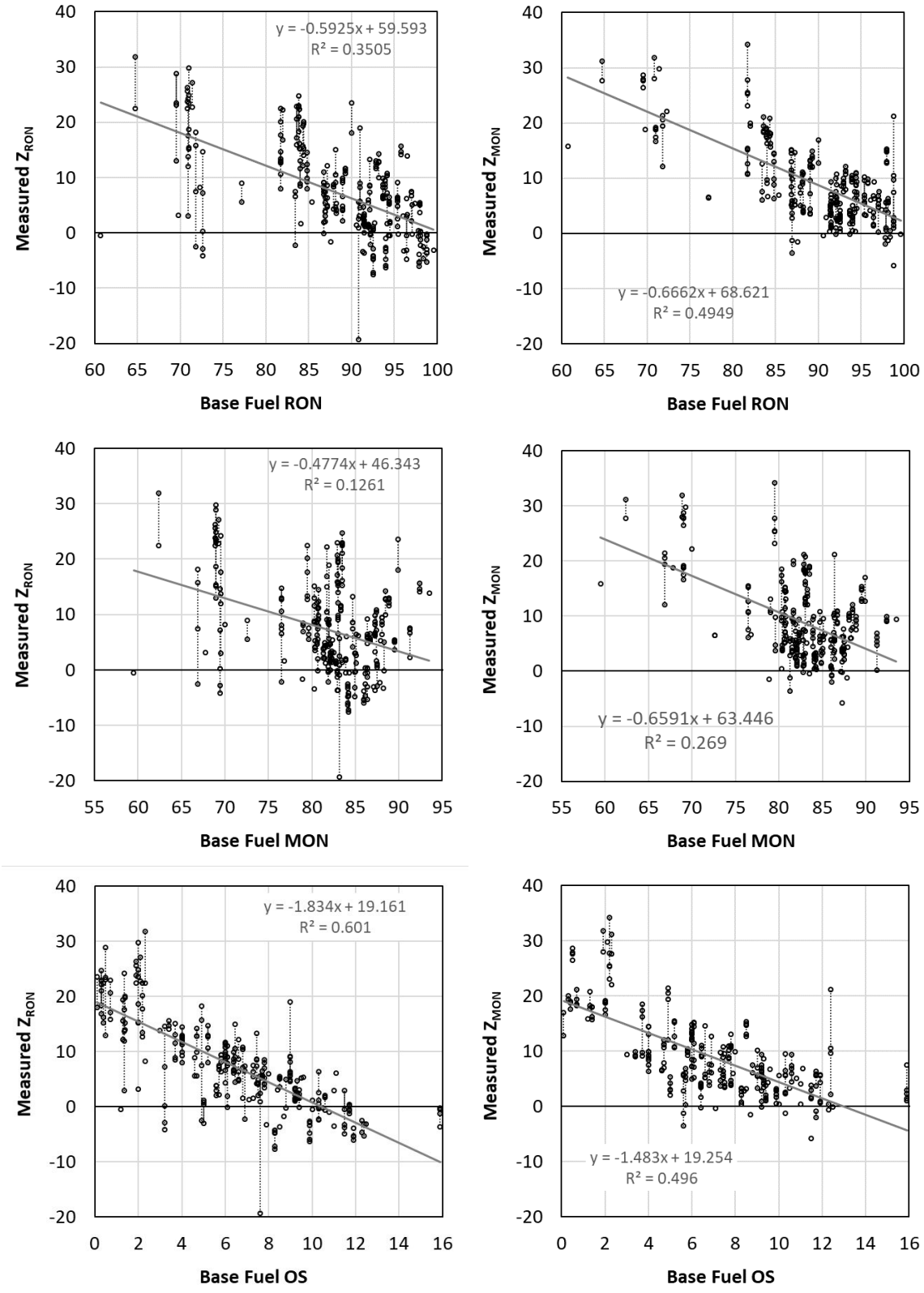

Figure S25. Measured Z_{RON} and Z_{MON} values plotted versus base fuel RON, base fuel MON and base fuel OS.

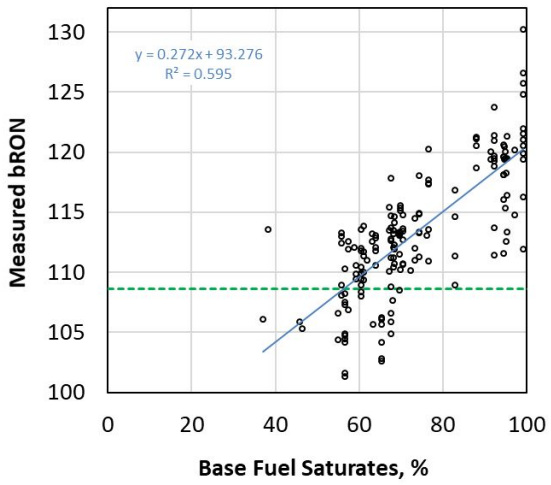
y = 0.272x + 93.276
R² = 0.595
Measured bRON
Base Fuel Saturates, %

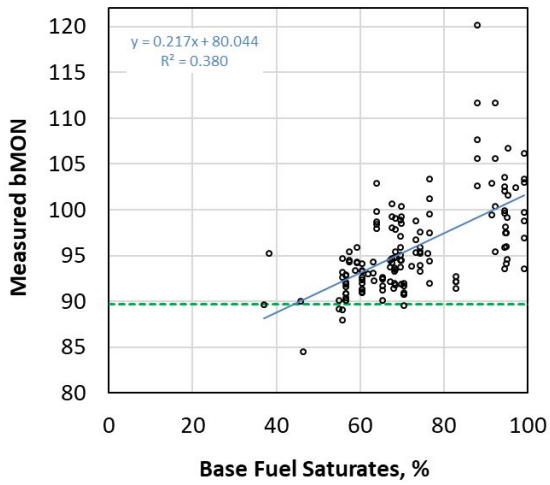
y = 0.217x + 80.044
R² = 0.380
Measured bMON
Base Fuel Saturates, %

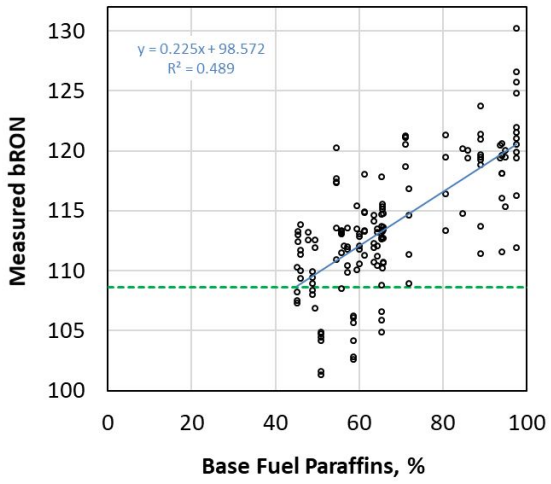
y = 0.225x + 98.572
R² = 0.489
Measured bRON
Base Fuel Paraffins, %

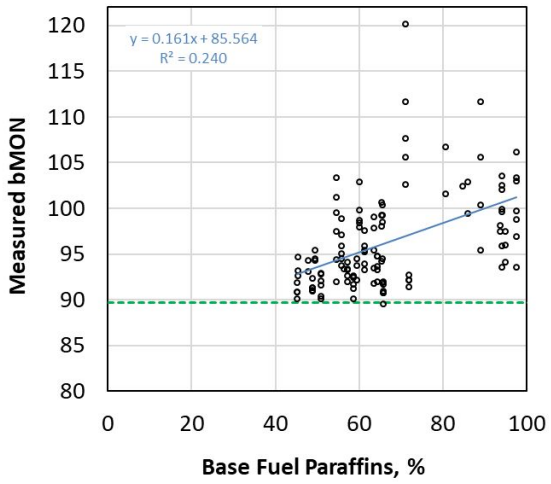
y = 0.161x + 85.564
R² = 0.240
Measured bMON
Base Fuel Paraffins, %

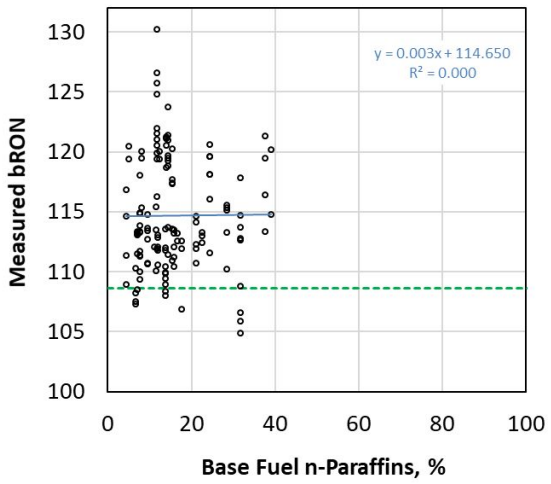
y = 0.003x + 114.650
R² = 0.000
Measured bRON
Base Fuel n-Paraffins, %

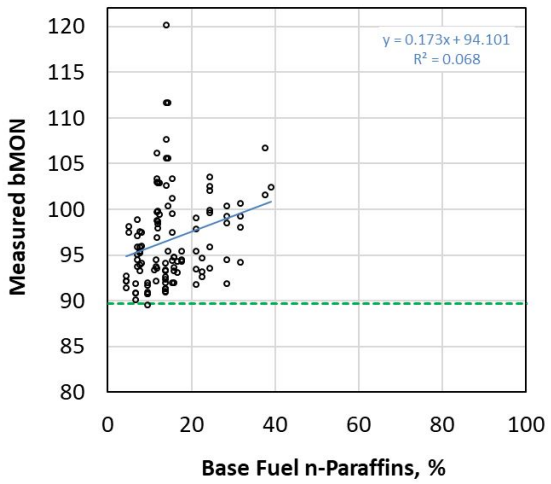
y = 0.173x + 94.101
R² = 0.068
Measured bMON
Base Fuel n-Paraffins, %

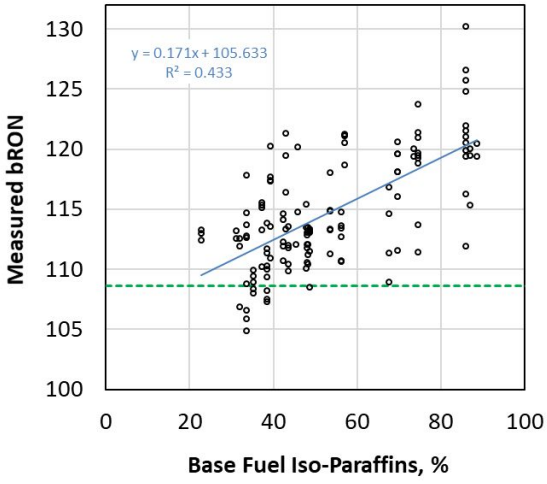
y = 0.171x + 105.633
R² = 0.433
Measured bRON
Base Fuel Iso-Paraffins, %

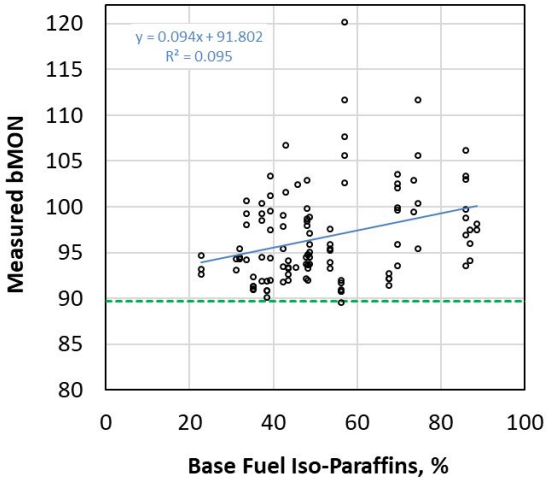
y = 0.094x + 91.802
R² = 0.095
Measured bMON
Base Fuel Iso-Paraffins, %

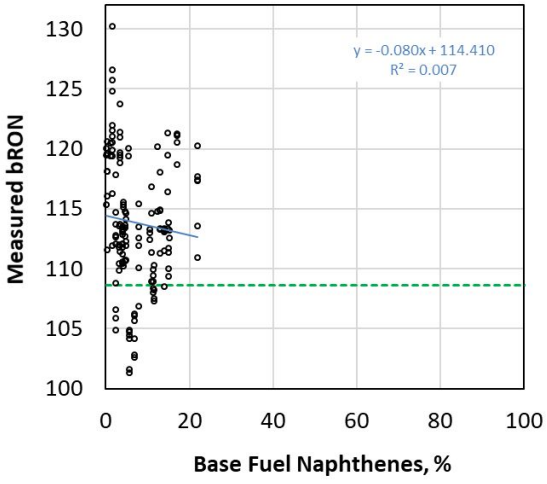
y = -0.080x + 114.410
R² = 0.007
Measured bRON
Base Fuel Naphthenes, %

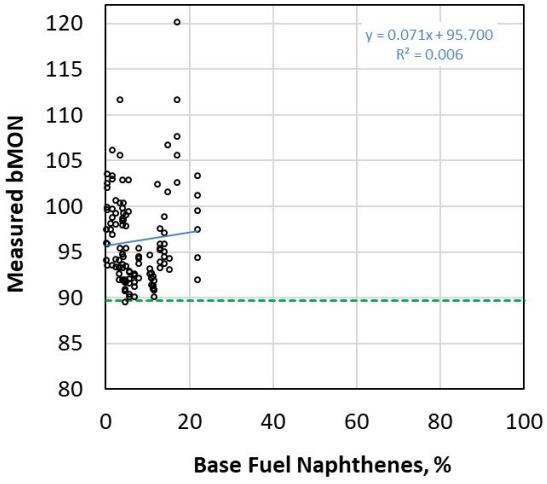
y = 0.071x + 95.700
R² = 0.006
Measured bMON
Base Fuel Naphthenes, %

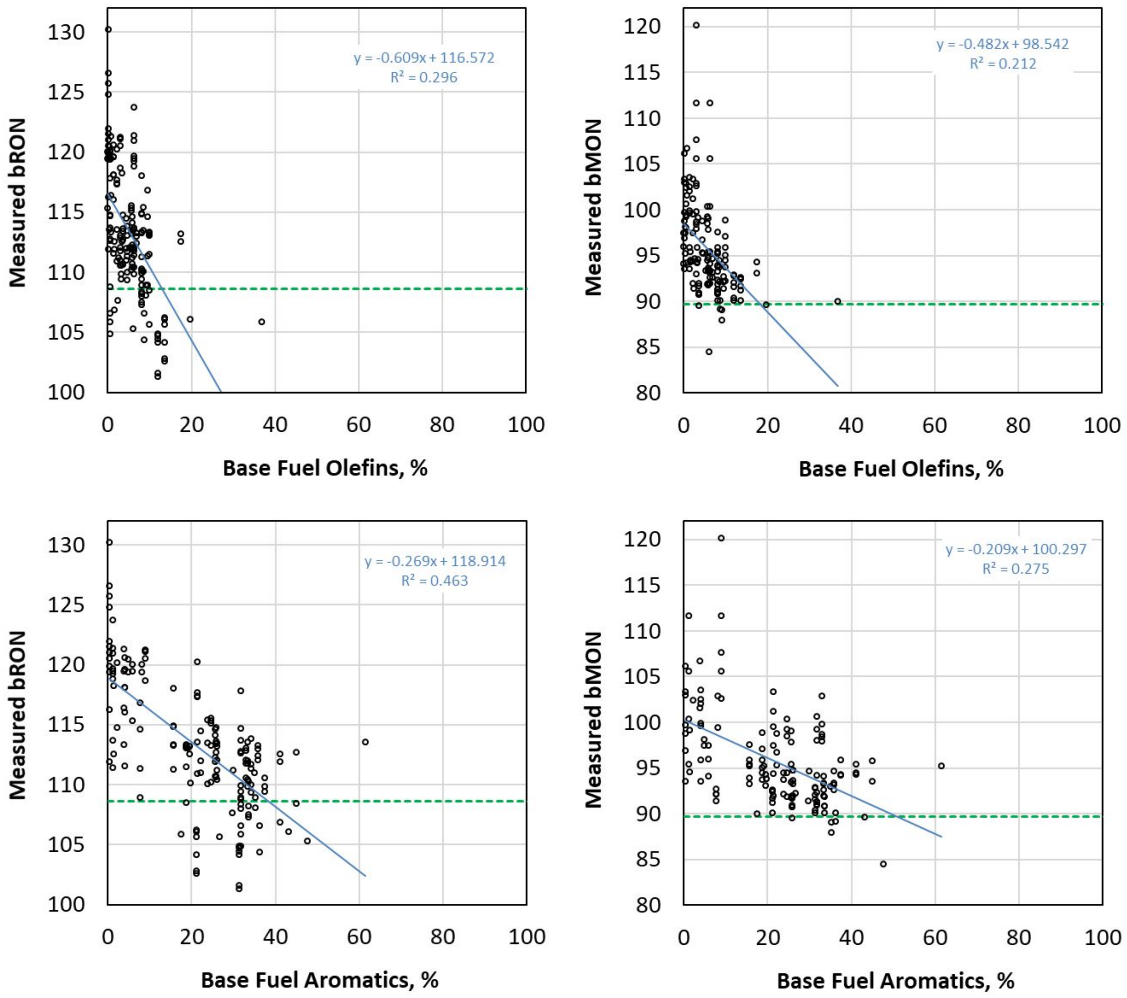

Figure S26. $bRON_{mol}$ and $bMON_{mol}$ values versus content of different base fuel hydrocarbon groups. Dashed green line indicates the RON or MON of neat ethanol.

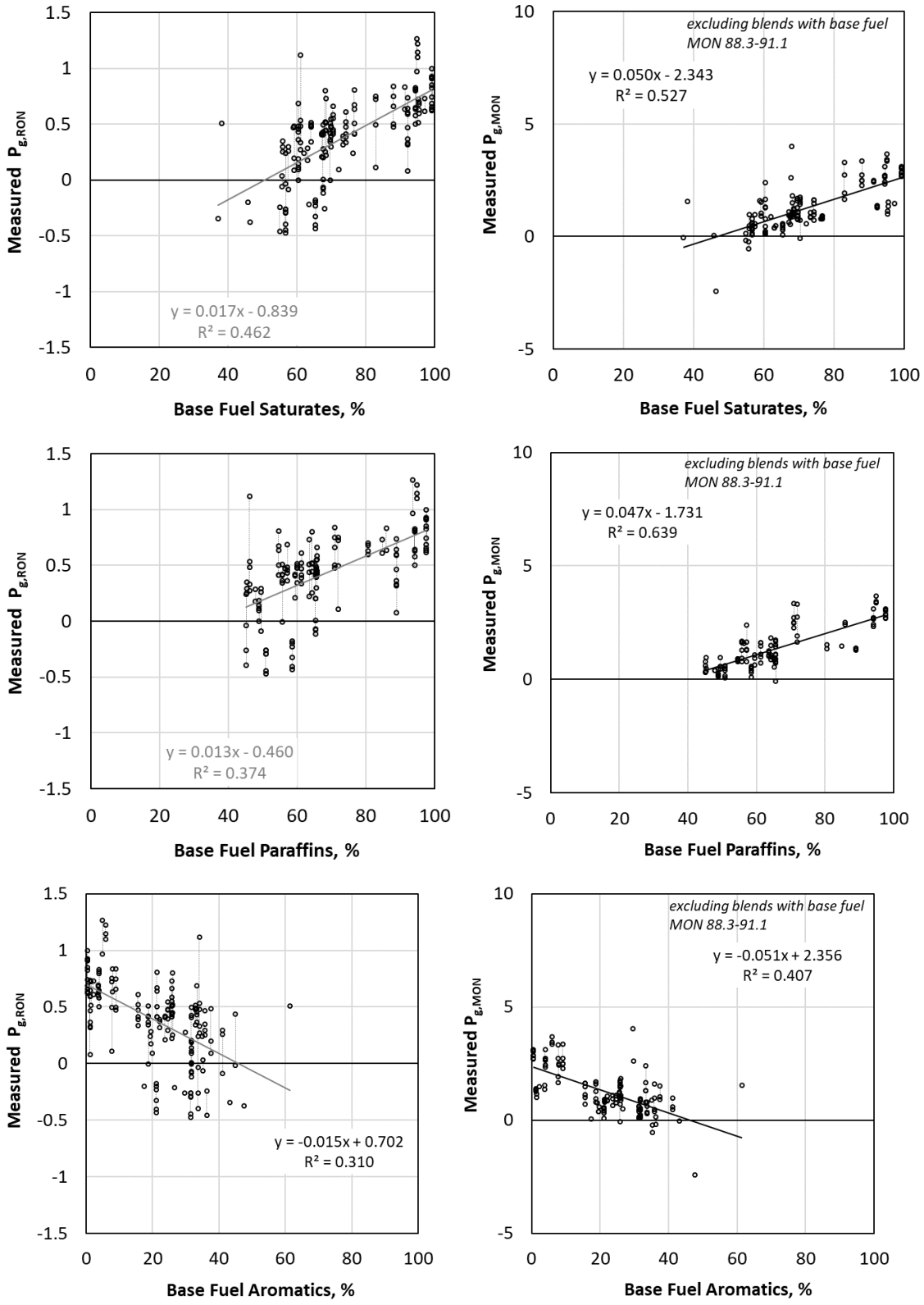

Figure S27. $P_{g,RON}$ and $P_{g,MON}$ values versus content of base fuel saturates, paraffins and aromatics content.

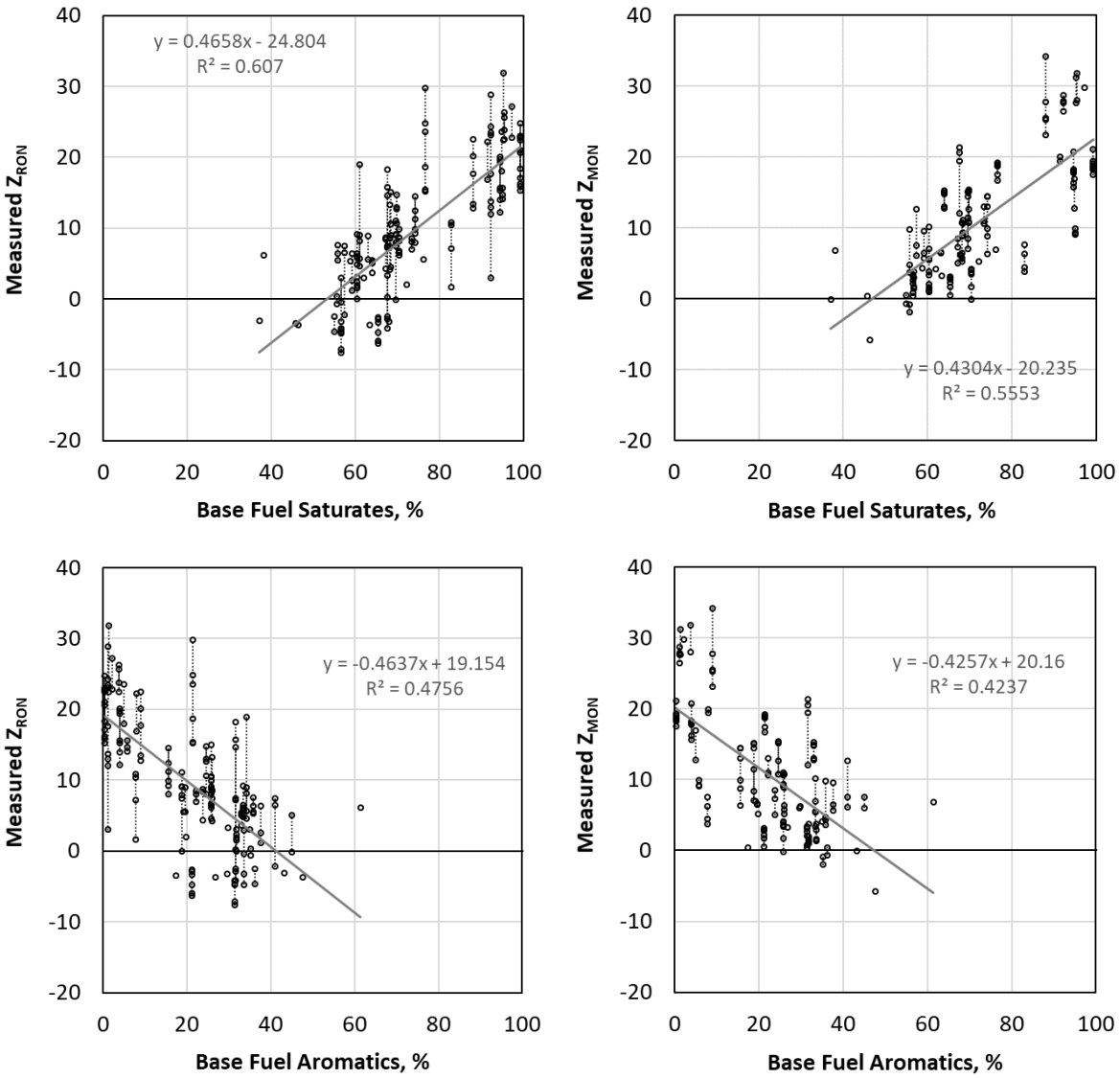

Figure S28. $Z_{,RON}$ and $Z_{,MON}$ values versus content of base fuel saturates and aromatics content.

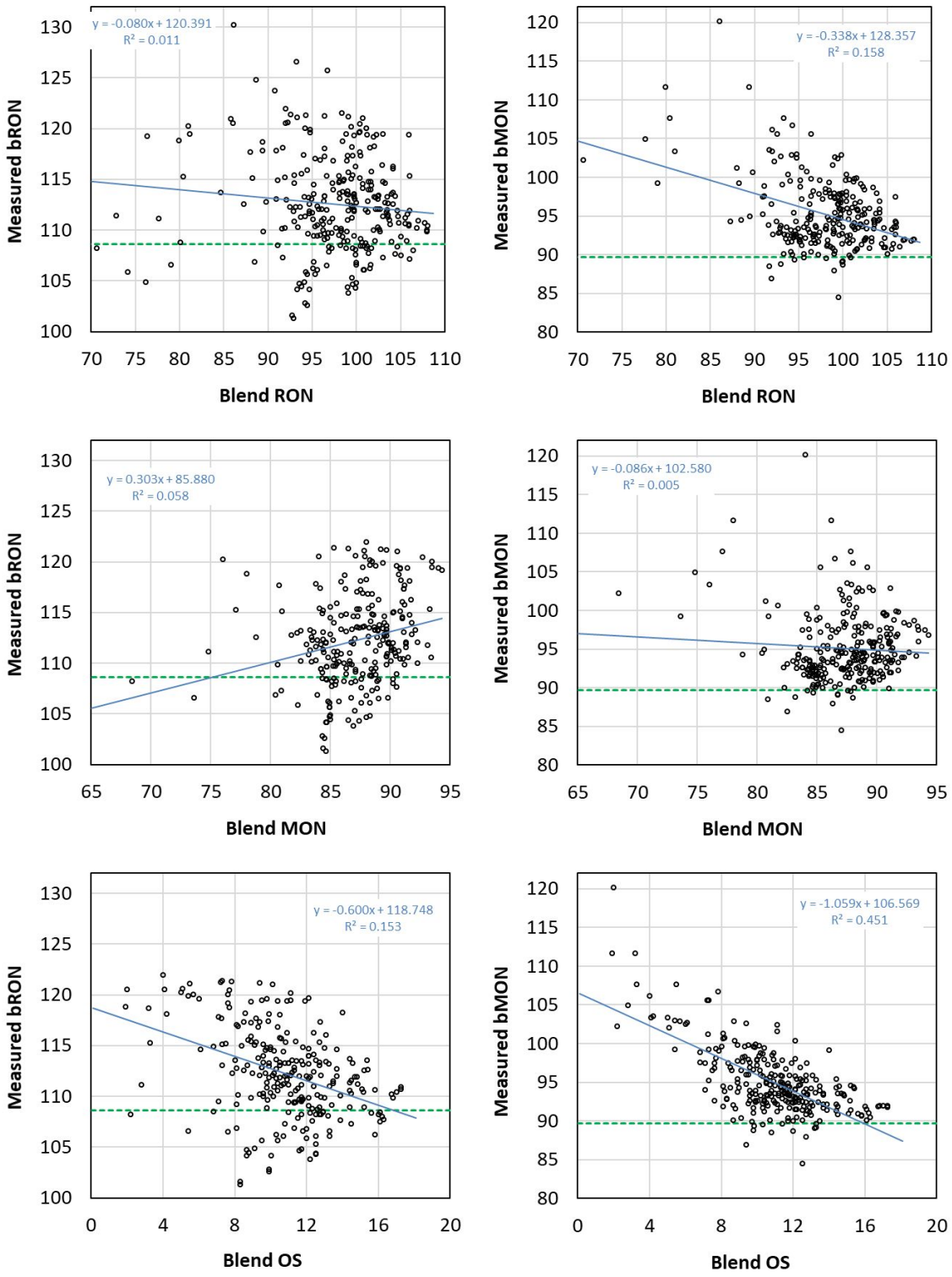

Figure S29. Molar-based bRON and bMON values for ethanol in complex base fuels plotted versus blend RON, blend MON and blend OS (rather than base fuel). Dashed green line indicates the RON or MON of neat ethanol.

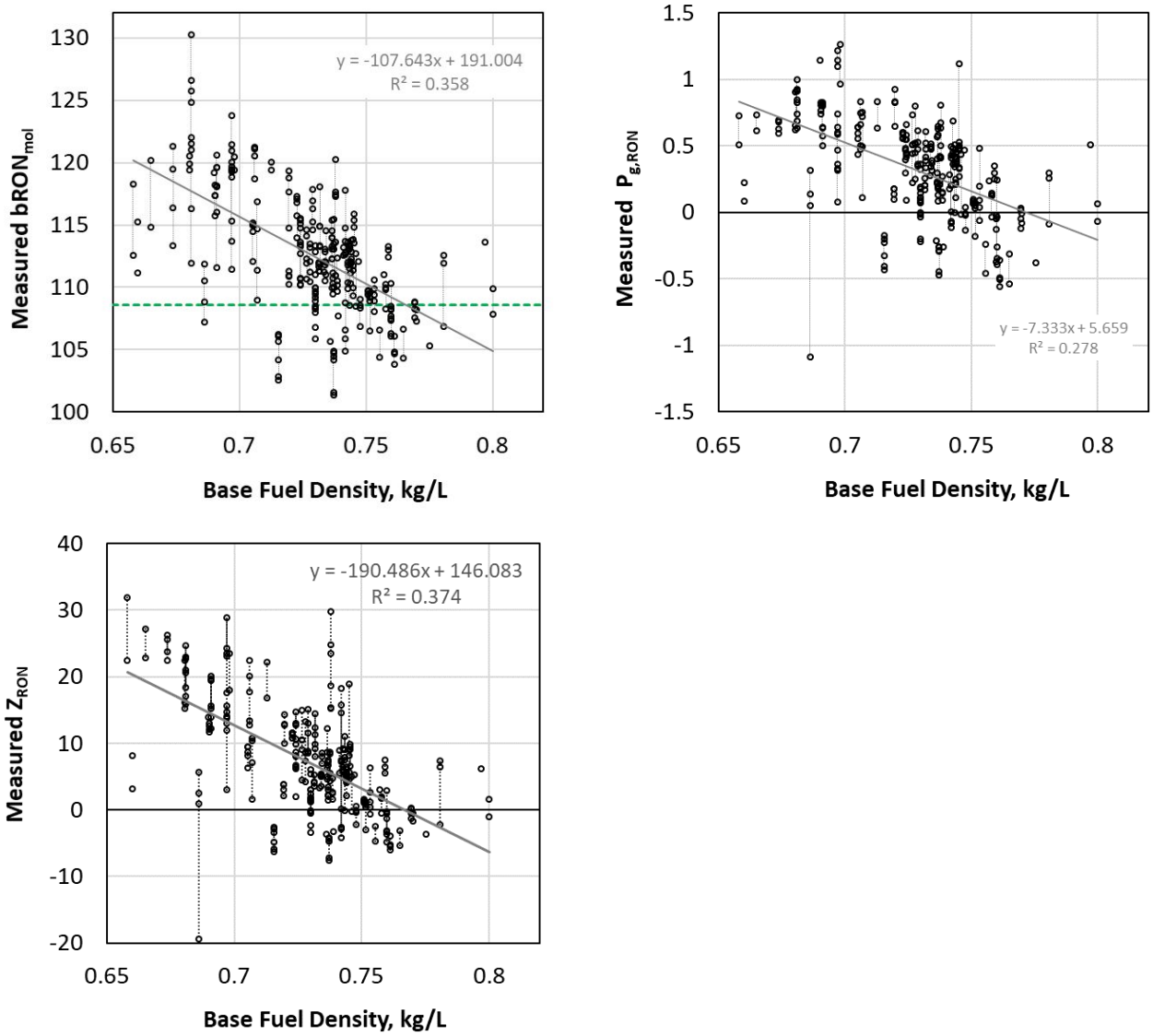

Figure S30. Measured $bRON_{mol}$, $P_{g,RON}$ and Z_{RON} values versus base fuel density. Dashed green line indicates the RON of neat ethanol.

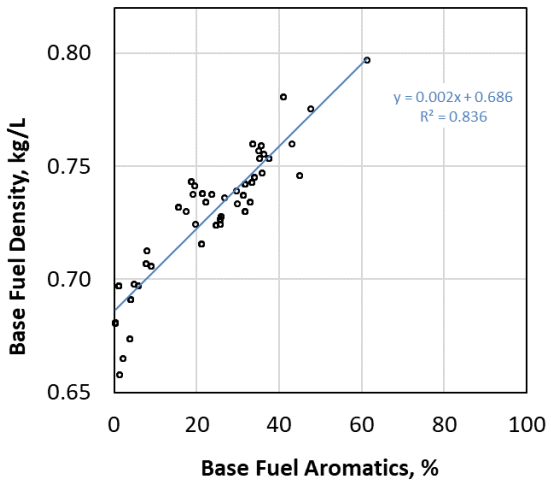

Figure S31. Density of base fuels versus aromatics content.

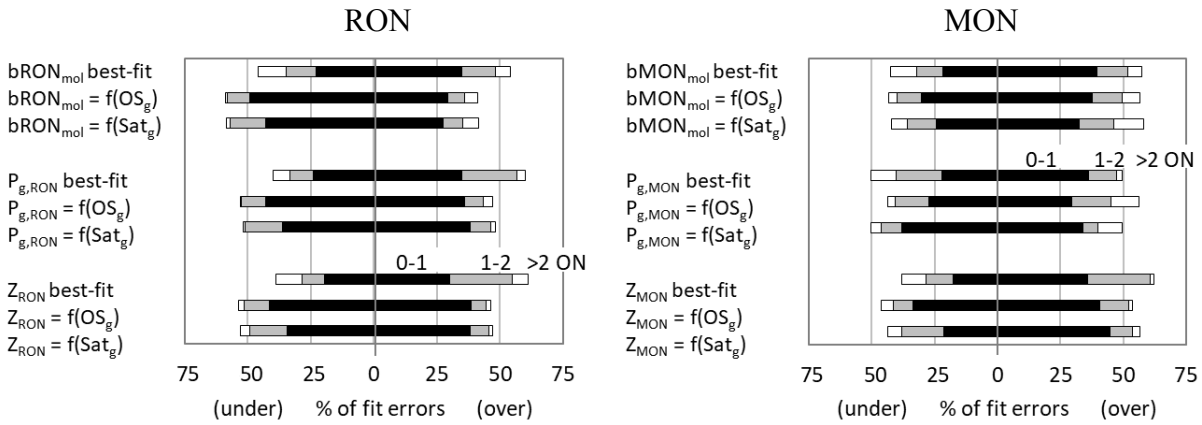

Figure S32. Goodness of fit for different ethanol octane blending models using least-squares regressed equations on base fuel OS ("= f(OS$_g$)") or saturates content ("= f(Sat$_g$)") and compared to versions with no base fuel dependence ("best-fit"). Bars show percentage of data with fit error of percentage of data with fit error 0-1 ON, 1-2 ON and >2 ON.

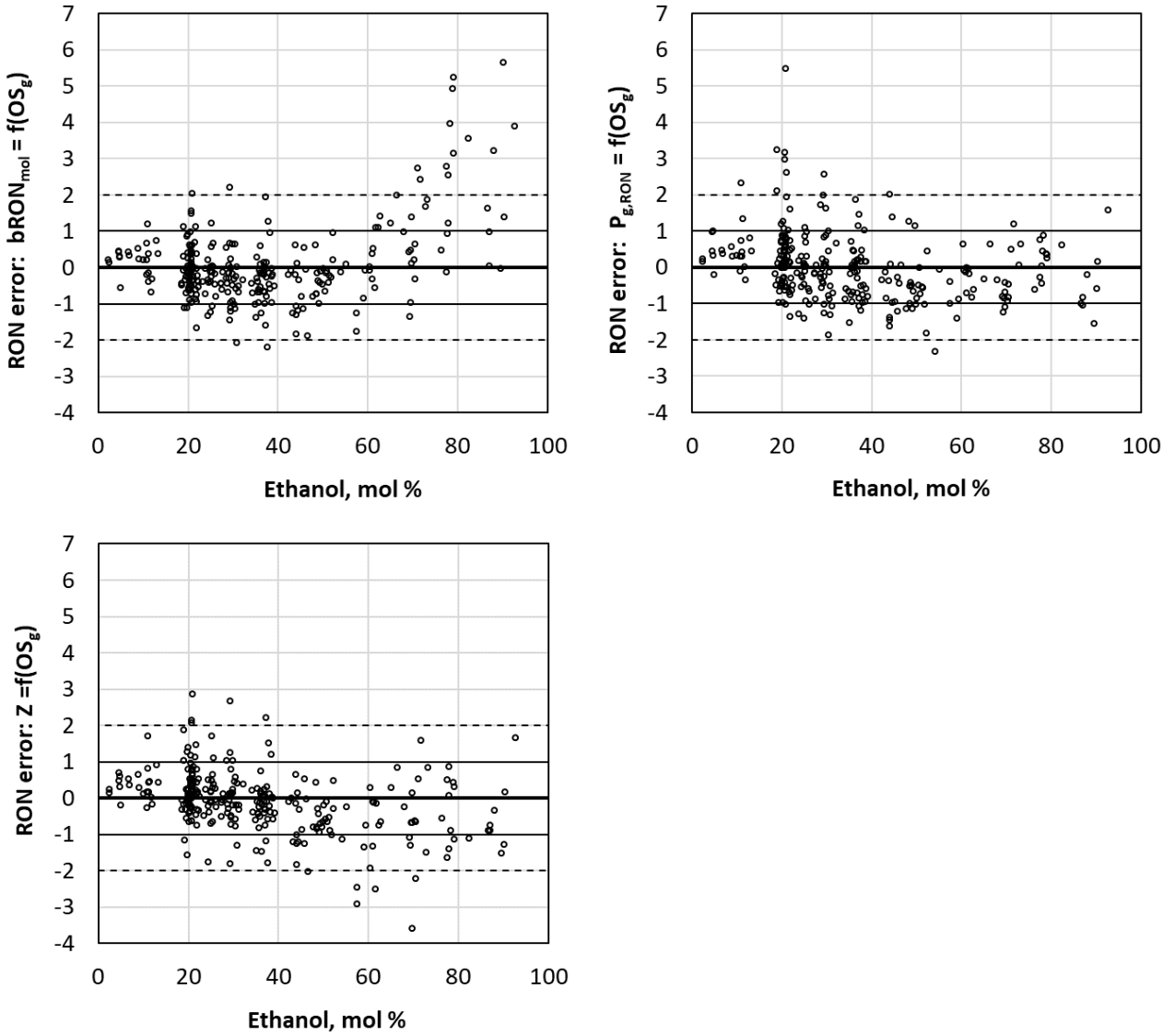

Figure S33. Error of RON prediction for ethanol blends using $bRON_{mol}$, $P_{g,RON}$, and Z_{RON} models incorporating base fuel OS data for fit equations shown in Table S5.

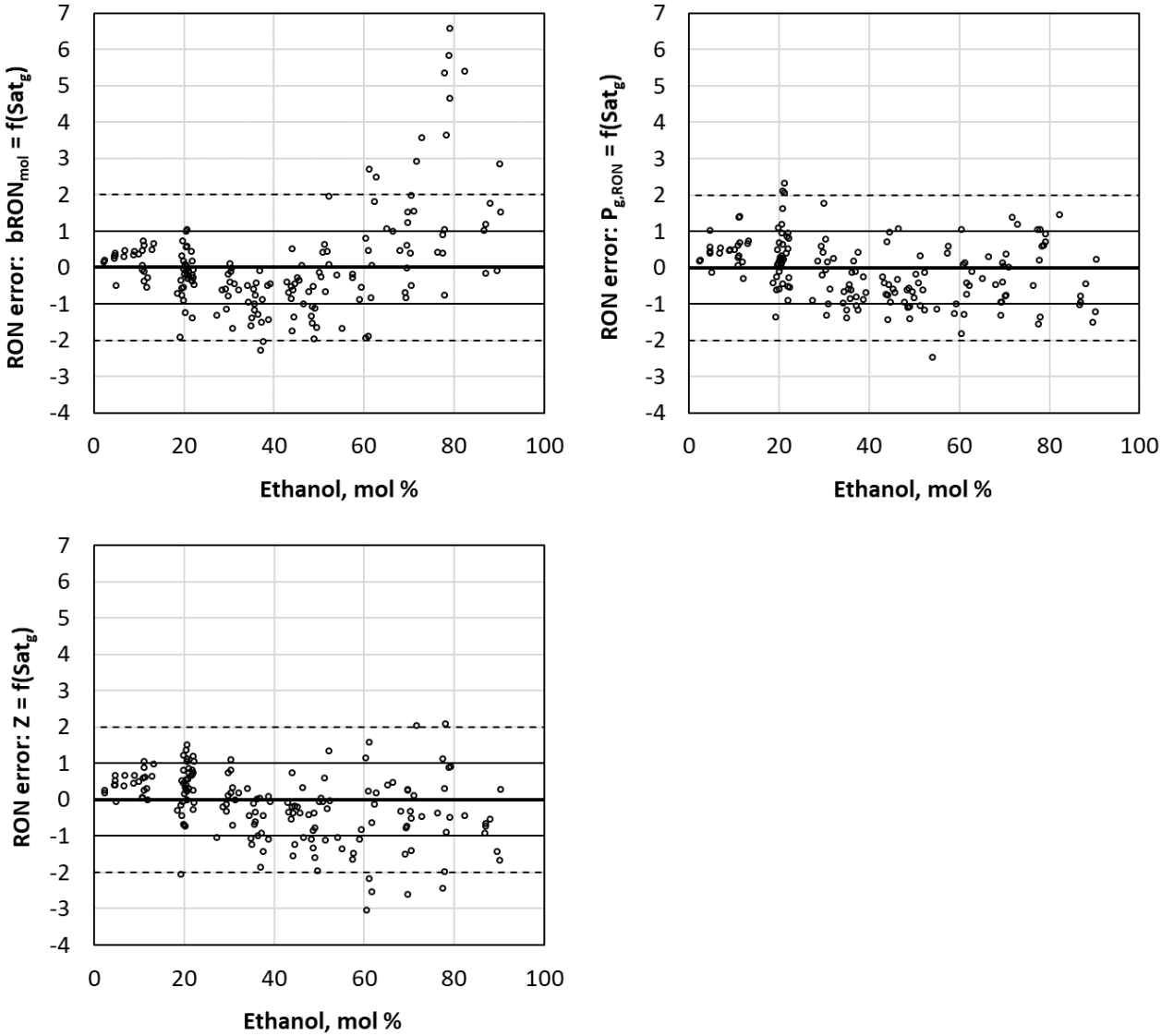

Figure S34. Error of RON prediction for ethanol blends using $bRON_{mol}$, $P_{g,RON}$, and Z_{RON} models incorporating base fuel saturates data for fit equations shown in Table S5.

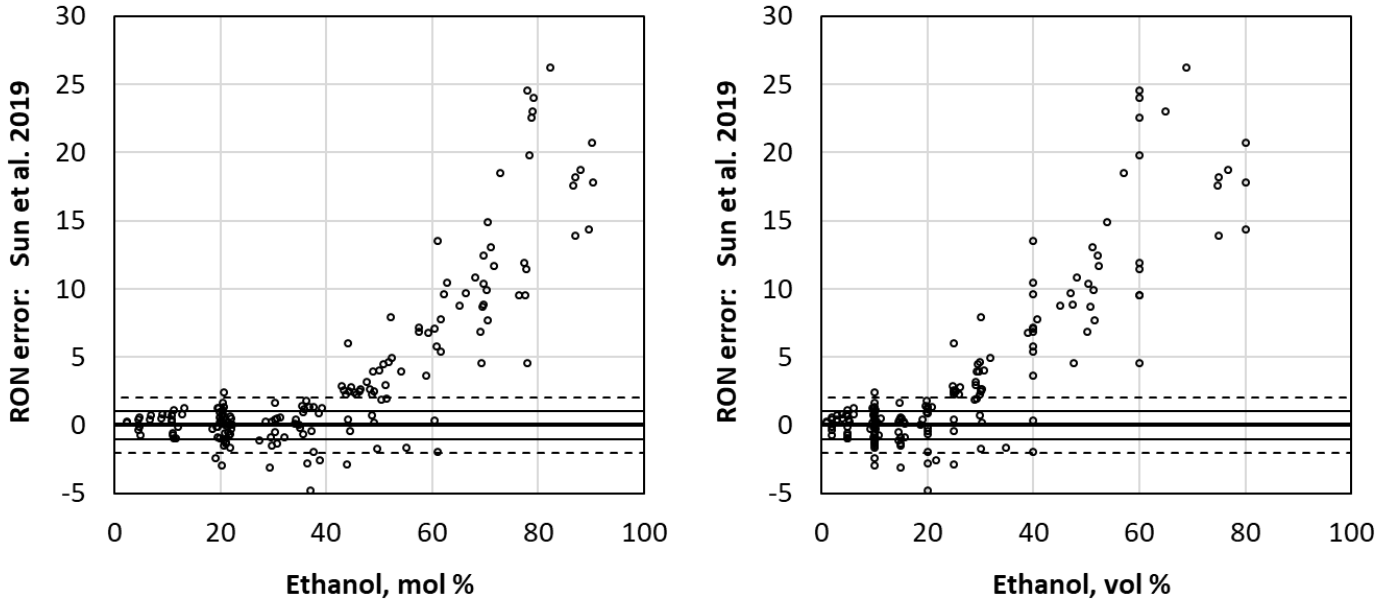

Figure S35. Error of RON prediction for ethanol blends using Sun et al. (2019) model [36] incorporating base fuel aromatics content with linear volume blending: $bRON_{vol} = 161.27 - 0.9117Arom_g$

SI-14.Models with dependence on multiple fuel properties

Table S7. Ethanol RON blending model equation coefficients (for $bRON_{mol}$, P_g and Z) from forward-step regression using molar ethanol content and either base fuel octane numbers (RON_g, OS_g) or blend octane numbers (RON_{blend}, OS_{blend}). Ethanol mol % = 0-100.

					equation coefficients for models					
parameters included	ON	model	n	adj. R^2	intercept	ethanol, mol %	RON_g	OS_g	RON_{blend}	OS_{blend}
ON_g	R	$bRON_{mol}$	280	60%	108.62		0.138559	-1.279		
ON_g+E	R	$bRON_{mol}$	280	60%	108.62	-	0.138559	-1.279		
ON_g	R	$P_{g,RON}$	280	54%	-0.813		0.0205	-0.1065		
ON_g+E	R	$P_{g,RON}$	280	58%	-1.118	0.00400	0.0223	-0.1053		
ON_g	R	Z_{RON}	280	60%	19.16		-	-1.834		
ON_g+E	R	Z_{RON}	280	67%	14.41	0.1109	-	-1.716		
ON_{blend}	R	$bRON_{mol}$	253	33%	71.30				0.578	-1.449
ON_{blend}+E	R	$bRON_{mol}$	253	51%	86.81	0.1294			0.403	-1.730946
ON_{blend}	R	$P_{g,RON}$	253	33%	-4.725				0.0631	-0.1068
ON_{blend}+E	R	$P_{g,RON}$	253	49%	-3.485	0.01033			0.0492	-0.1293
ON_{blend}	R	Z_{RON}	253	15%	-67.49				0.937	-1.614
ON_{blend}+E	R	Z_{RON}	253	52%	-28.39	0.3260			0.497	-2.325

Table S8. Ethanol MON blending model equation coefficients (for $bRON_{mol}$, P_g and Z) from forward-step regression using molar ethanol content and either base fuel octane numbers (RON_g, OS_g) or blend octane numbers (RON_{blend}, OS_{blend}). Ethanol mol % = 0-100.

					equation coefficients for models					
parameters included	ON	data set	n	adj. R^2	intercept	ethanol, mol %	RON_g	OS_g	RON_{blend}	OS_{blend}
ON_g	M	$bMON_{mol}$	272	39%	109.78		-0.118	-0.606		
ON_g+E	M	$bMON_{mol}$	272	44%	114.40	-0.0549	-0.145	-0.628		
ON_g	M	$P_{g,MON}$	272	32%	-0.813		0.0205	-0.1065		
ON_g+E	M	$P_{g,MON}$	272	41%	-1.118	0.00400	0.0223	-0.1053		
ON_g	M	Z_{MON}	272	58%	49.53		-0.386	-0.866		
ON_g+E	M	Z_{MON}	272	60%	44.39	0.0610	-0.356	-0.842		
ON_{blend}	M	$bMON_{mol}$	253	49%	81.15				0.310	-1.511
ON_{blend}+E	M	$bMON_{mol}$	253	68%	97.17	0.1335			0.130	-1.802
ON_{blend}	M	$P_{g,MON}$	236	50%	-21.94				0.294	-0.492
ON_{blend}+E	M	$P_{g,MON}$	236	56%	-19.21	0.0199			0.262	-0.527
ON_{blend}	M	Z_{MON}	253	18%	-34.01				0.636	-1.777
ON_{blend}+E	M	Z_{MON}	253	62%	21.47	0.3515			-	-2.305

Table S9. Ethanol RON blending model equation coefficients (for $bRON_{mol}$, P_g and Z) from forward-step regression using SOA hydrocarbon content (% = 0-100), molar ethanol content (% = 0-100), base fuel octane numbers (RON_g, OS_g) and density (kg/L) for the subset of fuels with base fuel SOA composition. Also shown are similar regressions using only base fuel octane numbers and ethanol content for the same fuel subset.

					equation coefficients for models						
parameters included	ON	data set	n	adj. R^2	intercept	ethanol, mol %	RON_g	OS_g	Sat_g	$Arom_g$	ρ_g
SOA	R	$bRON_{mol}$	168	61%	77.88				0.428	0.188	
SOA+E	R	$bRON_{mol}$	168	61%	77.88	-			0.428	0.188	
SOA+ON_g+E	R	$bRON_{mol}$	168	65%	89.06	-	0.097	-0.886	0.242	0.148	
SOA+ON_g+E+D	R	$bRON_{mol}$	168	65%	32.39	-	-	-0.381	0.324	-	81.8
ON_g (SOA set)	R	$bRON_{mol}$	168	62%	107.89		0.158	-1.466			
ON_g+E (SOA set)	R	$bRON_{mol}$	168	62%	107.89	-	0.158	-1.466			
SOA	R	$P_{g,RON}$	168	54%	-2.725				0.0357	0.0226	
SOA+E	R	$P_{g,RON}$	168	59%	-2.569	0.00390			0.0323	0.0196	
SOA+ON_g+E	R	$P_{g,RON}$	168	67%	-2.816	0.00475	0.0196	-0.0786	0.0192	0.0161	
SOA+ON_g+E+D	R	$P_{g,RON}$	168	67%	-2.816	0.00475	0.0196	-0.0786	0.0192	0.0161	-
ON_g (SOA set)	R	$P_{g,RON}$	168	53%	-0.786		0.0205	-0.1078			
ON_g+E (SOA set)	R	$P_{g,RON}$	168	64%	-1.219	0.00536	0.0230	-0.1080			
SOA	R	Z_{RON}	168	63%	-52.62				0.748	0.340	
SOA+E	R	Z_{RON}	168	75%	-47.82	0.1200			0.643	0.246	
SOA+ON_g+E	R	Z_{RON}	168	76%	-17.86	0.1220	-	-1.180	0.343	0.181	
SOA+ON_g+E+D	R	Z_{RON}	168	76%	-17.86	0.1220	-	-1.180	0.343	0.181	-
ON_g (SOA set)	R	Z_{RON}	168	63%	20.89		-	-2.032			
ON_g+E (SOA set)	R	Z_{RON}	168	74%	14.99	0.1303	-	-1.920			

Table S10. Ethanol MON blending model equation coefficients (for $bRON_{mol}$, P_g and Z) from forward-step regression using SOA hydrocarbon content (% = 0-100), molar ethanol content (% = 0-100), base fuel octane numbers (RON_g, OS_g) and density (kg/L) for the subset of fuels with base fuel SOA composition. Also shown are similar regressions for the same fuel subset using only base fuel octane numbers and ethanol content.

					equation coefficients for models						
parameters included	ON	data set	n	adj. R^2	intercept	ethanol, mol %	RON_g	OS_g	Sat_g	$Arom_g$	ρ_g
SOA	M	$bMON_{mol}$	145	39%	66.13				0.358	0.173	
SOA+E	M	$bMON_{mol}$	145	48%	62.80	-0.0680			0.427	0.227	
SOA+ON_g+E	M	$bMON_{mol}$	145	58%	89.27	-0.0829	-0.188	-0.295	0.318	0.234	
SOA+ON_g+E+D	M	$bMON_{mol}$	145	58%	89.27	-0.0829	-0.188	-0.295	0.318	0.234	-
ON_g (SOA set)	M	$bMON_{mol}$	145	44%	101.64		-	-0.987			
ON_g+E (SOA set)	M	$bMON_{mol}$	145	53%	113.68	-0.0725	-0.109	-0.910			
SOA	M	$P_{g,MON}$	145	37%	-5.924				0.0860	0.0533	
SOA+E	M	$P_{g,MON}$	145	41%	-5.282	0.01111			0.0738	0.0432	
SOA+ON_g+E	M	$P_{g,MON}$	145	61%	-11.608	0.01562	0.0917	-0.1682	0.0633	0.0401	
SOA+ON_g+E+D	M	$P_{g,MON}$	145	61%	-11.608	0.01562	0.0917	-0.1682	0.0633	0.0401	-
ON_g (SOA set)	M	$P_{g,MON}$	145	44%	-5.214		0.0989	-0.3259			
ON_g+E (SOA set)	M	$P_{g,MON}$	145	57%	-6.959	0.01771	0.1099	-0.3167			
SOA	M	Z_{MON}	145	57%	-41.91				0.650	0.269	
SOA+E	M	Z_{MON}	145	58%	-39.54	0.0485			0.601	0.231	
SOA+ON_g+E	M	Z_{MON}	145	77%	13.85	-	-0.532	0.074	0.511	0.281	
SOA+ON_g+E+D	M	Z_{MON}	145	77%	13.85	-	-0.532	0.074	0.511	0.281	-
ON_g (SOA set)	M	Z_{MON}	145	71%	51.70		-0.380	-1.272			
ON_g+E (SOA set)	M	Z_{MON}	145	71%	51.70	-	-0.380	-1.272			

Table S11. Ethanol RON blending model equation coefficients (for $bRON_{mol}$, P_g and Z) from forward-step regression using PIONA hydrocarbon content (% = 0-100), molar ethanol content (% = 0-100), base fuel octane numbers (RON_g, OS_g) and density (kg/L) for the subset of fuels with base fuel PIONA composition. Also shown are similar regressions for the same fuel subset using only base fuel octane numbers and ethanol content or only SOA hydrocarbon composition and ethanol content.

					equation coefficients for models									
parameters included	ON	data set	n	adj. R^2	intercept	ethanol, mol %	RON_g	OS_g	Sat_g	$Arom_g$	$nPar_g$	$iPar_g$	$Naph_g$	ρ_g
PIONA	R	$bRON_{mol}$	134	54%	119.68					-0.266	-	-	-	
PIONA+E	R	$bRON_{mol}$	134	61%	122.13	-0.0586				-0.259	-	-	-	
PIONA+ON_g+E	R	$bRON_{mol}$	134	65%	114.66	-0.0489	0.097	-0.791		-0.122	-	-	0.078	
PIONA+ON_g+E+D	R	$bRON_{mol}$	134	65%	114.66	-0.0489	0.097	-0.791		-0.122	-	-	0.078	-
ON_g (PIONA set)	R	$bRON_{mol}$	134	59%	106.21		0.178	-1.331						
ON_g+E (PIONA set)	R	$bRON_{mol}$	134	63%	108.95	-0.0434	0.164	-1.332						
SOA (PIONA set)	R	$bRON_{mol}$	134	58%	95.57				0.249	-				
SOA+E (PIONA set)	R	$bRON_{mol}$	134	65%	98.65	-0.0556			0.241	-				
PIONA	R	$P_{g,RON}$	134	44%	-0.244					-	0.00622	0.0118	-	
PIONA+E	R	$P_{g,RON}$	134	48%	-0.401	0.00284				-	0.00630	0.0123	-	
PIONA+ON_g+E	R	$P_{g,RON}$	134	59%	-1.354	0.00316	0.0264	-0.1052		-	-	-0.000783	-	
PIONA+ON_g+E+D	R	$P_{g,RON}$	134	59%	-1.354	0.00316	0.0264	-0.1052		-	-	-0.000783	-	-
ON_g (PIONA set)	R	$P_{g,RON}$	134	54%	-1.105		0.0240	-0.0947						
ON_g+E (PIONA set)	R	$P_{g,RON}$	134	59%	-1.304	0.00317	0.0250	-0.0998						
SOA (PIONA set)	R	$P_{g,RON}$	134	44%	-1.599				0.0242	0.0122				
SOA+E (PIONA set)	R	$P_{g,RON}$	134	47%	-1.786	0.00229			0.0251	0.0129				
PIONA	R	Z_{RON}	134	63%	-49.55					0.276	0.778	0.678	1.028	
PIONA+E	R	Z_{RON}	134	69%	-55.18	0.0911				0.297	0.783	0.704	0.997	
PIONA+ON_g+E	R	Z_{RON}	134	69%	15.50	0.1113	-	-1.560		-0.129	-	-	0.141	
PIONA+ON_g+E+D	R	Z_{RON}	134	71%	77.42	0.1031	-	-1.472		-	-	-	0.211	-90.0
ON_g (PIONA set)	R	Z_{RON}	134	56%	20.36		-	-1.831						
ON_g+E (PIONA set)	R	Z_{RON}	134	67%	15.58	0.1213	-	-1.959						
SOA (PIONA set)	R	Z_{RON}	134	56%	-19.42				0.407	-				
SOA+E (PIONA set)	R	Z_{RON}	134	64%	-25.17	0.1037			0.422	-				

Table S12. Ethanol MON blending model equation coefficients (for $bRON_{mol}$, P_g and Z) from forward-step regression using PIONA hydrocarbon content (% = 0-100), molar ethanol content (% = 0-100), base fuel octane numbers (RON_g, OS_g) and density (kg/L) for the subset of fuels with base fuel PIONA composition. Also shown are similar regressions for the same fuel subset using only base fuel octane numbers and ethanol content or only SOA hydrocarbon composition and ethanol content.

					equation coefficients for models									
parameters included	ON	data set	n	adj. R^2	intercept	ethanol, mol %	RON_g	OS_g	Sat_g	$Arom_g$	$nPar_g$	$iPar_g$	$Naph_g$	ρ_g
PIONA	M	$bMON_{mol}$	111	40%	57.51					0.219	0.555	0.412	0.638	
PIONA+E	M	$bMON_{mol}$	111	61%	67.28	-0.1155				0.167	0.532	0.360	0.591	
PIONA+ON_g+E	M	$bMON_{mol}$	111	61%	89.48	-0.1158	-0.096	-0.372		-	0.310	0.140	0.311	
PIONA+ON_g+E+D	M	$bMON_{mol}$	111	61%	89.48	-0.1158	-0.096	-0.372		-	0.310	0.140	0.311	-
ON_g (PIONA set)	M	$bMON_{mol}$	111	36%	101.80		-	-1.015						
ON_g+E (PIONA set)	M	$bMON_{mol}$	111	57%	117.64	-0.1158	-0.138	-0.737						
SOA (PIONA set)	M	$bMON_{mol}$	111	30%	80.82				0.211	-				
SOA+E (PIONA set)	M	$bMON_{mol}$	111	49%	86.43	-0.1106			0.204	-				
PIONA	M	$P_{g,MON}$	111	43%	-0.321					-	-	0.0381	-	
PIONA+E	M	$P_{g,MON}$	111	47%	-0.788	0.00896				-	-	0.0390	-	
PIONA+ON_g+E	M	$P_{g,MON}$	111	59%	-7.271	0.01061	0.0925	-0.1950		-	0.0307	0.019798	-	
PIONA+ON_g+E+D	M	$P_{g,MON}$	111	59%	-7.271	0.01061	0.0925	-0.1950		-	0.0307	0.019798	-	-
ON_g (PIONA set)	M	$P_{g,MON}$	111	50%	-5.773		0.1043	-0.2961						
ON_g+E (PIONA set)	M	$P_{g,MON}$	111	55%	-6.654	0.01150	0.1092	-0.3116						
SOA (PIONA set)	M	$P_{g,MON}$	111	32%	-1.412				0.0406	-				
SOA+E (PIONA set)	M	$P_{g,MON}$	111	35%	-1.872	0.00835			0.0415	-				
PIONA	M	Z_{MON}	111	66%	-47.09					0.243	0.972	0.618	1.019	
PIONA+E	M	Z_{MON}	111	65%	-47.09	-				0.243	0.972	0.618	1.019	
PIONA+ON_g+E	M	Z_{MON}	111	67%	43.64	-	-0.308	-0.770		-0.165	0.167	-	-	
PIONA+ON_g+E+D	M	Z_{MON}	111	67%	124.05	-	-0.466	-0.579		-	-	-	-	-94.6
ON_g (PIONA set)	M	Z_{MON}	111	64%	47.95		-0.332	-1.346						
ON_g+E (PIONA set)	M	Z_{MON}	111	64%	47.95	-	-0.332	-1.346						
SOA (PIONA set)	M	Z_{MON}	111	45%	-16.59				0.388	-				
SOA+E (PIONA set)	M	Z_{MON}	111	45%	-16.59	-			0.388	-				

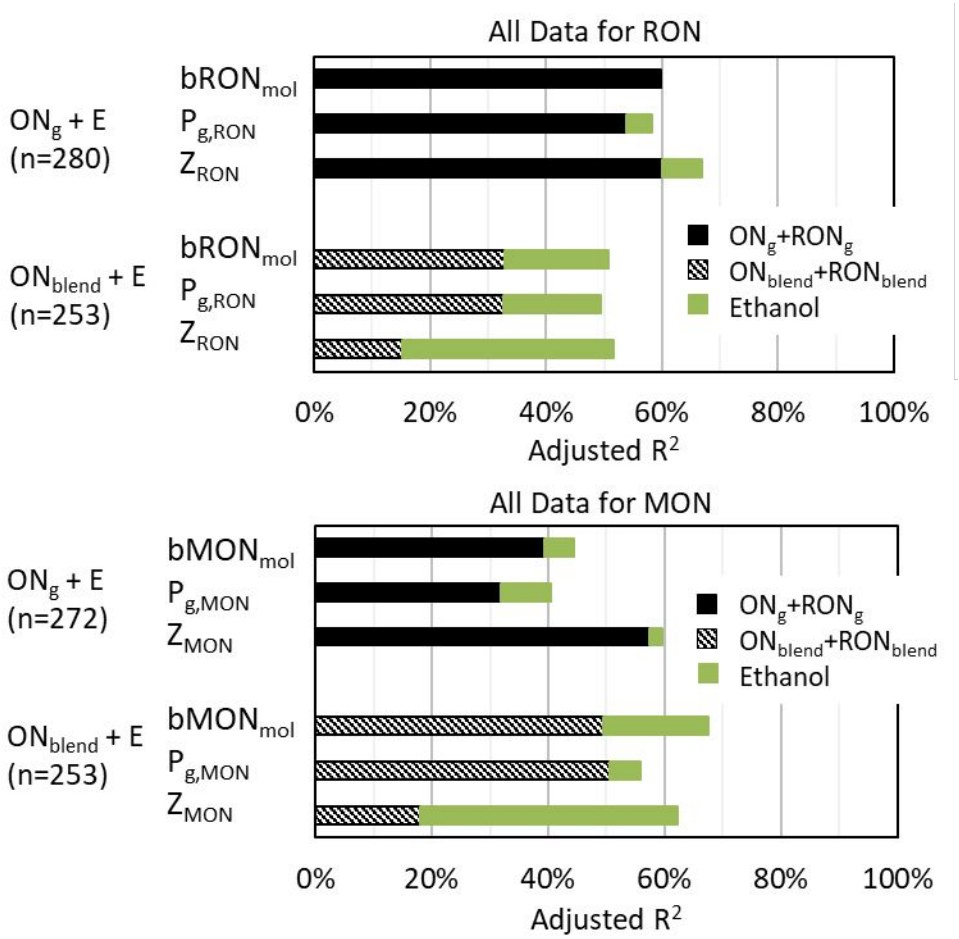

Figure S36. Increasing adjusted R^2 of fits for ethanol RON (top) and MON (bottom) model equation coefficients using entire data set from forward-step regression for bON_{mol}, P_g and Z approaches. "ON_g + E" stacked bars show results starting with only base fuel octane numbers (OS_g and RON_g) and then after adding ethanol content. "ON_{blend} + E" stacked bars show results starting with only blend octane numbers (OS_{blend} and RON_{blend}) and then adding ethanol content.

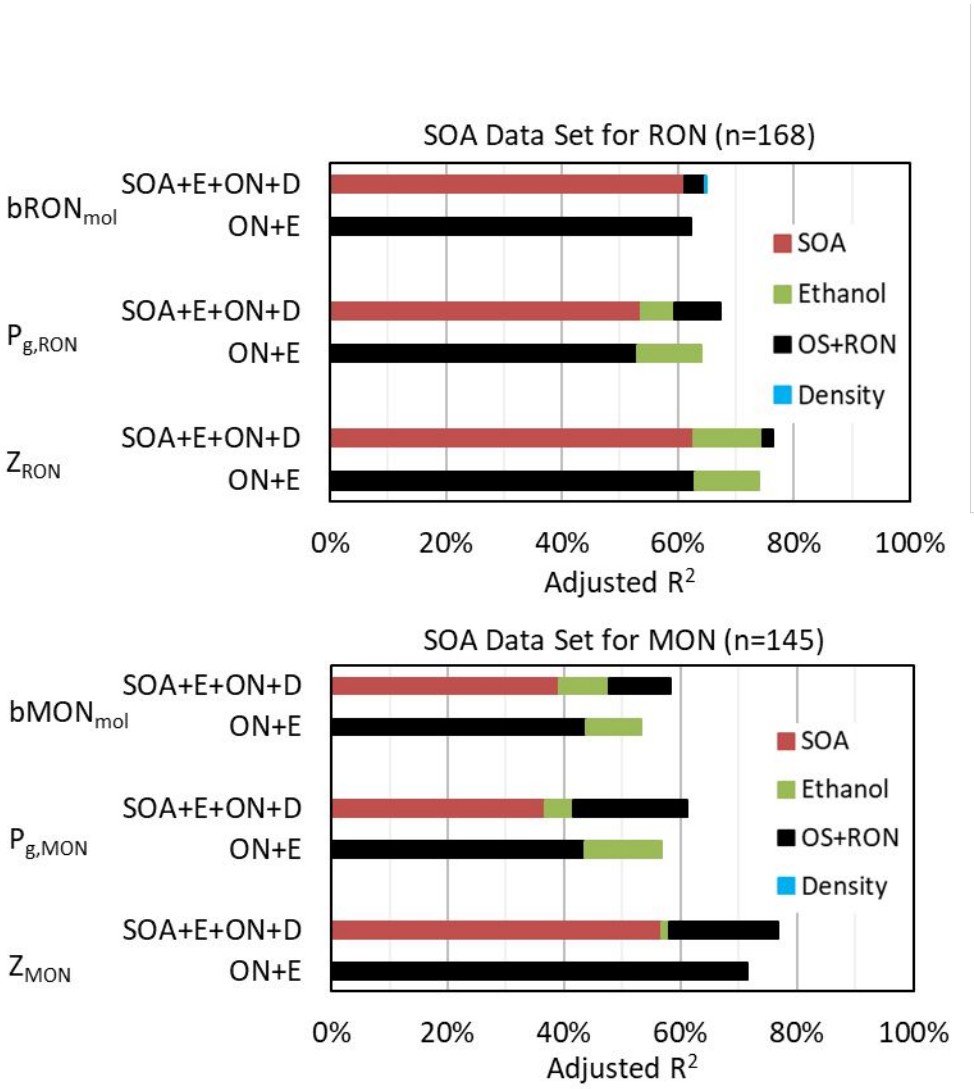

Figure S37. Increasing adjusted R^2 of fits for ethanol RON (top) and MON (bottom) model equation coefficients using consistent SOA data set from forward-step regression for bON_{mol}, P_g and Z approaches. "SOA" stacked bars show results starting with only base fuel hydrocarbon composition (saturates, olefins, aromatics), then successively adding ethanol content, base fuel octane numbers (OS_g and RON_g) and base fuel density. "ON" bars show result for same data set (only blends with SOA data) starting with base fuel octane numbers and then adding ethanol content. n=168 for all RON cases; n=145 for all MON cases.

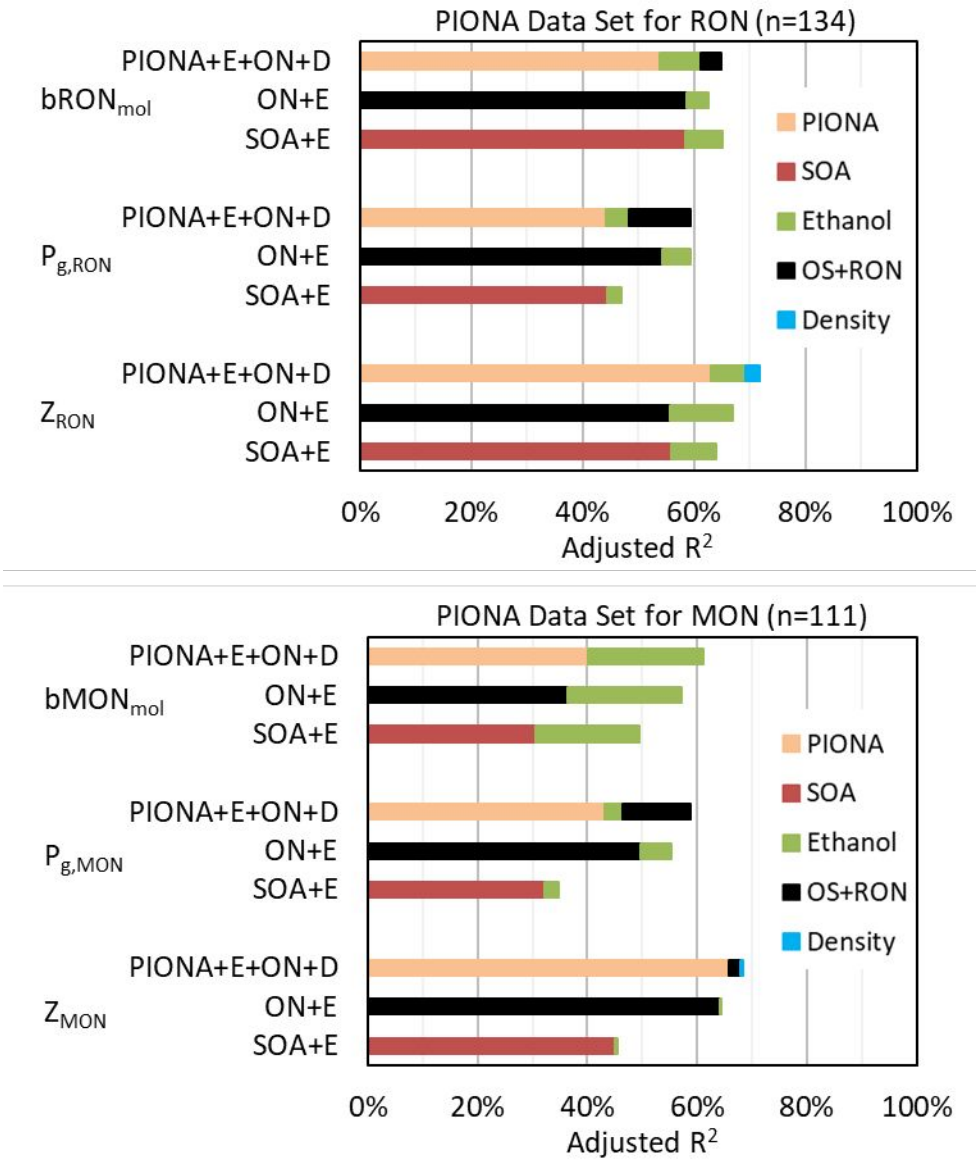

Figure S38. Increasing adjusted R^2 of fits for ethanol RON (top) and MON (bottom) model equation coefficients using consistent SOA data set from forward-step regression for bON_{mol}, P_g and Z approaches. "PIONA+E+ON+D" stacked bars show results starting with only base fuel hydrocarbon composition (n-paraffins, iso-paraffins, naphthenes, olefins, aromatics), then successively adding ethanol content, base fuel octane numbers (OS_g and RON_g) and base fuel density. "ON+E" stacked bars show result for same data sets (only blends with PIONA data) starting with base fuel octane numbers and then adding ethanol content. "SOA" stacked bars show result for same data sets (only blends with PIONA data) starting with base fuel SOA hydrocarbon composition (saturates, olefins, aromatics) and then adding ethanol content. n=134 for all RON cases; n=111 for all MON cases.

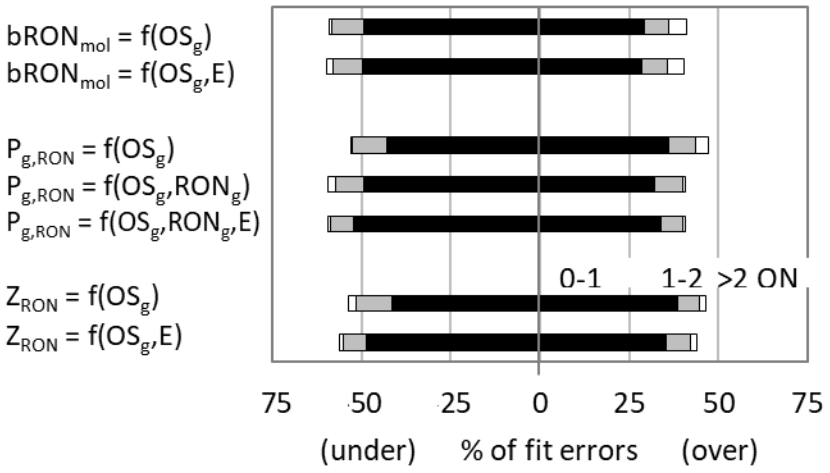

Figure S39. Goodness of fit for univariate and multivariate ethanol RON blending models utilizing base fuel octane numbers (OS_g, RON_g) and molar ethanol content (E). Bar segments show percentage of data with positive and negative fit error of 0-1 ON, 1-2 ON, and >2 ON. Model coefficients given in Tables S5 and S7. n=280.

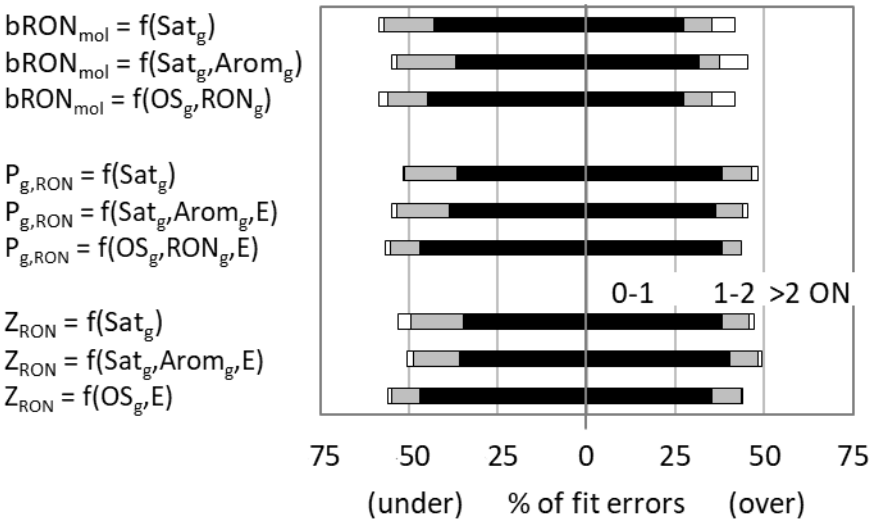

Figure S40. Goodness of fit for univariate and multivariate ethanol RON blending models utilizing SOA hydrocarbon composition (Sat_g, $Arom_g$) and molar ethanol content (E). Comparisons shown for same data set for models utilizing base fuel octane numbers (OS_g, RON_g) and molar ethanol content. Bar segments show percentage of data with positive and negative fit error of 0-1 ON, 1-2 ON, and >2 ON. Model coefficients given in Tables S5 and S8. n=168.

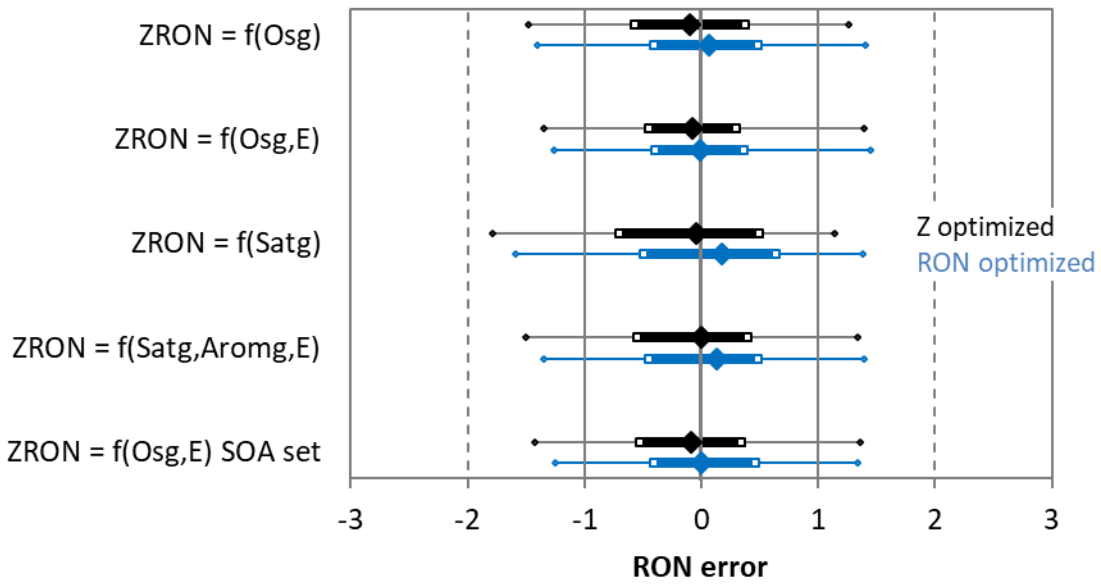

Figure S41. Box plots of fitting errors for ethanol RON blending models using base fuel octane numbers (OS_g, RON_g), hydrocarbon type content (Sat_g, $Arom_g$) and/or molar ethanol content. Black lines and symbols show results for models optimized around Z values (forward-step linear regression on Z values); blue lines and symbols show models optimized around RON values (minimizing sum of squared RON errors). Central diamonds = 50th percentile (median), inner dark bars = 25-75th percentile, and outer whiskers = 5-95th percentile of errors.

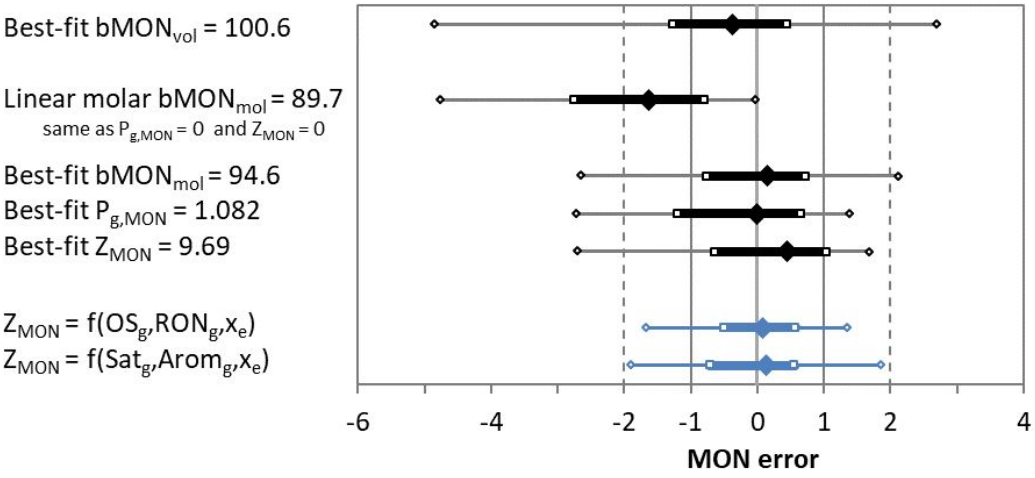

Figure S42. Box plots of MON_{blend} fitting errors for ethanol MON blending models using base fuel octane numbers (OS_g, RON_g), hydrocarbon type content (Sat_g, $Arom_g$) and/or molar ethanol content (two blue lines). For reference, plots for generic models without base fuel dependence (black lines) are also shown. Central diamonds = 50th percentile (median), inner dark bars = 25-75th percentile, and outer whiskers = 5-95th percentile of errors.

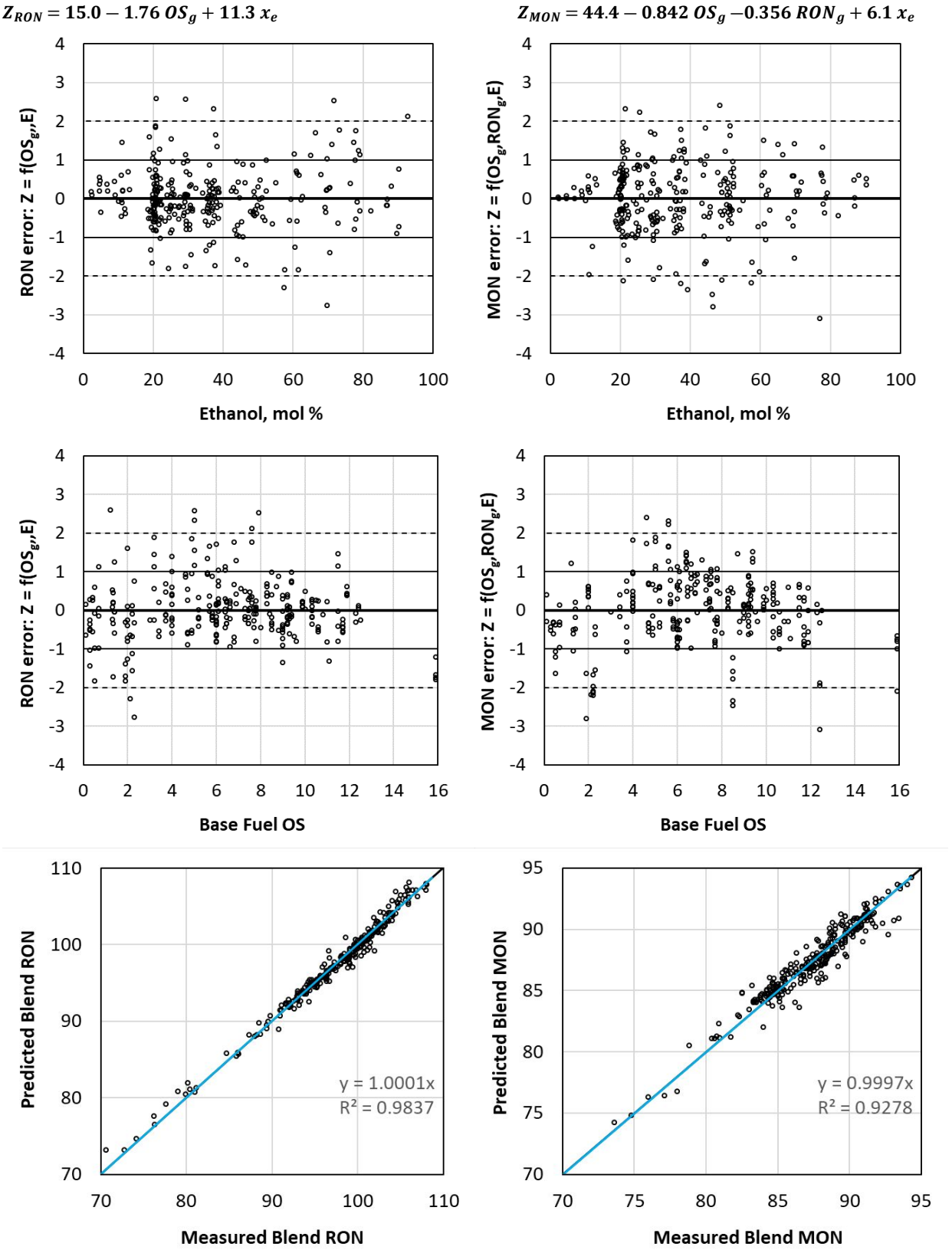

Figure S43. Error of RON and MON predictions for ethanol blends using Z models based on base fuel octane ratings and ethanol content, plotted versus ethanol content (top) and base fuel OS (middle), and predicted versus measured (bottom).

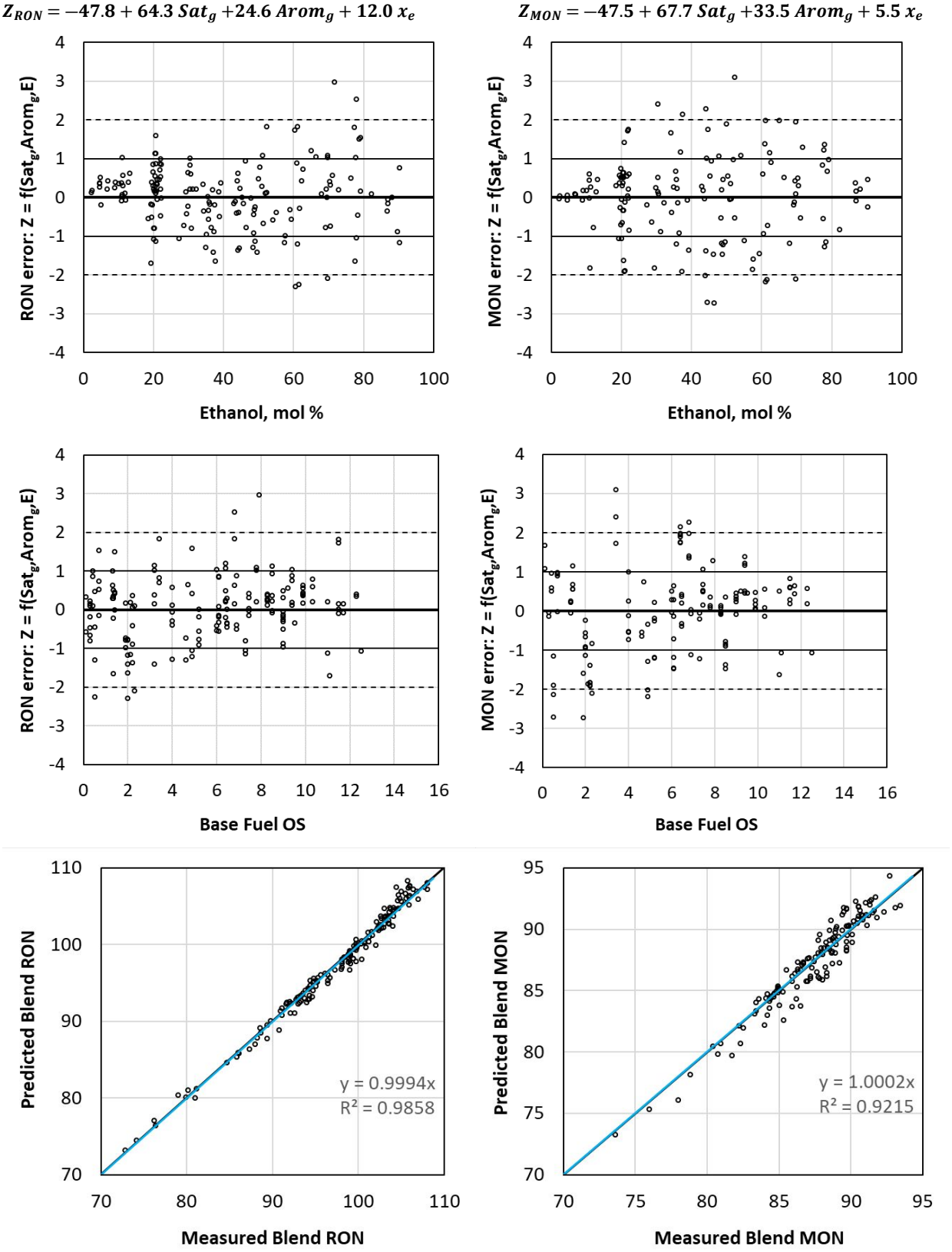

Figure S44. Error of RON and MON predictions for ethanol blends using Z models based on base fuel hydrocarbon composition and ethanol content, plotted versus ethanol content (top) and base fuel OS (middle), and predicted versus measured (bottom)

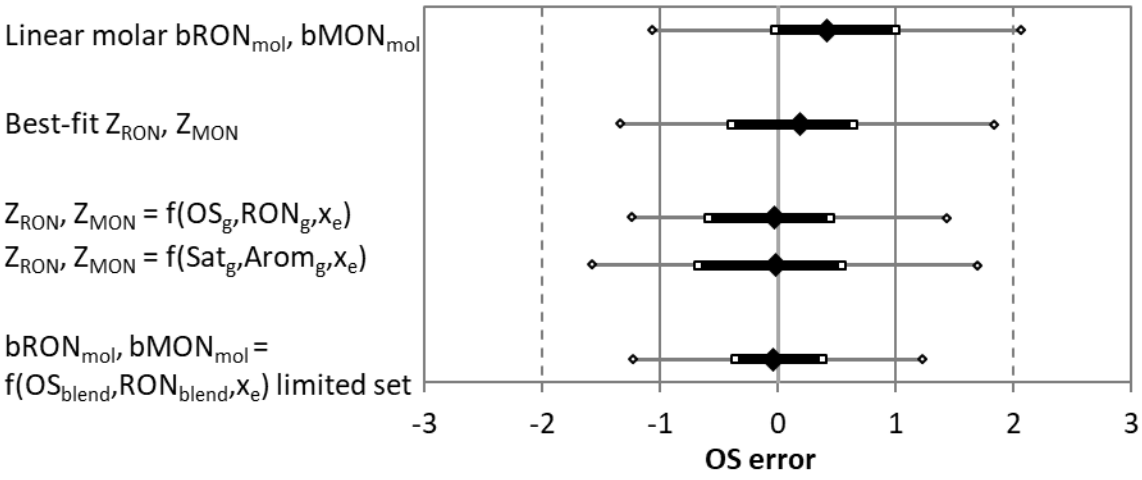

Figure S45. Box plot of OS_{blend} errors resulting from ethanol $bRON_{mol}$ and $bMON_{mol}$ blending models over limited ethanol and RON range (ethanol < 35 vol % and RON_{blend} = 91-100) based on blend octane numbers (OS_{blend}, RON_{blend}) and/or molar ethanol content (bottom set). For comparison, similar OS_{blend} error distributions are shown for Z-based models based on base fuel octane numbers (OS_g, RON_g), hydrocarbon type content (Sat_g, $Arom_g$) and/or molar ethanol content (middle sets). For reference, plots for two generic models without base fuel dependence are also shown (top sets). Central diamonds = 50th percentile (median), inner dark bars = 25-75th percentile, and outer whiskers = 5-95th percentile of errors.

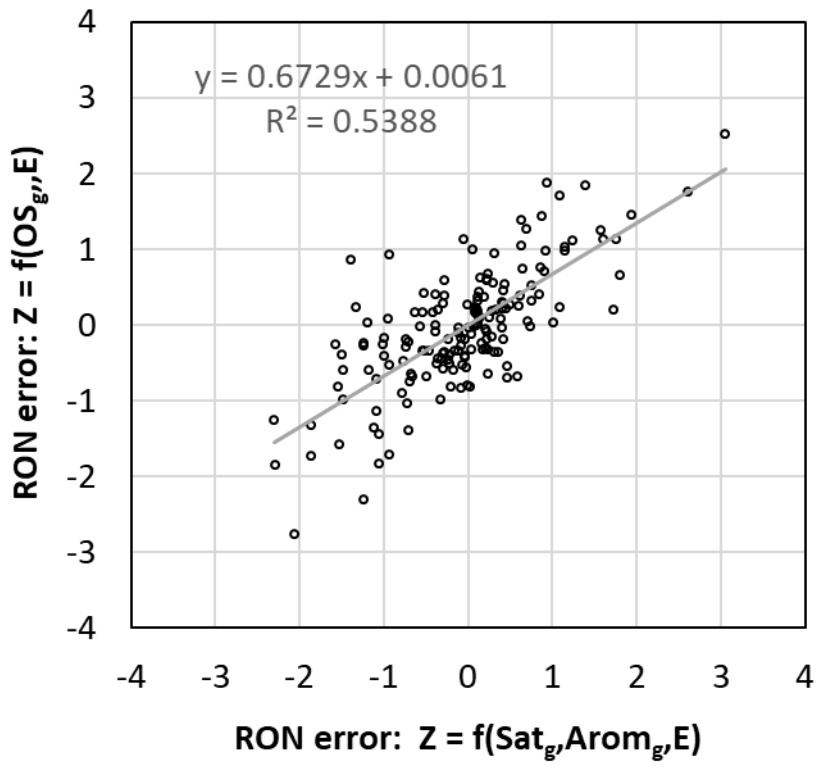

Figure S46. Comparison of RON_{blend} prediction errors for Z_{RON} models using (x axis) base fuel saturates and aromatic content and blend ethanol content or (y axis) base fuel octane sensitivity and blend ethanol content.

SI-15. Solving for base fuel octane ratings from blend octane ratings using Z blending model equations

The equations in Table 2 (summarized below) provide estimates of blend octane ratings (RON_{blend}, MON_{blend}) using known base gasoline octane ratings (RON_g, MON_g), the Z_{RON} and Z_{MON} parameters (which are themselves functions of RON_g and OS_g or MON_g), and the molar ethanol fraction (x_e=0-1).

$$RON_{blend} = (1 - x_e)RON_g + x_e RON_e + Z_{RON}\, x_e(1 - x_e)$$

$$MON_{blend} = (1 - x_e)MON_g + x_e MON_e + Z_{MON}\, x_e(1 - x_e)$$

$$Z_{RON} = a + b\, RON_g + c\, OS_g + d\, x_e$$

where a = 15.0, b = 0, c = -1.76 and d = 11.3

$$Z_{MON} = a' + b'\, RON_g + c'\, OS_g + d'\, x_e$$

where a′ = 44.4, b′ = -0.356, c′ = -0.842 and d′ = 6.1

With the appropriate algebraic manipulations, these equations can be solved for the octane ratings of the base gasoline. The resulting equations are shown below.

$$RON_g = \left(A_R/C_R + B_R A_M/(C_R C_M)\right)/\left(1 + B_R B_M/(C_R C_M)\right)$$

$$MON_g = \left(A_M - B_M RON_g\right)/C_M$$

where

$$A_R = RON_{blend} - x_e RON_e + x_e(1 - x_e)(\mathrm{a} + \mathrm{d}x_e)$$

$$B_R = x_e(1 - x_e)\ \mathrm{c}$$

$$C_R = (1 - x_e)(1 + x_e(\mathrm{b} + \mathrm{c}))$$

$$A_M = MON_{blend} - x_e MON_e - x_e(1 - x_e)(\mathrm{a}' + \mathrm{d}' x_e)$$

$$B_M = x_e(1 - x_e)(\mathrm{b}' + \mathrm{c}')$$

$$C_M = (1 - x_e)(1 - \mathrm{c}'\, x_e)$$

SI-16. Models developed for limited ethanol and RON range

To mitigate the limitation of the bON_{mol} approach for high ethanol content blends, additional forward-step linear regressions were conducted for a data subset including only low- to mid-level ethanol content blends (<35 vol %) with blend RON of 91-100. Results are shown in Tables S13-S14 and Figures S45-S51.

Table S13. Ethanol RON blending model equation coefficients from forward-step regression fitted over limited ethanol and RON range (ethanol < 35 vol % and RON_{blend} = 91-100) using base fuel octane numbers (RON_g, OS_g) or blend octane numbers (RON_{blend}, OS_{blend}), and ethanol content (% = 0-100).

					equation coefficients for models					
parameters included	ON	model	n	adj. R^2	intercept	ethanol, mol %	RON_g	OS_g	RON_{blend}	OS_{blend}
ON_g	R	$bRON_{mol}$	152	67%	121.58		-	-1.327		
ON_g+E	R	$bRON_{mol}$	152	69%	118.79	0.0752	-	-1.218		
ON_g	R	$P_{g,RON}$	152	55%	0.832		-	-0.084		
ON_g+E	R	$P_{g,RON}$	152	62%	-1.407	0.0105	0.0231	-0.100		
ON_g	R	Z_{RON}	152	71%	37.33		-0.226	-1.635		
ON_g+E	R	Z_{RON}	152	76%	12.99	0.1699	-	-1.702		
ON_{blend}	R	$bRON_{mol}$	145	33%	64.35				0.669	-1.691
ON_{blend}+E	R	$bRON_{mol}$	145	61%	87.998	0.2340			0.355	-1.646
ON_{blend}	R	$P_{g,RON}$	145	29%	-4.43				0.060	-0.113
ON_{blend}+E	R	$P_{g,RON}$	145	53%	-2.870	0.0154			0.039	-0.110
ON_{blend}	R	Z_{RON}	145	29%	-62.25				0.935	-2.277
ON_{blend}+E	R	Z_{RON}	145	67%	-22.33	0.3934			0.405	-2.201

Table S14. Ethanol MON blending model equation coefficients from forward-step regression fitted over limited ethanol and RON range (ethanol < 35 vol % and RON_{blend} = 91-100) using base fuel octane numbers (RON_g, OS_g) or blend octane numbers (RON_{blend}, OS_{blend}), and ethanol content (% = 0-100).

					equation coefficients for models					
parameters included	ON	data set	n	adj. R^2	intercept	ethanol, mol %	RON_g	OS_g	RON_{blend}	OS_{blend}
ON_g	M	$bMON_{mol}$	151	50%	102.48		-	-1.046		
ON_g+E	M	$bMON_{mol}$	151	50%	102.48	-	-	-1.046		
ON_g	M	$P_{g,MON}$	145	38%	-8.53		0.139	-0.391		
ON_g+E	M	$P_{g,MON}$	145	41%	-11.96	0.0201	0.173	-0.412		
ON_g	M	Z_{MON}	151	56%	44.77		-0.319	-1.181		
ON_g+E	M	Z_{MON}	151	57%	15.14	0.1123	-	-1.481		
ON_{blend}	M	$bMON_{mol}$	145	57%	49.73				0.679	-2.012
ON_{blend}+E	M	$bMON_{mol}$	145	70%	65.274	0.1530			0.472	-1.984
ON_{blend}	M	$P_{g,MON}$	139	62%	-26.05				0.342	-0.569
ON_{blend}+E	M	$P_{g,MON}$	139	62%	-26.05	-			0.342	-0.569
ON_{blend}	M	Z_{MON}	145	46%	-64.83				1.039	-2.774
ON_{blend}+E	M	Z_{MON}	145	72%	-31.99	0.3238			0.603	-2.711

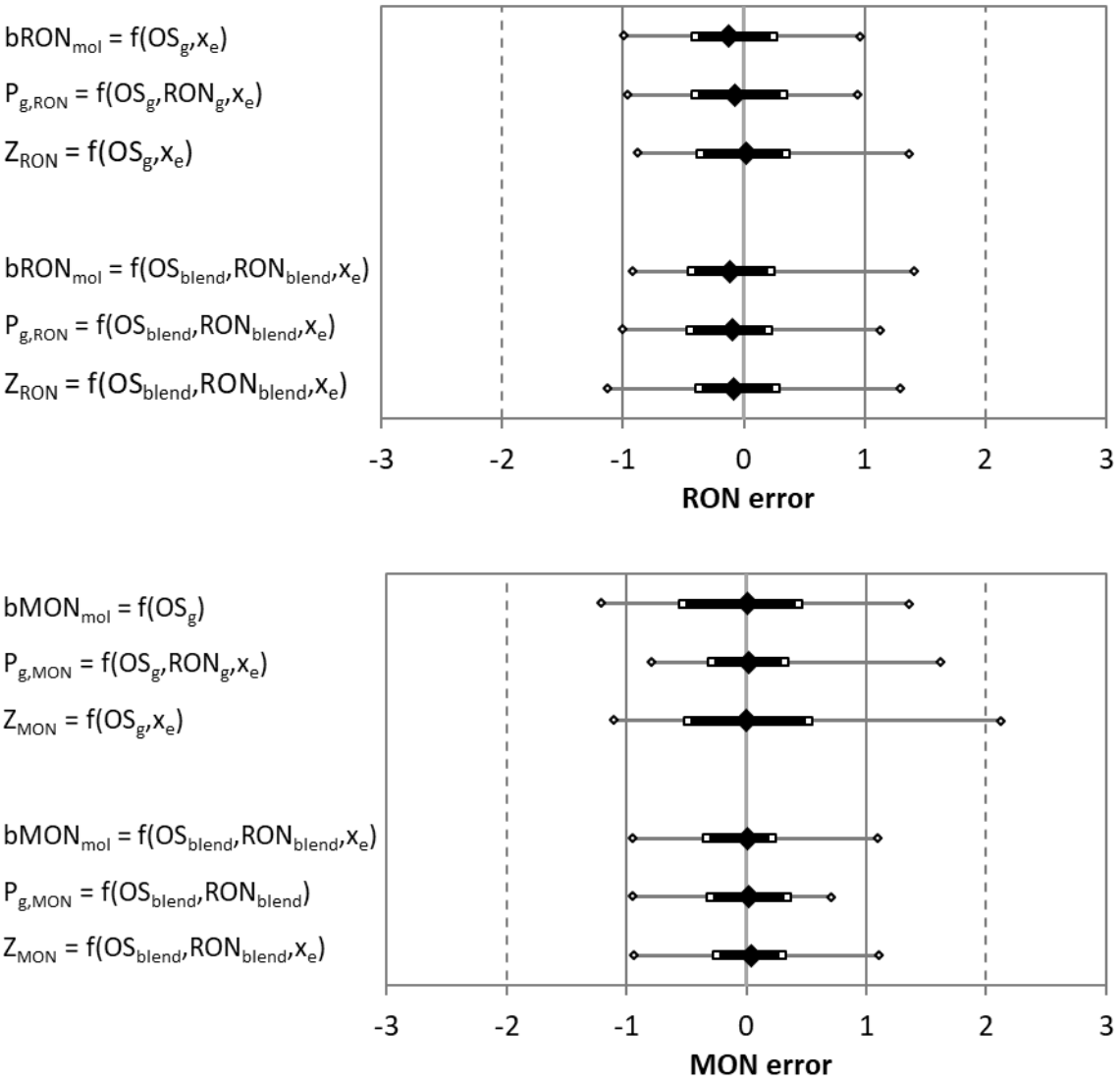

Figure S47. Box plots of ON_{blend} fitting errors for ethanol RON (top) and MON (bottom) blending models fitted over limited ethanol and RON range (ethanol < 35 vol % and RON_{blend} = 91-100) using base fuel octane numbers (OS_g, RON_g), blend octane numbers (OS_{blend}, RON_{blend}), and/or molar ethanol content. Central diamonds = 50th percentile (median), inner dark bars = 25-75th percentile, and outer whiskers = 5-95th percentile of errors.

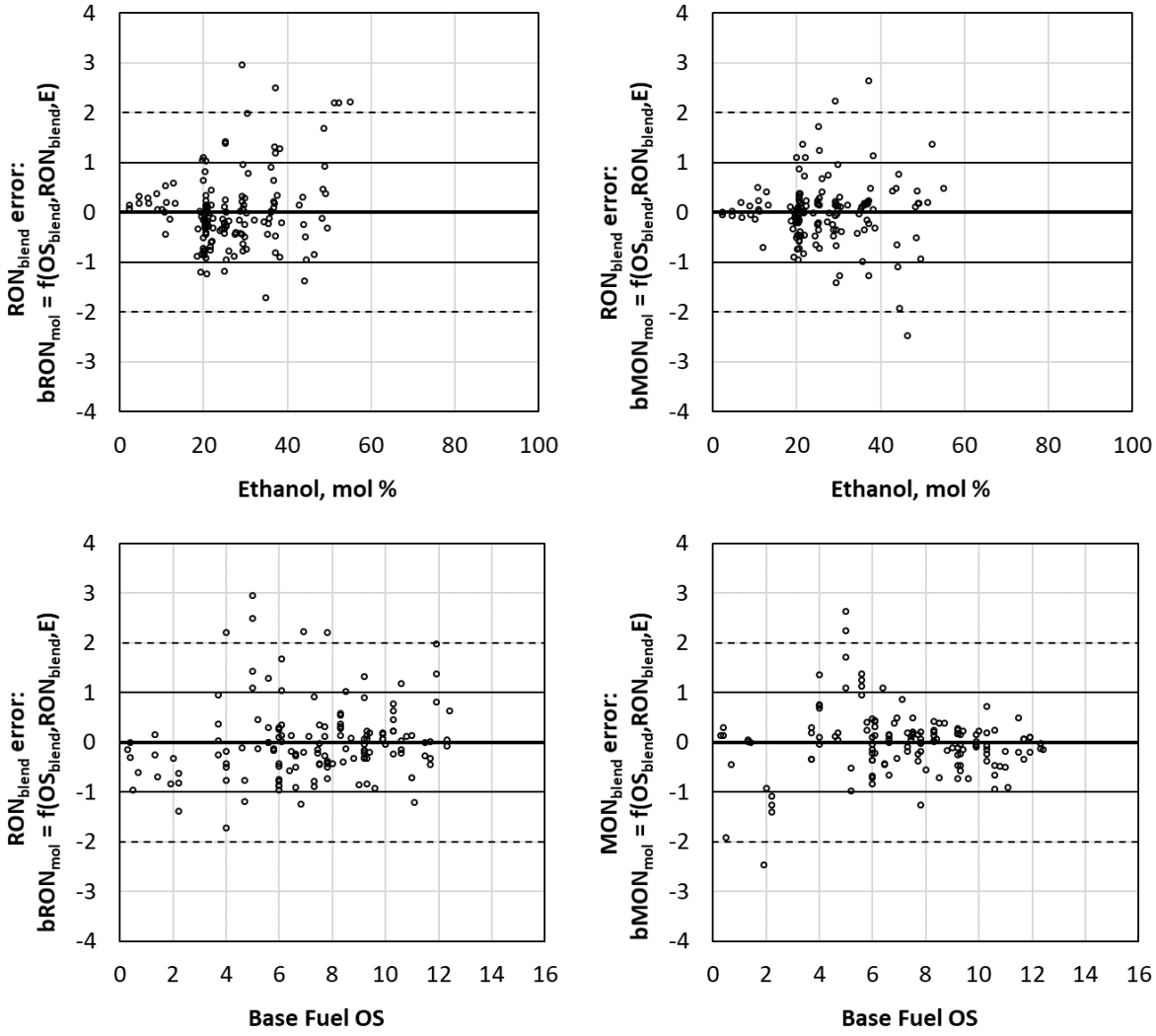

Figure S48. Error of RON and MON predictions for ethanol blends using bON_{mol} models fitted over limited ethanol and RON range (ethanol < 35 vol % and RON_{blend} = 91-100) and based on ethanol blend octane ratings (OS_{blend} and RON_{blend}) and molar ethanol content (x_e), plotted versus ethanol content (top) and base fuel OS (bottom).

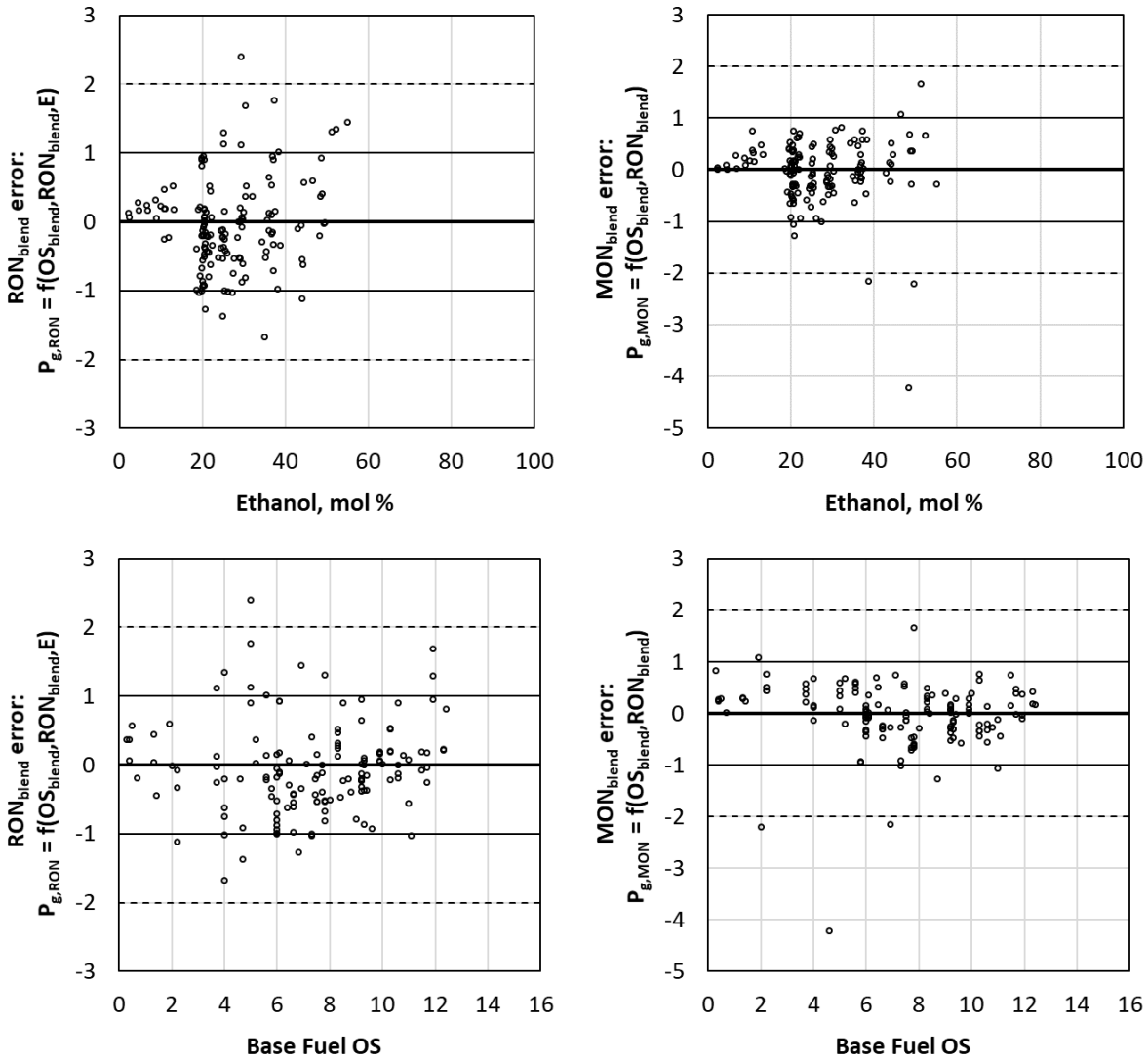

Figure S49. Error of RON and MON predictions for ethanol blends using P_g models fitted over limited ethanol and RON range (ethanol < 35 vol % and RON_{blend} = 91-100) and based on ethanol blend octane ratings (OS_{blend} and RON_{blend}) and molar ethanol content (x_e), plotted versus ethanol content (top) and base fuel OS (bottom).

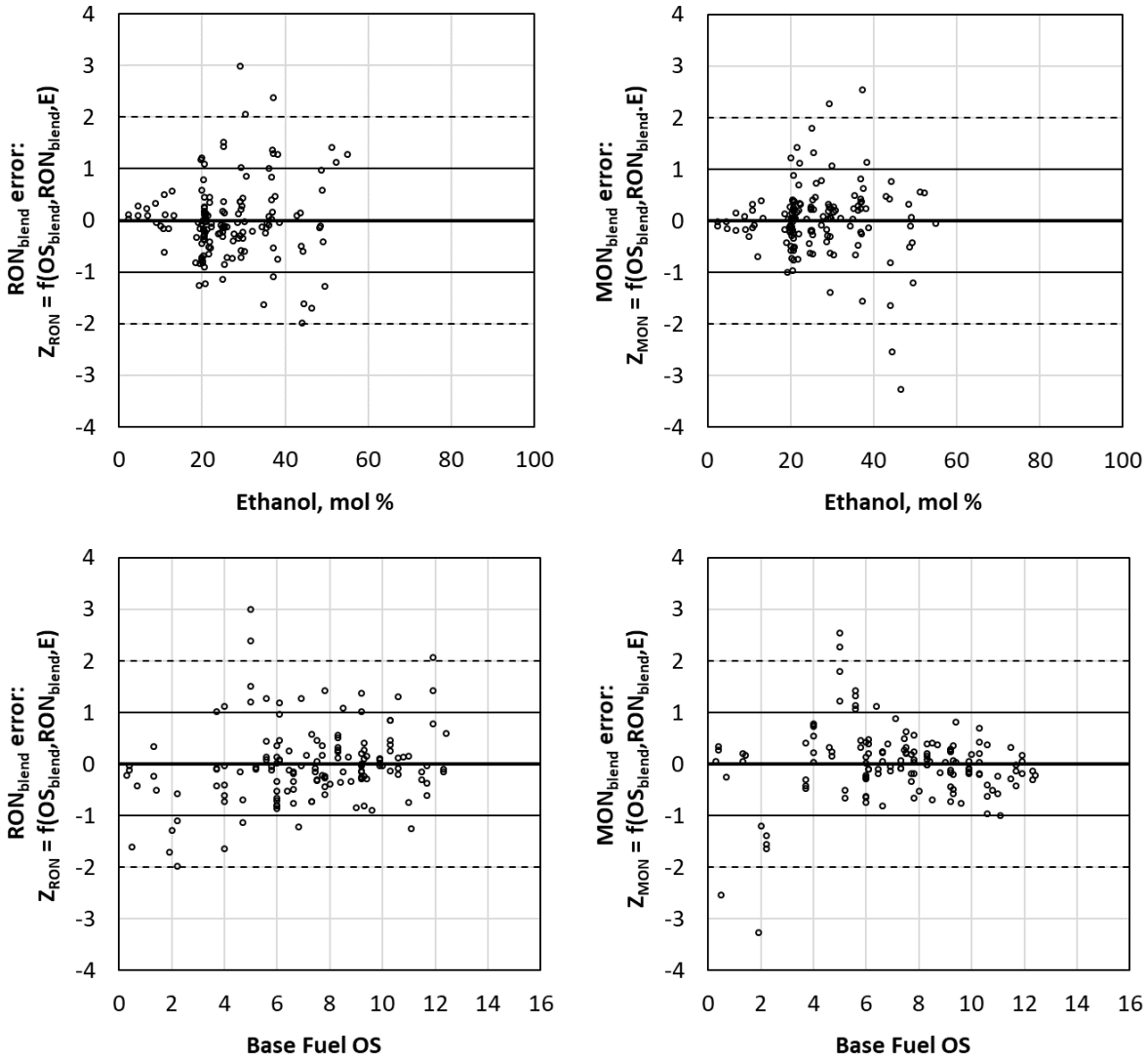

Figure S50. Error of RON and MON predictions for ethanol blends using Z models fitted over limited ethanol and RON range (ethanol < 35 vol % and RON_{blend} = 91-100) and based on ethanol blend octane ratings (OS_{blend} and RON_{blend}) and molar ethanol content (x_e), plotted versus ethanol content (top) and base fuel OS (bottom).

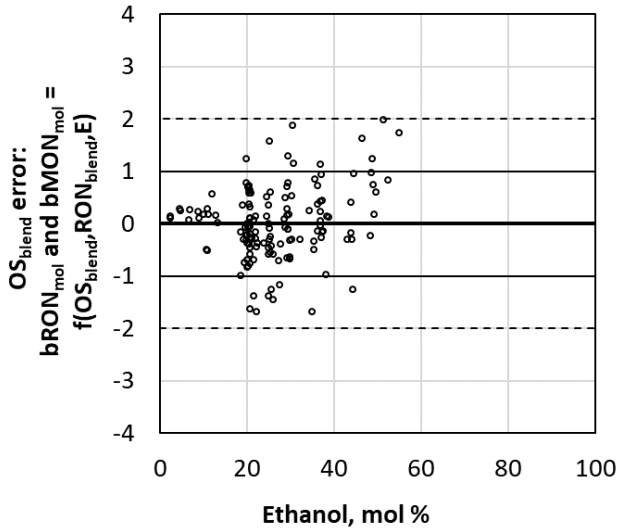

Figure S51. Error of OS predictions for ethanol blends using $bRON_{mol}$ and $bMON_{mol}$ models fitted over limited ethanol and RON range (ethanol < 35 vol % and RON_{blend} = 91-100) and based on ethanol blend octane ratings (OS_{blend} and RON_{blend}) and molar ethanol content (x_e), plotted versus ethanol content.

The red symbols in Fig. S52 show the error of blend RON and MON prediction when extrapolated for use blends with 100-102 RON (red symbols) using the model equations developed from the more limited ethanol and RON data subset (ethanol < 35 vol % and RON_{blend} = 91-100). The black symbols are the same as in Fig. S48.

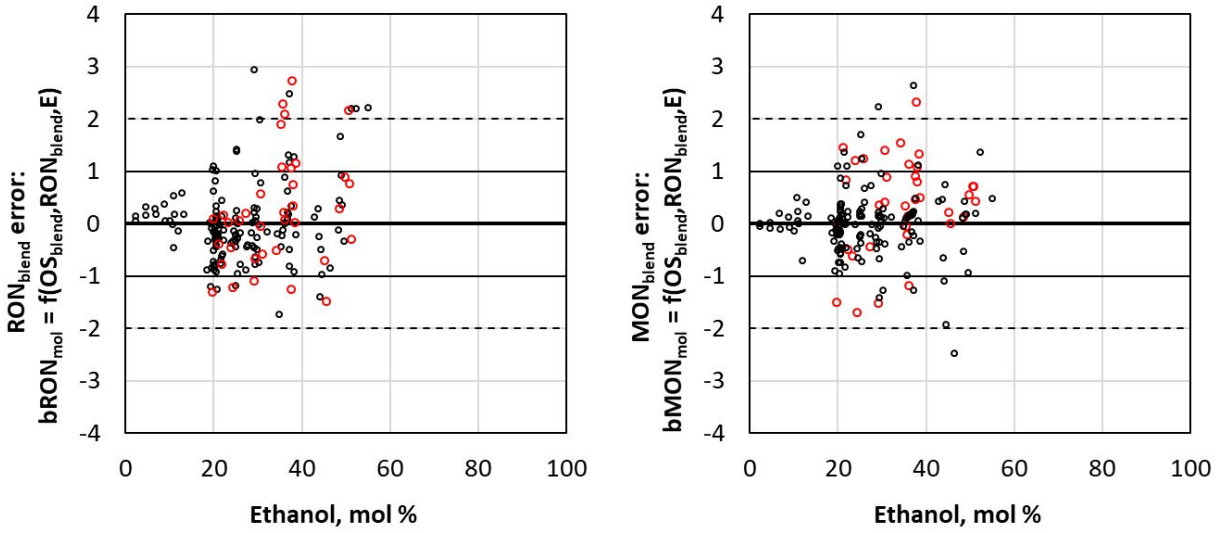

Figure S52. Error of RON and MON predictions for ethanol blends using bON_{mol} models fitted over limited ethanol and RON range (ethanol < 35 vol % and RON_{blend} = 91-100) and based on ethanol blend octane ratings (OS_{blend} and RON_{blend}) and molar ethanol content (x_e), plotted versus ethanol content. Black symbols show data over fitted range (ethanol < 35 vol % and RON_{blend} = 91-100). Red symbols show extrapolation to higher RON_{blend} range (ethanol < 35 vol % and RON_{blend} = 100-102)

SI-17. Estimation of potential octane ratings for U.S. gasoline with higher ethanol content

The analysis uses U.S. gasoline survey data from summer 2016 and winter 2017 provided by the Alliance of Automobile Manufacturers.[32] Samples with nominal E10 ethanol content (excluding samples with less than 9 vol % ethanol and greater than 11 vol % ethanol) comprised approximately 95% of the data, including 229 samples of summer regular-grade (minimum 87 AKI) and 179 samples of summer premium-grade (minimum 91 or 93 AKI). For the winter season samples, 218 and 168 samples were E10 regular and premium grades, respectively. The reported data included RON, MON, density, and ethanol content, among other properties. The reported data are only for E10 blends, however—data for their BOBs (base fuels without ethanol) were estimated as part of the analysis.

The molar ethanol content of the each E10 fuel was estimated from the reported volumetric ethanol content assuming a BOB MW of 100 g/mol (for all BOBs since this data was not reported) and its estimated BOB density (calculated from the reported E10 density using the reported ethanol content and ethanol density of 0.785 kg/L). Molar ethanol content for E15, E20, E25 and E30 were calculated using the same approach.

Next, RON and MON of the BOB for each E10 blend was estimated using the *base fuel* octane-based Z_{RON} and Z_{MON} equations in Table 2, by simultaneously solving these two equations for RON_g and MON_g. Estimated BOB RON and MON values for both winter and summer are compared with the measured E10 RON and MON values in Fig. S53. The data are plotted versus E10 AKI to better indicate which samples represent regular-grade (typically minimum 87 AKI) and premium fuels (minimum 91 or 93 AKI, depending on location). The degree of scatter is similar to that seen in the data compiled in the present study in which measured RON and MON values are available for both the E10 fuels and their BOBs (Fig. S54).

The blend RON and MON for E15, E20, E25, and E30 were then estimated using the same base fuel octane-based Z_{RON} and Z_{MON} equations (from Table 2). Plots of RON, MON and OS are shown for summer samples in Fig. S55 and for winter samples in Fig. S56.

(An alternative approach would be to first use the *blend* octane equations to estimate the BOB RON and MON and then use the *base fuel* octane equations to estimate RON and MON of the higher ethanol blends. However, using these two different sets of regression equations resulted in additional error accumulation as indicated by some RON-dependent bias in the RON and MON estimates for the round-trip from E10 to BOB and back to E10. This bias does not occur when using the same regression equations in both directions.)

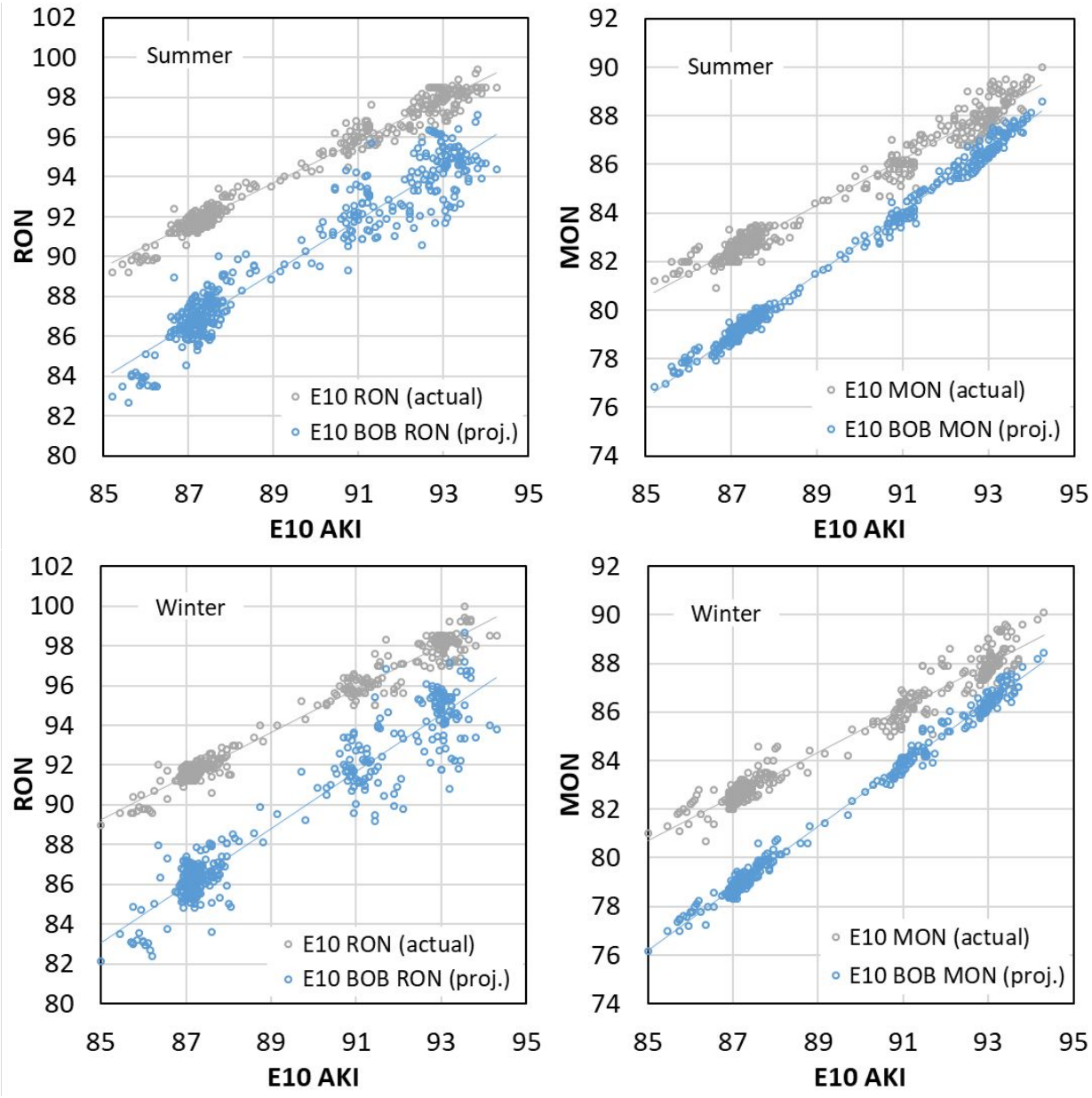

Figure S53. RON (left) and MON (right) for summer (top) and winter (bottom) E10 ethanol blends and projected values for their BOBs versus the E10 AKI for the fuels included in this study. Projected BOB ONs were calculated by solving the base fuel octane-based Z_{RON} and Z_{MON} equations simultaneously for RON_g and MON_g for each blend.

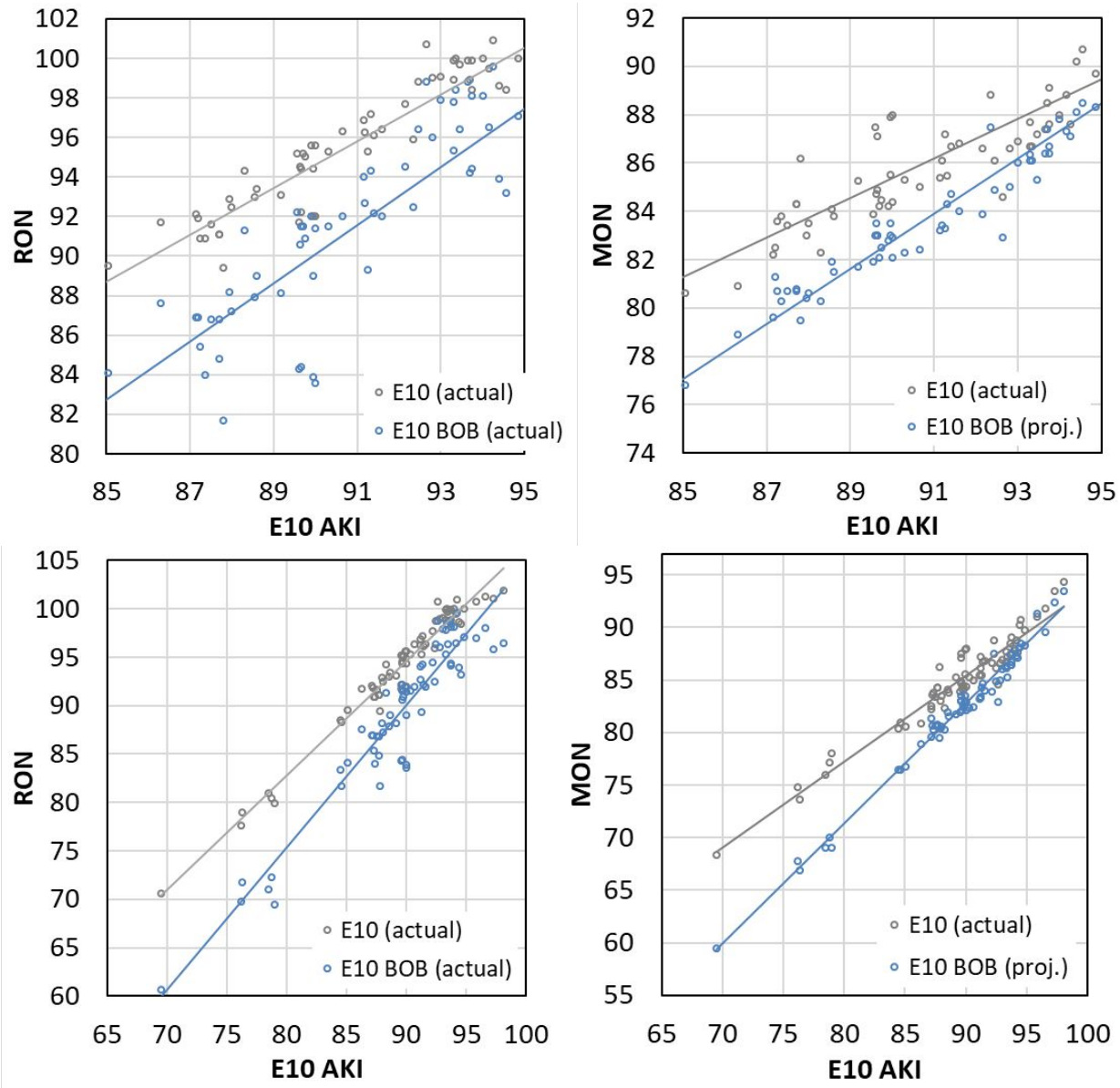

Figure S54. RON (left) and MON (right) for E10 ethanol blends and their BOBs versus the E10 AKI for the fuels included in this study. All RON and MON data are measured for both E10 and BOBs, none are estimated. Top row shows same data with scale matching Fig. S53. Bottom row shows entire data set.

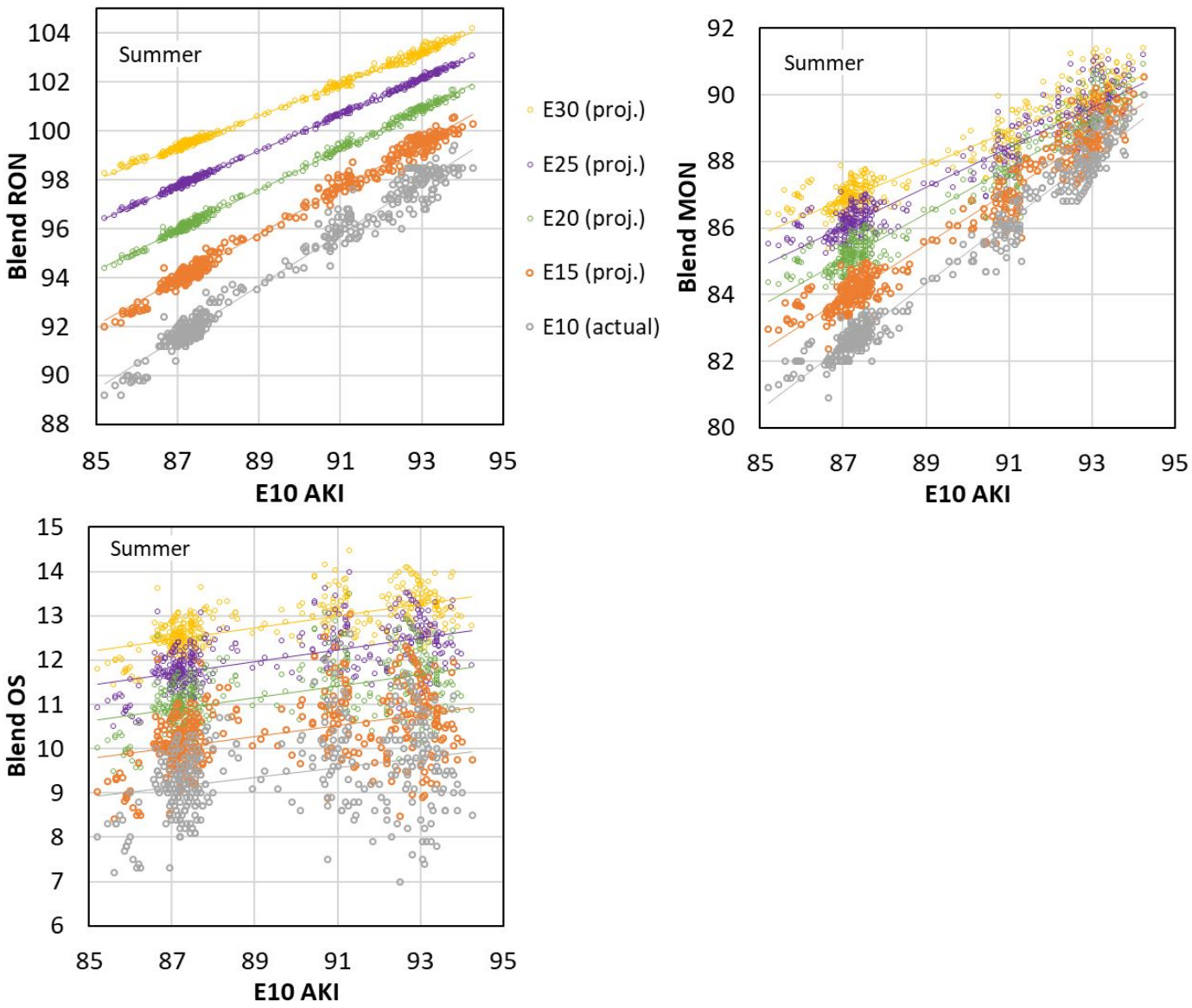

Figure S55. RON, MON and OS of U.S. E10 summer gasolines (grey symbols) versus AKI. Also shown are projected RON, MON and OS of each fuel after blending to higher ethanol content (E15, E20, E25, E30) calculated using blend octane-based Z_{RON} and Z_{MON} equations and using base fuel RON and MON values solved using Z_{RON} and Z_{MON} models.

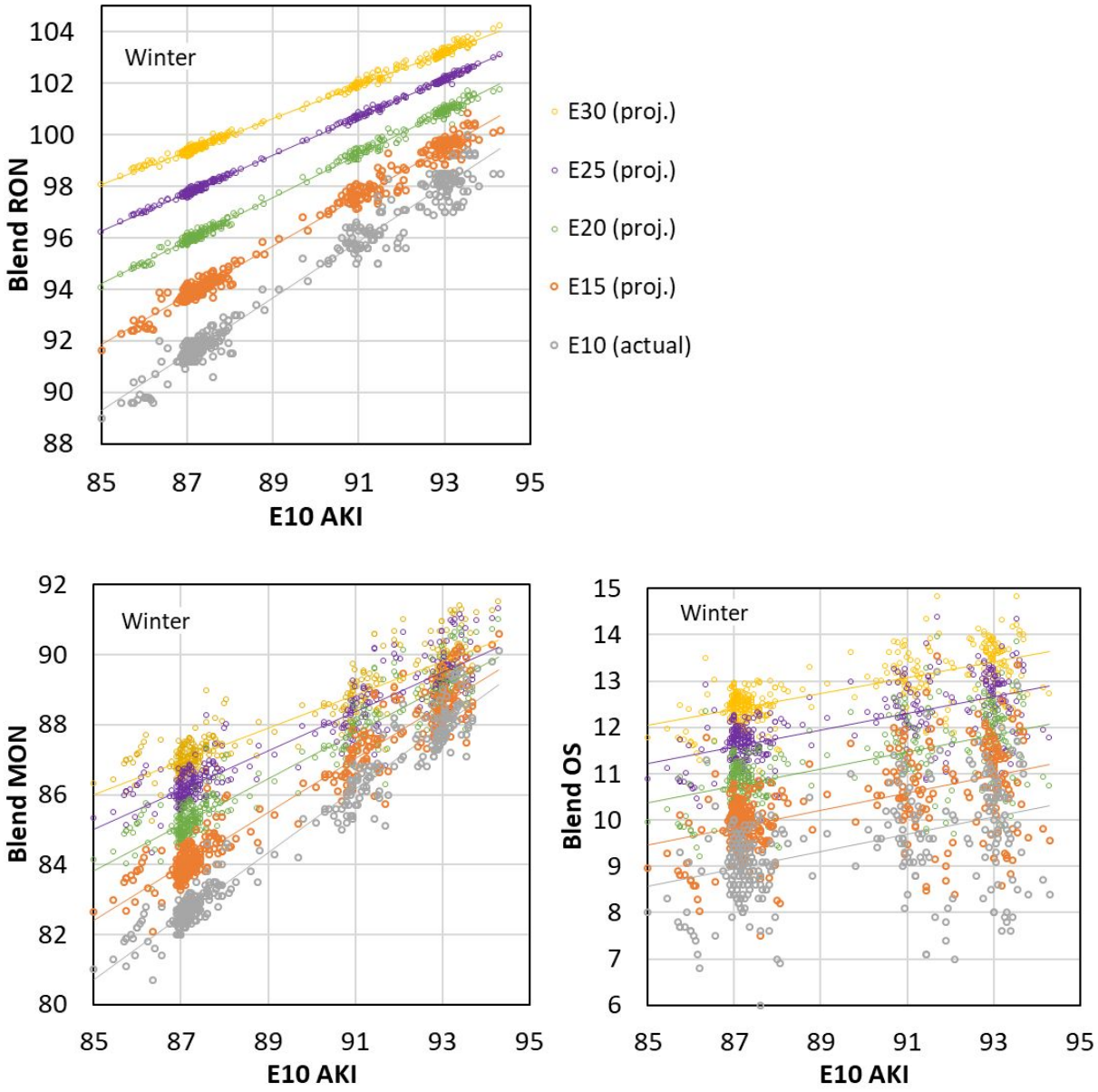

Figure S56. RON, MON and OS of U.S. E10 winter gasolines (grey symbols) versus AKI. Also shown are projected RON, MON and OS of each fuel after blending to higher ethanol content (E15, E20, E25, E30) calculated using blend octane-based Z_{RON} and Z_{MON} equations and using base fuel RON and MON values solved using Z_{RON} and Z_{MON} models.

SI-18. Uncertainty discussion

Data quality in octane rating measurements likely contributes to the variability in the model fits including outliers. As noted in the main text, RON and MON measurements have reproducibility estimates as low as 0.7 RON and 0.9 MON (where estimated), with larger values at higher RON and MON and with greater ethanol content. Models utilizing data from multiple sources cannot be expected to obtain fitting errors much below these levels.

It is also possible that individual studies may have reported erroneous or biased ON or fuel property data that was not detected and screened out during the data evaluation phase.

Density and MW are used in the volume-to-mole conversion for ethanol content as discussed in SI section SI-8. Typical values for density and molecular weight were assumed for base fuels when these values were not reported. Density and molecular weight generally fall within a relatively small range (much smaller than the other parameters considered), thus this should have a relatively limited impact on the results. To quantify the associated uncertainty, the errors of RON fitting were recalculated after assuming a different density or MW without reoptimizing the octane blending equations. RON projections with the octane rating-based Z equations in Table 2 were considered. The density (0.73 kg/L at 25 °C) and MW (100 g/mol) default assumptions were the average of reported values for US gasoline BOBs and finished E0 gasolines as described in SI section SI-8. Changing the assumed density from 0.73 to 0.77 kg/L (25 °C) increases the sum of squared RON prediction error by 0.1% and does not change the number of blends outside the ± 1 RON prediction error range (remains at 84.3%). The lack of impact is because the density was not known for only 8 of the 90 base fuels. In contrast, for MW, 49 of the 90 base fuels (and 160 of the 299 ethanol blends) had no reported MW. Changing the assumed MW value from 100 to 110 g/mol results in a 16% increase in the sum of squared RON prediction error and reduces the number of blends inside the ± 1 RON error band from 83.4% to 80.4%. Thus, the results are relatively insensitive to changes in the default assumptions for density and MW.

Volume and mass fractions for hydrocarbon groups in SOA and PIONA were used interchangeably, because insufficient speciation information was reported to allow interconversion or to convert them to molar

concentrations. This adds some unavoidable uncertainty to these data. Conversion of the hydrocarbon type fractions to molar fractions, if it were possible, would have relatively little impact on results since the molecular weights of the hydrocarbon fractions are relatively similar to each other.

Finally, some of the data sets may not be well suited for inferring octane blending behavior. For example, 7 of the 8 lowest measured $bRON_{mol}$ values (and 9 of the 12 lowest, ranging from 101.3 to 104.8 RON implying antagonistic blending) were from the two base fuels in the Karonis et al. study and all contained 10 vol % ethanol or less.[10] The increase in RON for many of these blends (relative to their base fuels) was less than 1 ON as was the increase in MON for all of the blends. These small differences make it difficult to measure blending information with high precision. These relatively low ON errors may have undue influence on the resulting correlations with octane blending values.

References

1. Brinkman, N. D., Gallopoulos, N. E., Jackson, M. W. Exhaust emissions, fuel economy, and driveability of vehicles fueled with alcohol-gasoline blends. SAE Technical Paper No. 750120, 1975.

2. Keller, J. L. *Hydrocarbon Processing* **1979**, *58*, 127-138.

3. Marceglia, G., Oriani, G. *Chem. Econ. Eng. Rev.* **1982**, *14*, 39-45.

4. Kisenyi, J. M., Savage, C. A., Simmonds, A. C. The Impact of Oxygenates on Exhaust Emissions of Six European Cars. SAE Technical Paper No. 940929, 1994.

5. Reynolds, R. E. Fuel Specifications and Fuel Property Issues and their Potential Impact on the Use of Ethanol as a Transportation Fuel. Downstream Alternatives Inc.: South Bend, IN; 2002.

6. da Silva, R., Cataluña, R., de Menezes, E. W., Samios, D., Piatnicki, C. M. S. *Fuel* **2005**, *84*, 951.

7. Yucesu, H. S., Topgul, T., Cinar, C., Okur, M. *Appl. Thermal Eng.* **2006**, *26*, 2272.

8. Nakata, K., Uchida, D., Ota, A., Utsumi, S., Kawatake, K. The Impact of RON on SI Engine Thermal Efficiency. SAE Technical Paper No. 2007-01-2007, 2007.

9. Martini, G., Manfredi, U., Mellios, G., Krasenbrink, A., De Santi, G., McArragher, S., Thompson, N., Baro, J., Zemroch, P. J., Boggio, F., Celasco, A., Cucchi, C., Cahill, G. F. Effects of Gasoline Vapour Pressure and Ethanol Content on Evaporative Emissions from Modern European Cars. SAE Technical Paper No. 2007-01-1928, 2007.

10. Karonis, D., Anastopoulos, G., Lois, E., Stournas, S. *SAE Int. J. Fuels Lubr.* **2008**, *1*, 1584-1594.

11. Milpied, J., Jeuland, N., Plassat, G., Guichaous, S., Dioc, N., Marchal, A., Schmelzle, P. *SAE Int. J. Fuels Lubr.* **2009**, *2*, 118-126.

12. Wheeler, J. Ethanol Effects on Gasoline-like HCCI Combustion. CRC Report No. AVFL-13b; Coordinating Research Council, Inc.: Alpharetta, GA; 2009.

13. American Petroleum Institute. Determination of the Potential Property Ranges of Mid-Level Ethanol Blends: Final Report. 2010.

14. Moore, W., Foster, M., Hoyer, K. Engine Efficiency Improvements Enabled by Ethanol Fuel Blends in a GDi VVA Flex Fuel Engine. SAE Technical Paper No. 2011-01-0900, 2011.

15. Christensen, E., Yanowitz, J., Ratcliff, M., McCormick, R. L. *Energy Fuels* **2011**, *25*, 4723-4733.

16. Anderson, J. E., Leone, T. G., Shelby, M. H., Wallington, T. J., Bizub, J. J., Foster, M., Lynskey, M. G., Polovina, D. Octane Numbers of Ethanol-Gasoline Blends: Measurements and Novel Estimation Method from Molar Composition. SAE Technical Paper No. 2012-01-1274, 2012.

17. Storey, J. M. E., Barone, T. L., Thomas, J. F., Huff, S. P. Exhaust Particle Characterization for Lean and Stoichiometric DI Vehicles Operating on Ethanol-Gasoline Blends. SAE Technical Paper No. 2012-01-0437, 2012.

18. Szybist, J. P., West, B. H. *SAE Int. J. Fuels Lubr.* **2013**, *6*, 44-54.

19. Foong, T. M., Morganti, K. J., Brear, M. J., da Silva, G., Yang, Y., Dryer, F. L. *Fuel* **2014**, *115*, 727-739.

20. Cannella, W., Foster, M., Gunter, G., Leppard, W. FACE Gasolines and Blends with Ethanol: Detailed Characterization of Physical and Chemical Properties. Coordinating Research Council, Inc.: Alpharetta, GA; 2014.

21. Alleman, T. L., McCormick, R. L., Yanowitz, J. *Energy Fuels* **2015**, *29*, 5095-5102.

22. Chupka, G. M., Christensen, E., Fouts, L., Alleman, T. L., Ratcliff, M. A., Mccormick, R. L. *SAE Int. J. Fuels Lubr.* **2015**, *8*, 251-263.

23. Rankovic, N., Bourhis, G., Loos, M., Dauphin, R. *Fuel* **2015**, *150*, 41-47.

24. Waqas, M., Naser, N., Sarathy, M., Morganti, K., Al-Qurashi, K., Johansson, B. Blending Octane Number of Ethanol in HCCI, SI and CI Combustion Modes. SAE Technical Paper No. 2016-01-2298, 2016.

25. Badra, J., AlRamadan, A. S., Sarathy, S. M. *Applied Energy* **2017**, *203*, 778-793.

26. Anderson, J. E., Vander Griend, S. J., Stein, R. A. previously unpublished ethanol blend data set, see Supporting Information. 2019.

27. Anderson, J. E., Kramer, U., Mueller, S. A., Wallington, T. J. *Energy Fuels* **2010**, *24*, 6576-6585.

28. Wang, C., Zeraati-Rezaei, S., Xiang, L., Xu, H. *Applied Energy* **2017**, *191*, 603-619.

29. Shen, Y. Fuel Chemistry Impacts in Gasoline HCCI (CRC Project No. AVFL-13). Coordinating Research Council, Inc.: Alpharetta, GA; 2007.

30. Pahl, R. H., McNally, M. J. Fuel Blending and Analysis for the Auto/Oil Air Quality Improvement Research Program. SAE Technical Paper No. 902098, 1990.

31. Alliance of Automobile Manufacturers. North American Fuel Survey, Summer 2008 and Winter 2009. Washington, DC; 2009.

32. Alliance of Automobile Manufacturers. North American Fuel Survey, Summer 2016 and Winter 2017. Washington, DC; 2017.

33. Anderson, J. E., DiCicco, D. M., Ginder, J. M., Kramer, U., Leone, T. G., Raney-Pablo, H. E., Wallington, T. J. *Fuel* **2012**, *97*, 585-594.

34. Hunwartzen, I. Modification of CFR Test Engine Unit to Determine Octane Numbers of Pure Alcohols and Gasoline-Alcohol Blends. SAE Technical Paper No. 820002, 1982.

35. *Standard Test Method for Research Octane Number of Spark-Ignition Engine Fuel*, D2699-16; ASTM International: 2016.

36. Sun, P., Elgowainy, A., Wang, M. Well-to-Wheels Energy and Greenhouse Gas Emission Analysis of Bio-Blended High-Octane Fuels for High-Efficiency Engines. Argonne National Laboratory: 2019.